Title

Patch Dynamics, Behavioral Responses, and Kelp Forest Stability Across a Mosaic of Ecosystem States

Permalink

https://escholarship.org/uc/item/0q16g293

Author

Smith, Joshua Gray

Publication Date

2021

UNIVERSITY OF CALIFORNIA
SANTA CRUZ

PATCH DYNAMICS, BEHAVIORAL RESPONSES, AND KELP FOREST STABILITY ACROSS A MOSAIC OF ECOSYSTEM STATES

A dissertation submitted in partial satisfaction
of the requirements for the degree of

DOCTOR OF PHILOSOPHY

in

ECOLOGY AND EVOLUTIONARY BIOLOGY

by

Joshua G. Smith

June 2021

The Dissertation of Joshua G. Smith is approved:

Professor Mark H. Carr, chair

Professor Pete T. Raimondi

Professor Anne K. Salomon

M. Tim Tinker, Ph.D.

Quentin Williams
Interim Vice Provost and Dean of Graduate Studies

Table of Contents

List of Figures

Abstract

PATCH DYNAMICS, BEHAVIORAL RESPONSES, AND KELP FOREST STABILITY ACROSS A MOSAIC OF ECOSYSTEM STATES

by Joshua G. Smith

Empirical evaluations of the ecological processes that enhance or dampen the likelihood of shifts between top-down (i.e., predator-driven) and bottom-up (i.e., resource-driven) forcing are essential to understanding the potential for cascading effects that can underpin community functioning, productivity, and stability. This suite of research used an extraordinary herbivore-outbreak in kelp forests along the central coast of California as a natural field setting to disentangle: (1) how alternations in the foraging behavior of a primary consumer drives patch state transition dynamics, (2) whether predation or resource abundance are the predominant drivers of community regulation, and (3) community-wide consequences to the formation of alternative ecosystem states. This dissertation was motived by a rapid and dramatic decline in the abundance of a sea star predator (*Pycnopodia helianthoides*) of sea urchins, and a decline of a primary producer (*Macrocystis pyrifera,* ‘kelp’) that initiated a fundamental change in purple sea urchin (*Strongylocentrotus purpuratus*) foraging behavior and condition, resulting in a spatial mosaic of remnant kelp forests interspersed with patches of sea urchin barrens. In Chapter 1, I demonstrate the important role of grazer behavior in mediating

switching among patch states. I show that the 2014 sea urchin outbreak along the Monterey Peninsula, California, USA is explicable by a shift in sea urchin grazing behavior, not by a demographic (i.e., recruitment or survivorship) response. During this six-year study, kelp forests recovered to an area that was once an expansive sea urchin barren. I show that this remarkable recovery of kelp forests in 2019 to an area in deep water was evidenced by sea urchin movement to shallow water. These results highlight the role of grazer behavior in facilitating patch transition dynamics. In Chapter 2, I demonstrate how the behavioral response of an apex predator to changes in prey behavior and condition can dramatically alter the role and relative contribution of top-down forcing, depending on the spatial organization of ecosystem states. I show that the mosaic of adjacent alternative ecosystem states led to an increase in the number of sea otters (*Enhydra lutris nereis*) specializing on urchin prey, a population-level increase in urchin consumption, and an increase in sea otter survivorship. I further show that the spatial distribution of sea otter foraging effort for urchin prey was not directly linked to high prey density, but rather was predicted by energetically profitable prey patches. Finally, in Chapter 3 I examine whether the spatial mosaic of sea urchin barrens interspersed with remnant patches of kelp forest resulted in a departure of community structure from the long-standing configuration that proceeded the formation of the mosaic. I found that beginning in 2013, many sites across the study region departed from a common multivariate ("forested") state, which had persisted for the previous six-years, and drifted into a new multivariate configuration ("urchin barrens"). Although sites trended toward a common reconfiguration, community trajectories were highly variable, and sites exhibited regional cohesion in their trajectories (Carmel, Monterey Bay). These results suggest that outbreaks of grazers associated with punctuated environmental (e.g., marine heatwaves) and biotic (loss of predators, sea urchin outbreaks) perturbations can drive apparently stable kelp forest communities to alternative potentially stable states. Collectively, the results of this dissertation highlight how patch dynamics, behavioral responses, and biotic and environmental perturbations underpin the structure and stability of ecosystems.

To those who influenced my curiosity for the natural world –
your inspiration led me here.

- and -

The mighty kelp forests of Monterey Bay, where I discovered my love for ecology.

Acknowledgements

Advisors and Reading Committee

I extend a very deep thank you to my dissertation committee for contributing to my growth as a scientist. First, I owe so much to my advisor Mark Carr for providing me guidance and direction in becoming an independent scientist, mentor, and teacher. Mark, thank you for supporting my research, academic, and professional interests, and for always investing in me. Our discussions about natural history, general ecology, and 'terrestrial equivalents' have made me a better ecologist. Your enthusiasm for the natural world motivated me through this long process. Thank you to Pete Raimondi, who consistently offered conceptual advice that taught me to think more deeply about science. Pete, thank you for your open-door policy and your willingness to explain statistics, even over the phone while you were out mountain biking. Thanks to Anne Salomon for insightful comments during committee meetings. Anne, your broad-level feedback taught me different ways of knowing and interpreting results that substantially improved my dissertation. Your breadth of knowledge and ways of drawing important inferences made our discussions so intellectually rewarding. And thanks to Tim Tinker, who pushed me to expand my quantitative skillset and welcomed me to the sea otter community. Tim, thank you for supporting my doctoral journey by encouraging me to incorporate natural history with my own research interests and questions. Thank you for setting my foundational quantitative skillset and for teaching me so much about sea otter ecology.

Mentors and those behind-the-scenes

I owe the completion of this dissertation to several other mentors outside my reading committee. Dr. William "Bill" Head is responsible for my decision to earn a PhD degree. Bill, thank you for helping me find my voice and identity as a scholar, and for teaching me the importance of drinking PBR from a glass bottle. Thank you to James Lindholm and Frank Degnan, who first introduced me to the underwater realm and established my foundational scientific skillset.

Several individuals supported the many operational and logistical aspects of my dissertation research. First, to Emily Saarman – thank you for helping me navigate the permitting process and ArcGIS, and for truly saving the day when things just weren't going right. Thank you to Dan Malone for answering all my repeated questions about PISCO data. To Steve Clabuesch and Dave Benet, thank you for making me a better diver and vessel operator. And thank you to my trusty HeatWave – a true relic with 20-mm of neoprene on the core – that [barely] survived to the end of my final field season before it unstitched at every seam.

Many parts of this dissertation would simply not have been possible without the extraordinary long-term subtidal monitoring dataset collected and hosted by the Partnership for Interdisciplinary Studies of Coastal Oceans. Thank you to the individuals who maintain this important ongoing effort. I extend a special thanks to the dozens of individuals who collected data over multiple years. To Colin and Tristin McHugh, Shannon Myers, and Hillary Krumholz – thank you for leading these efforts during my time at UCSC, and to all those past and present who continue this important ecological monitoring enterprise.

Thank you to Joe Tomoleoni, Michelle Staedler, Sophia Lyon, and Jessica Fujii for welcoming me to the sea otter community with my benthic ecology lens.

Thank you to the amazing scientists, artists, and photographers who provided images, illustrations, and graphics for this dissertation – Jessica Kendall-Bar, Michael Langhans, Kate Vylet, Kenan Chan, and Steve Lonhart.

Interns and volunteers

This work is made possible through the enormous contributions of dozens of student interns and volunteers. To my dive team – Casey Juliussen, Celine de Jong, Cheyenne Jarman, Kyle Mooers, Marisa Lovos, Liana Gaspar, Sabrina Garcia, and Torrey Gorra – thank you for enduring many long hours underwater in the cold, murky Pacific Ocean. Together we completed 774 SCUBA dives and logged over 500 hours underwater. Thanks to Logan Grady for keeping our SCUBA bottles at optimal psi. Thank you to the dozens of individuals who contributed to sea urchin dissections, conducted laboratory experiments, and collected data from hundreds of hours of videos and thousands of photoqaudrats – Adelyne Wedell, Adrian Apostol, Alan Mao, Alexa Dean, Alice Feng, Amelia Reynolds, Bonnie Goslin, Brayanna Monterosa, Caroline Banh, Cassandra Wood, Christina Langford, Daniela Asar, Dylan Meek, Echo Vanier, Edris Sherdil, Gabby Smith, Giovanna Sainz, Grace Tuohey, Haley Sutton, Holly Chen, Isabella Bolstad, Isabella Brown, Jacqueline

Shwartz, Jean-Marc Beddow, Jeannette Peters, Jess Manalo, Jovani Porras, Julia Bickford, June Leung, Kaetlyn Rodriguez, Kathleen Mayer, Kathryn Dressendorfer, Katie Lewis, Kyle Lim, Lauren Puffer, Liana Beld, Linnea Gullikson, Madelyn Saranto, Mara Salisbury, Maria Velazquez, Marissa King, Melissa Gutterman, Michael Langhans, Nick Eberle, Nick Scott, Olivia Bott, Owen Forest, Patrick Lee, Paula Kaltenbrunner, Pranav Tadepalli, Quinabil Rizal, Sabrina Ng, Sanika Bharvirkur, Sebastian Velasquez, Stefania Moore, Thomas Kurzawinski, and dozens of other volunteers.

Funding

My stipend and tuition at UC Santa Cruz (UCSC) were supported by the National Science Foundation (NSF) Graduate Research Fellowship and a UCSC Dissertation Year Fellowship from the Graduate Division. Research supplies and operational costs were supported by the NSF Graduate Research Internship, NSF Grant OCE-1538582 (awarded to PIs Dr. Mark Carr and Dr. Tim Tinker), the Future Leaders in Coastal Science Award at UC Santa Cruz, the Koret Graduate Student Mentor Fellowship, the Department of Ecology and Evolutionary Biology at UCSC, the Friends of Long Marine Lab Student Research Award, and the Earl and Ethel Myers Oceanographic Trust. I sincerely thank these entities for their support that made this research possible. Finally, operational and logistical support were provided by the US Geological Survey, The Monterey Bay Aquarium, and the California Department of

Fish and Wildlife. The funders had no role in study design, data collection and analysis, decision to publish, or preparation of this dissertation.

Family and friends

I am deeply grateful to my family for their support. To my wife Bree, who has supported me since long before graduate school was even on the horizon – thank you for always believing in me. Thank you for creating space for me to pursue this PhD degree. I am so grateful for you as my partner. Thank you for listening to my many questions about nature and ecology. I've enjoyed our time spent together in Monterey Bay venturing to the kelp forests, the rocky intertidal, and storming around the redwoods in the rain searching for mycoflora. Thank you for being the reason I finished this PhD degree strong and focused on the future. Thank you to Sarah for bringing me so much joy. To my sister Jennifer, thank you for always inspiring me with your enthusiasm for science and conservation. To my parents, thank you for pointing me towards nature at such a young age. How can I ever thank you enough for all that you have done to provide me a strong educational foundation? Your support provided the means for me to succeed. Thank you to the Perry family – Nick and Lisa – and to Lacey and James for supporting me throughout this journey with your encouragement and genuine interest in my research.

My incredible support team extends to many other individuals. To Kyle and Ashlyn, Rick and Michelle, Marc Johnson, and so many others – thank you for keeping me grounded with your support. Thanks to those who substantially improved the quality of my homebrew during grad school, and to Mark Carr for his annual contribution of fresh hops.

And finally, I acknowledge the many wonderful and diverse ecosystems that surround Monterey Bay. The rugged coastline where redwoods, live oak woodlands, and cypress trees meet the ocean is a fantastically beautiful landscape. At the edge of these ecosystems lies Monterey's iconic kelp forests – my motivation for what follows in this dissertation.

This dissertation is published in the following papers and datasets:

Chapter publications

Chapter 1 is reproduced from the following submitted manuscript:

Smith JG. Alternations in the foraging behavior of a primary consumer drives state transition dynamics in a temperate rocky reef ecosystem.

Chapter 2 is reproduced from the following published article:

Smith JG, J Tomoleoni, M Staedler, S Lyon, J Fujii, M. Tim Tinker. (2021). Behavioral responses across a mosaic of ecosystem states restructure a sea otter-urchin trophic cascade. *Proceedings of the National Academy of Sciences* 118(11) DOI: 10.1073/pnas.2012493118.

Chapter 3 is reproduced from the following submitted manuscript:

Smith JG, D. Malone, MH Carr. Spatial cohesion in community structure destabilization following the outbreak of a dominant reef grazer.

Other publications and datasets resulting from this dissertation

Smith JG and S. Garcia. (2021). Variation in purple sea urchin (*Strongylocentrotus purpuratus*) morphological traits in relation to resource availability. *PeerJ* 9: e11352 DOI 10.7717/peerj.11352

Smith JG, J Tomoleoni, M Staedler, S Lyon, J Fujii, M. Tim Tinker. (2021). Behavioral responses across a mosaic of ecosystem states restructure a sea otter-urchin trophic cascade, Dryad, Dataset, https://doi.org/10.7291/D1566H

Smith JG and S. Garcia. (2021). Variation in purple sea urchin (*Strongylocentrotus purpuratus*) morphological traits in relation to resource availability, Dryad, Dataset, https://doi.org/10.7291/D11M38

Introduction

The role of trophic interactions in organizing and maintaining the structure, persistence, functioning, and stability of ecological communities is one of the oldest subjects in the ecological literature (Muller 1940; Lewontin 1969; Holling 1973, Sutherland 1990). Although the methods by which changes in natural populations and communities are measured has been debated for decades (Lewontin 1969; Holling 1973; Connell and Sousa 1983), it is widely accepted that ecological communities can experience slow or rapid changes through time, or remain relatively unchanged (i.e., stable) across multiple generations of the constituent species. However, ecological communities do not vary randomly and often transition between multiple configurations (hereafter, “states”) as a result of biotic and environmental perturbations (Scheffer et al. 2001, Scheffer and Carpenter 2003, Schröder et al. 2005, Dudgeon et al. 2010). Identifying the mechanisms that structure ecological communities, that facilitate alternations between states, or that enhance the ability for a system to absorb or return from perturbations remains a central objective in community and ecosystem ecology (Beisner et al. 2003, Dudgeon et al. 2010, Staver et al. 2011).

The capacity to explain and predict ecosystem dynamics is dependent upon accurate estimates of biotic (e.g., species composition, diversity, trophic structure) and abiotic (e.g., disturbance events, punctuated or continuous environmental perturbations) processes that facilitate the numerical and functional ways to which species impact one another, including interactions between organisms and their environments (Worm et al. 2006; Cardinale et al. 2006; Watson and Estes 2011). There are now multiple theoretical and empirical examples of how demographic rates, species interactions, life-histories, behavior, and abiotic stressors can independently and interactively influence the structure and functioning of communities, and ultimately scale-up to shape the stability of entire ecosystems (Hairston et al. 1960; May 1973; Dayton et al. 1984; Dublin et al. 1990; Scheffer et al. 2001). However, empirical advances on the mechanisms that destabilize multispecies assemblages are often limited to opportunistic events (such as herbivore outbreaks) in space and time that erode persistent community configurations and reveal the biotic or environmental boundaries at which shifts occur (Tilman 1996, Loreau and De Mazancourt 2013).

Because of their high productivity, species diversity and ecological dynamics, ecologists have long studied the mechanisms of stability in kelp forest ecosystems around the world (Ebeling et al. 1985, Steneck et al. 2002). Some kelp forests persist for decades, while others show strong inter-annual variation, including rapid shifts from an algal-dominated state to an alternative sea urchin “barrens” state that is void of macroalgae (Graham et al. 1997, Tegner et al. 1997, Steneck et al. 2002). Forward state shifts (from forests to sea urchin barrens) can result from spatially explicit and episodic sea urchin recruitment (Lafferty and Kushner 2000, Basket and Salomon 2010, Ling et al. 2015), sea urchin migration (Harrold and Reed 1985), or from punctuated environmental disturbances (e.g., severe storms) that result in the rapid loss of kelp biomass (Harrold and Reed 1985). Reverse state shifts (from barrens to forests) can result from sea urchin disease epidemics (Carpenter and Chang 1988, Feehan and Scheibling 2014) and from severe storms that physically dislodge exposed sea urchins (Ebeling et al. 1985). Changes in predator diversity or abundance are also widely cited as mechanisms that facilitate state transition dynamics in kelp forest ecosystems (Estes and Palmisano 1974, McClanahan 2000, Hamilton and Caselle 2015).

Although multiple studies support the paradigm that two or more stable end-states may exist in kelp forest ecosystems (Estes and Duggins 1995, Filbee-Dexter and Scheibling 2014), several questions prevail about the generalization and predictability of state shifts, and the scale over which physical and environmental drivers may influence shifts (Dudgeon et al. 2010). Moreover, local drivers and processes may be highly influential in determining community states (Krumhansl et al. 2016, Kenner and Tinker 2018). Local processes may also create mosaics of barrens and forests that function as asynchronous patches that can be completely independent or linked together at multiple spatial scales (Dayton et al. 1984, Young et al. 2016). These ‘patch dynamics’ are reflective of various physical and biological forces that act on the ecosystem at different levels. Patch dynamics is a conceptual approach to understanding the structure, functioning, and dynamics of ecological communities that comprise an ecosystem’s landscape (Pickett and White 2013). The idea was first introduced by plant ecologists in the 1940’s who defined the spatial successional communities of vegetation as distinct patches within a landscape (Muller 1940). Levin and Paine (1974) later described the first model for patch dynamics, including patch maintenance and formation as a function of disturbance regimes and community structure. More recently, quantitative approaches to understanding patch dynamics have revealed explicit linkages between patch extent and community stability, highlighting that formerly continuous spatial ecosystems that become over dispersed mosaics often collapse (Scheffer et al. 2009).

Patch dynamics as they relate to stability have been extensively studied in kelp forest ecosystems and there is now a great body of literature that documents the ways that physical and biological forces interact to determine patchiness in kelp forest community structure (Dayton et al. 1984, Dayton et al. 1992, Reed et al. 2006). For example, variation in predator diversity, distribution, and abundance has repeatedly led to mosaic patches of sea urchin barrens and, consequently, marked differences in kelp forest community structure (Duggins 1983, Cowen 1983, Nichols et al. 2015, Hamilton and Caselle 2015, Burt et al. 2018). Physical forces, such as large storm-generated waves can also directly contribute to the patchy distribution of kelp across a landscape (Scheibling and Lauzon-Guay 2010) through the removal of kelp from exposed points or breaks within a continuous forest. These types of disturbance events may also have indirect effects on grazer foraging behavior, where the reduction of kelp biomass leads to increased sea urchin grazing activity that enhances the formation of barrens (Harrold and Reed 1985). Additionally, variation in the distribution of barren patches may result from differential recruitment dynamics, leading to feedback loops at patch locations where adult urchins are most abundant (Baskett and Salomon 2010). These multiple biotic and environmental perturbations can drive the spatial dynamics of barren and forest patches through time and space

(Harrold and Reed 1985). Ultimately, patch dynamics can have a profound influence on the resistance and resilience of ecosystems to biotic and abiotic disturbances (Dayton et al. 1984, Harrold and Reed 1985, Reed et al. 2006, Eisaguirre et al. 2020).

Temperate coastlines around the world have reported increased outbreaks of sea urchin barrens in the last four decades (Steneck 2002, Filbee-Dexter and Scheibling 2014). In 2014, kelp forests along the west coast of North America experienced a rapid and pronounced shift from highly expansive forests to large swaths of unproductive sea urchin barrens (Rogers-Bennett and Catton 2019, Beas-Luna et al. 2020, McPherson et al. 2021, Smith et al. 2021). Of particular concern is whether (and how) this widespread kelp deforestation resulted in a marked shift in the predominant source of primary production and decreased food web complexity. Recent studies have identified considerable geographic variation in species responses and key functional groups to a marine heatwave and decline in kelp, most notably in Mexico and northern California kelp forests, where the extent of forest loss was region-wide (Beas-Luna et al. 2020, McPherson 2021). In contrast to these region-wide shifts in system state, forest loss in central California was spatially heterogenous, resulting in mosaics of forests and barrens (Smith et al. 2021). These mosaics allow for concurrent comparison of community structure in forest and barrens subjected to similar past and present environmental (oceanographic, geomorphological) conditions.

In this dissertation, I evaluate the patch dynamics of kelp forest and sea urchin barren communities in relation to ecological stability. Beginning in 2013, a series of biotic (a catastrophic sea star wasting syndrome, decline in kelp productivity) and environmental (episodic marine heatwave) perturbations initiated an abrupt outbreak of purple sea urchins (*Strongylocentrotus purpuratus*) that shifted a once expansive kelp forest landscape into a mosaic of sea urchin barrens interspersed with remnant patches of forest. I used this kelp forest-urchin barrens mosaic as a natural field setting to explore mechanisms of community regulation and stability. In **Chapter 1**, I explore the spatial extent of kelp forests and sea urchin barren patches and relate this to the mechanisms that facilitate switching among patch states. In **Chapter 2**, I test a series of hypotheses related to the behavioral mechanisms that underpin community regulation across of the mosaic. Finally, in **Chapter 3**, I examine whether the spatial mosaic of sea urchin barrens interspersed with remnant patches of kelp forest resulted in a departure of community structure from the long-standing configuration that proceeded the formation of the mosaic.

In **Chapter 1**, I explore whether (and how) alternations in sea urchin foraging behavior explain state transition dynamics in patches of forests and barrens across the mosaic landscape. Understanding the role of animal behavior in linking individuals to ecosystems is central to advancing knowledge surrounding community structure, functioning, stability, and transition dynamics (Schmitz 1998, Ovadia and Schmitz 2002, Werner and Peacor 2003, Sih et al. 2012). Using 17-years of long-term subtidal monitoring and a size-structured population model, I show that the 2014 sea urchin outbreak is primarily evidenced by a behavioral shift, not by a demographic response (i.e., survival or recruitment). I then tracked the behavior of sea urchins for three years (2017-2019) following the outbreak and reduced availability of detrital algae to determine how behavior shapes alternations between kelp-dominated and urchin-dominated (hereafter, ‘barren’) states. In this chapter, I show that sea urchin behavior is a strong predictor of patch (forested or barren) transition dynamics in patches across the kelp forest-urchin barrens mosaic. Finally, in 2019, I observed a remarkable recovery of forests to a subset of deep (14-20 m) survey sites that were expansive sea urchin barrens just two years prior (2017). I show that this isolated recovery of kelp forest patches was associated with sea urchin movement to shallow water. This is evidenced by a dramatic reduction in medium (30-38 mm) and large (> 38 mm) urchins at deep reefs, simultaneous increase of those size classes inshore, and a pronounced reduction of foliose red macroalgae in shallow water. These results demonstrate the important role of grazer behavior in facilitating switching among alternative ecosystem states.

In **Chapter 2**, I demonstrate how the behavioral response of an apex predator to changes in prey behavior and condition can dramatically alter the role and relative contribution of top-down forcing, depending on the spatial organization of ecosystem states. In 2014, a rapid and dramatic decline in the abundance of a mesopredator (*Pycnopodia helianthoides*) and primary producer (*Macrocystis pyrifera*) coincided with a fundamental change in purple sea urchin (*Strongylocentrotus purpuratus*) foraging behavior and condition, resulting in a spatial mosaic of kelp forests interspersed with patches of sea urchin barrens. I show that this mosaic of adjacent alternative ecosystem states led to an increase in the number of sea otters (*Enhydra* *lutris nereis*) specializing on urchin prey, a population-level increase in urchin consumption, and an increase in sea otter survivorship. I further show that the spatial distribution of sea otter foraging efforts for urchin prey was not directly linked to high prey density but rather was predicted by the distribution of energetically profitable prey. Therefore, I infer that spatially explicit sea otter foraging enhances the resistance of remnant forests to overgrazing but does not directly contribute to the resilience (recovery) of forests. These results highlight the role of consumer and predator trait-mediated responses to resource mosaics that are common throughout natural ecosystems and enhance understanding of reciprocal feedbacks between top-down and bottom-up forcing on the regional stability of ecosystems.

Finally, in **Chapter 3**, I examine whether the spatial mosaic of sea urchin barrens interspersed with remnant patches of kelp forest resulted in a departure of community structure from the long-standing configuration that proceeded the formation of the mosaic. Ecological communities can be stable over multiple generations, or rapidly shift into structurally and functionally different configurations (Holling 1973, Connell and Sousa 1983, Tilman 1996, Dudgeon et al. 2010). In kelp forest ecosystems, overgrazing by sea urchins can abruptly shift forests into alternative states that are void of macroalgae and primarily dominated by actively roaming sea urchins. Beginning in 2013, a series of biotic and environmental perturbations initiated a widespread sea urchin outbreak along northern and central California. While forest loss was region-wide along the northern coast of California, central California forests shifted into a patchy mosaic of remnant forests interspersed with sea urchin barrens.

In this chapter, I used a 14-year subtidal monitoring dataset of invertebrates, algae, and fishes to explore changes in community structure associated with the loss of forests at 23 sampling sites in central California (Carmel Bay and southern Monterey Bay) to determine: (1) whether the spatial mosaic of barrens and forests resulted in a shift in community structure relative to the years preceding the formation of the mosaic, (2) how the spatial dynamics of community structure trajectory vary across the mosaic (and which species align well with observed dynamics), and (3) whether community structure dynamics were spatially cohesive among sample sites and regions (Monterey and Carmel Bay). I found that beginning in 2013, many sites across the study region departed from a common multivariate ("forested") state, which had persisted for the previous six-years, and drifted into a new multivariate configuration ("urchin barrens"). Although sites trended toward a common reconfiguration, community trajectories were highly variable, and sites exhibited regional cohesion in their trajectories (Carmel, Monterey Bay). These results suggest that outbreaks of grazers associated with punctuated environmental (e.g., marine heatwaves) and biotic (loss of predators, sea urchin outbreaks) perturbations can drive apparently stable kelp forest communities to alternative potentially stable states.

The results of this dissertation highlight how patch dynamics, behavioral responses, and biotic and environmental perturbations underpin the structure and stability of ecosystems. This study advances the field of community ecology by enhancing understanding of how the strengths of behaviorally mediated interactions can reorganize community regulation. Finally, this study highlights the importance of resource mosaics in mediating reciprocal feedbacks between top-down and bottom-up forces that ultimately scale-up to affect community dynamics and ecosystem stability.

CHAPTER ONE

ALTERNATIONS IN THE FORAGING BEHAVIOR OF A PRIMARY CONSUMER DRIVES STATE TRANSITION DYNAMICS IN A TEMPERATE ROCKY REEF ECOSYSTEM

Chapter 1: Alternations in the foraging behavior of a primary consumer drives state transition dynamics in a temperate rocky reef ecosystem.

Abstract

Understanding the role of animal behavior in linking individuals to ecosystems is central to advancing knowledge surrounding community structure, functioning, stability, and transition dynamics. In 2014, a widespread sea urchin outbreak along the central coast of California, USA shifted a once expansive kelp forest to a mosaic of remnant forests interspersed with patches of sea urchin barrens. Using 17-years of long-term subtidal monitoring and a size-structured population model within a Bayesian state-space framework, I show that the 2014 sea urchin outbreak is primarily evidenced by a behavioral shift, not by a demographic response (i.e., survival or recruitment). I then tracked the behavior of sea urchins for three years (2017-2019) following the outbreak and reduced availability of detrital algae to determine how behavior shapes alternations between kelp-dominated and urchin-dominated states. I found that sea urchin behavior is a strong predictor of state (forested or barren) transition dynamics in patches across the kelp forest-urchin barrens mosaic. Finally, in 2019, I observed a remarkable recovery of forests at a subset of deep (14-20m) survey sites that were expansive sea urchin barrens just two years prior (2017). I show that this isolated recovery of kelp forest patches was associated with sea urchin movement to shallow water. This is evidenced by a dramatic reduction in medium (30-38 mm) and large (> 38 mm) urchins at deep reefs,

simultaneous increase of those size classes inshore, and a pronounced reduction of foliose red macroalgae in shallow water. These results demonstrate the important role of grazer behavior in facilitating alternative state dynamics.

Introduction

The importance of behavior in linking individuals to ecosystems is widely recognized in the ecological literature (Schmitz 1998, Ovadia and Schmitz 2002, Werner and Peacor 2003, Sih et al. 2012). Behavior can facilitate community structure and functioning by altering the relative influence of key species interactions (e.g., competition, predation, mutualisms), changing the distribution of resources, and through other non-consumptive response pathways (Estes et al. 1998, Pace et al. 1999, Werner and Peacor 2003). From a top-down perspective, the mere presence of predators can elicit changes in herbivore behavior that have profound influences on primary productivity (Schmitt 1998, Werner and Peacor 2003, Gil et al. 2020). However, bottom-up processes driven by resource distribution, abundance, or quality can also affect consumer and predator foraging behavior (Eldred 2019, Smith et al. 2021). Although the debate continues over the relative importance of density versus behaviorally mediated influences of predators and primary consumers, both occur widely in nature and are often associated with trophic cascades (Beckerman et al. 1997, Schmitz et al. 1997, Werner and Peacor 2003, Kauffman et al. 2010). Therefore, understanding how the presence of predators and resource availability reciprocally influence the behavior of primary consumers is central to advancing knowledge of community structure, functioning, stability, and transition dynamics.

Sea urchin grazing in marine ecosystems around the world is often considered a fundamental driver of shifts from algal-dominated habitats to alternative sea urchin ‘barrens’ that are void of macroalgae (Filbee-Dexter and Scheibling 2014, Ling et al. 2015). These shifts have profound consequences to the structure and functioning (e.g., productivity) of coral reef, kelp forest, and rocky intertidal ecosystems (Done 1992, Watson and Estes 2011, Filbee-Dexter and Scheibling 2014). Resource availability and predator-driven impacts are perhaps the two most well-documented factors known to influence patterns in sea urchin grazing behavior (Mann 1982, Cowen 1983, Harrold and Reed 1985, Burt et al. 2018). Cascading effects resulting from the loss of sea urchin predators provide strong evidence of density-mediated indirect interactions (Estes et al. 1998, Burt et al. 2018), whereas reductions in the availability of food or risk-cues have been associated with behaviorally mediated indirect interactions (Harding and Scheibling 2015, Spyksma 2017). However, the relative influence of these factors is often context-dependent and difficult to decouple from other more environmentally driven processes such as how prey respond to macro- and micro-topography, seasonality, swell, and water temperature (Vivian-Smith 1997, Konar et al. 2014). Therefore, the factors that contribute to modifications in sea urchin grazing behavior can have important implications for the state of communities and ecosystems.

In temperate kelp forest ecosystems, sea urchin behavior can be categorized into two fundamental modalities. In kelp forests where abundant detrital (i.e., ‘drift’) algae is available, urchins mainly employ a ‘cryptic’ passive-grazing modality (Sala and Zabala 1996). Detrital kelp is constantly produced within forests and deposited in the refuge space occupied by sea urchins (Duggins et al. 1989, Krumhansl and Scheibling 2012). Urchin concealment in the refuge of crevices is also a known anti-predator behavior (Tegner and Levin 1983). The presence of predators may elicit a direct response in sea urchins that influences cryptic behavior, or indirectly by maintaining forests (and therefore abundant drift) through trophic cascades (Cowen 1983, Estes et al. 1998). However, when the production of detrital kelp is limited (either through a reduction in predator abundance, or through environmental perturbations), urchins fundamentally shift their behavior to an active grazing modality, where they emerge from refuge and roam on an open reef surface in search of live macroalgae (Harrold and Reed 1985, Kriegisch et al. 2019). Additionally, because sea urchins have a dispersive larval-stage life history, kelp-urchin dynamics can also be strongly driven by spatially explicit and episodic recruitment (Lafferty and Kushner 2000, Okamoto et al. 2020).

Kelp forests along the west coast of North America recently experienced a rapid and pronounced shift from highly expansive forests to unproductive sea urchin barrens. Starting in 2013, an extreme marine heatwave event coincided with a continental-wide collapse of the urchin predator *Pycnopodia helianthoides* (hereafter, *Pycnopodia*; Harvell et al. 2019, McPherson et al. 2021). Shortly after (2014-2016), large-scale outbreaks of purple sea urchins (*Strongylocentrotus purpuratus*) and a reduction in kelp biomass were recorded along the mainland coasts of California, United States and Baja California, Mexico (Beas-Luna et al. 2020). In northern California where bull kelp (*Nereocystis luetkeana*) is the dominant structure-forming foundation species, over a 95% reduction in historical kelp biomass was documented (Rogers-Bennett and Catton 2019, McPherson et al. 2021). Similar large-scale loss of kelp biomass was recorded at the southern range limit of the giant kelp (*Macrocystis pyrifera*) near Bahía Asunción, Mexico (27.1°N; Arafeh-Dalmau et al 2019, Beas-Luna et al. 2020). However, along the central coast of California, giant kelp-dominated forests experienced a shift to a patchy-mosaic of forests interspersed with sea urchin barrens (Smith et al. 2021). As such, whether the observed 2014 sea urchin outbreak resulted from a behavioral shift (in response to the loss of *Pycnopodia* and a decline in kelp), or an anomalous recruitment event remains unresolved.

In this study, I explore how the regional extirpation of *Pycnopodia* and reduced productivity of kelp associated with the 2015-16 marine heatwave initiated a widespread behavioral shift in purple sea urchins. I then track the behavior of sea urchins in the years following the demise of sea stars and reduced availability of detrital algae to determine how behavior shapes alternations between kelp-dominated (hereafter, ‘forested’) and urchin-dominated (hereafter, ‘barren’) states. This study is motivated by the following hypotheses: (1) the regional collapse of *Pycnopodia*, the 2015-16 marine heatwave, and a decline in kelp production led to the emergence of sea urchins from refuge, (2) sea urchin behavior (passive or active) explains state (forested or barren) transition dynamics, and (3) sea urchin movement is associated with macroalgae recovery.

Methods

Study system

This study was conducted in the nearshore temperate reefs of southern Monterey Bay, California, USA (Figure 1.1). All marine algae and invertebrates within the region are protected from harvest within marine protected areas. The giant kelp, *Macrocystis pyrifera,* is the dominant habitat-forming alga and the purple sea urchin, *Strongylocentrotus purpuratus,* (hereafter, 'sea urchin') is the principal benthic herbivore, although bull kelp (*Nereocystis luetkeana*) and red sea urchins (*Mesocentrotus franciscanus*) also inhabit the region. In 2013, a coastwide sea star wasting syndrome locally extirpated the urchin predator *Pycnopodia helianthoides* (Harvell et al. 2020). Shortly thereafter, a dramatic increase in visually detectible sea urchins shifted the region to a patchy mosaic of remnant forests interspersed with sea urchin barrens (Smith et al. 2021). I used long-term benthic subtidal monitoring data to determine whether the initial urchin outbreak was primarily evidenced by a behavioral shift, or by a demographic response (i.e., sea urchin recruitment or survivorship). I then conducted a series of annual surveys designed to explore whether (and how) sea urchin behavior is associated with state transition dynamics in patches across the mosaic.

Urchin behavioral shifts at the regional scale

To determine the temporal point when the sea urchin outbreak occurred, I conducted change point analyses on a 17-year time series of subtidal data collected by the Partnership for Interdisciplinary Studies of Coastal Oceans (PISCO; Malone et al. 2021). First, I used a segmented regression to determine the most likely temporal change point locations on the annual sum of urchin counts recorded across a subset of 12 sites (to account for unequal sampling effort between years) surveyed in sequential years in Monterey, California. The segmented approach is useful for determining the number and position of change points when they are unknown a priori. However, static change points are considered independent and therefore confidence regions cannot be generated continuously across segments. Therefore, I used the temporal breakpoints identified in the segmented regression to inform a Bayesian regression with multiple change points in the 'mcp' package in the program R (Lindeløv 2020).

To determine whether the sea urchin outbreak is explained by a shift in sea urchin behavior from passive to active grazing, I examined the annual size-frequency of sea urchins recorded on PISCO surveys before and after the outbreak. Support for this hypothesis would be evidenced by increases in counts of all size classes of urchins as they emerged from crevices and became more visible on surveys. Alternatively, support for the recruitment hypothesis (i.e., that the urchin outbreak was associated with a recruitment event) would be evidenced by a dramatic and disproportionate increase in the frequency of sea urchins less than 3 cm. I used an analysis of variance test on the size-frequency of sea urchins across all years to evaluate annual changes in the mean size-class of urchins, and a Kolmogorov-Smirnov test to evaluate equality in urchin size-distribution across the critical 2013-2014 breakpoint (identified from the Bayesian regression).

Population state dynamics

To further explore whether the marked 2014 increase in counts of adult (>3 cm) sea urchins is explicable by a sea urchin behavioral shift, I developed a process model within a Bayesian hierarchical framework, fitting a size-structured population dynamics model to survey data to evaluate sea urchin recruitment, survival (growth), and detection probability as plausible drivers of observed population dynamics. The key demographic processes in this model are growth, survival, and recruitment, while a fourth observer process (detection probability) relates the latent dynamics of the true population to the observed survey data.

To estimate size-specific growth transition rates, I used a Tanaka (1982) growth function within a Bayesian framework adapted from Burt et al. 2018 to model the growth of *Strongylocentrotus purpuratus*:

$$D_{t+1} = \frac{1}{\sqrt{f}}\log\left[\left(2f\left(\frac{E}{4f}-\frac{a}{E}+1\right)+2\sqrt{f^2\left(\frac{E}{4f}-\frac{a}{E}+1\right)+f*a}\right)\right]+d+\varepsilon$$

$$E = e^{\sqrt{f}(D_t-d)}$$

where ε is a normal variate $\varepsilon \sim \mathrm{N}(0, \sigma^2)$, and with nearby (Bodega Bay, California, USA) area-specific parameters (a, d, f, σ) derived from Ebert (2010). The model was simulated to estimate one-year growth increments for 5000 individual urchins drawn randomly from the empirically derived size distribution from all sites across all years. I then used these growth increments to calculate size-specific transition probabilities (G_i) for 10 size-classes of urchins (for a seamless comparison with field size estimates measured to the nearest 1 cm). Specifically, I used the Tanaka function to construct a growth transition matrix consisting of the proportion of individuals that persisted within a size class or transitioned to class $G_i + 1$ (Appendix 1 Table T1).

The average instantaneous mortality rate for purple urchins was set at 0.197 based on previously published values (Russel 1987, Ebert 2010), and temporal variation in survival was modeled by allowing for an additive random effect on log mortality:

$$S_{i,t} = \exp\left(-\exp\left(\log(0.197) + \phi_{S,t}\right)\right)$$

where $\phi_{S,t}$ is a random effect estimated during model fitting, normally distributed with standard error σ_S and mean of 0 for years prior to 2014 and $\overline{\phi_S}$ for years 2014-2020, where both σ_S and $\overline{\phi_S}$ are parameters to be estimated.

For recruitment, I set an arbitrary baseline value for average recruitment that was large enough such that the other parameters in the process model could take on a wide range of meaningful values given the observed data. While I was interested in potential effects of changes to relative recruitment rates, the absolute values of recruitment are not identifiable if variation in survival and mean detection probability (see below) are also free parameters. However, average recruitment can be set arbitrarily and then the model solved for an equilibrium abundance given survival. If this abundance value is large to allow sufficient flexibility in the detection probability parameter (see below), it should not impact model results. I therefore set the average value of R to exp(6) = 400 recruits per year, but also evaluated a range of values to ensure that the value chosen did not qualitatively impact model results. Temporal variation in relative recruitment values was then modeled by allowing for an additive random effect on log recruitment:

$$R_t = \exp\left(6 + \phi_{R,t}\right)$$

where $\phi_{R,t}$ is a random effect estimated during model fitting, normally distributed with standard error σ_R and mean of 0 for years prior to 2014 and $\overline{\phi_R}$ for years 2014-2020, where both σ_R and $\overline{\phi_R}$ are parameters to be estimated. Combining these demographic processes, the number of expected individuals (N_{exp}) surviving and transitioning to larger size-classes was estimated as:

$$N_{exp_{1,t+1}} = [(N_{1_t})(1 - G_1) + R_t] * S_{a_{i,t}}$$

$$N_{exp_{2,t+1}} = [(N_{2_t})(1 - G_2) + N_{exp_{1,t}} G_1] * S_{a_{i,t}}$$

$$\dots$$

$$N_{exp_{10,t+1}} = [(N_{10_t})(1 - G_{10}) + N_{exp_{9,t}} G_9] * S_{a_{i,t}}$$

The actual number of urchins of each size class observed on transects each year ($Obs_{i,t}$) depended both on true abundance and on the likelihood that urchins were detected, given their size and behavior. Previous analyses (Burt et al. 2018) have shown that detection probability decreases for smallest size classes, therefore we modeled age-specific detection probability as a non-linear asymptotic logit function:

$$logit(D_{i,t}) = \exp\left(a - b\left(\frac{1}{i}\right)^2 + \phi_{D,t}\right)$$

where $D_{i,t}$ is the detectability of size class *i* at time *t*, a and b are estimated parameters, and $\phi_{D,t}$ is a random effect estimated during model fitting, normally distributed with standard error σ_D and mean of 0 for years prior to 2014 and $\overline{\phi_D}$ for ears 2014-2020, where both σ_D and $\overline{\phi_D}$ are parameters to be estimated.

The total number of urchins observed on transects each year was modeled as a gamma-distributed random variable, related to true (latent) abundance as:

$$\sum_i Obs_{i,t} \sim \text{Gamma}\left(\sum_i \left[Nexp_{i,t} \cdot D_{i,t}\right] \cdot \upsilon, \upsilon\right)$$

where ν is a model-estimated inverse scale parameter that determines the magnitude of observer error in annual survey counts.

The annual vectors of observed size distributions of urchins were modeled as Dirichelet-multinomial random variables, related to the true (latent) size distributions as:

$$\langle Obs_{i,t} \rangle \sim \text{Dirichlet} - \text{Multinomial}\left(\langle \left[Nexp_{i,t} \cdot D_{i,t} \right] \rangle \cdot \tau\right)$$

where the degree of over-dispersion in size frequency vectors (relative to that expected for a simple multinomial distribution) was determined by the fitted precision parameter τ.

Size-structured urchin population dynamics were fit to observed data using Markov Chain Monte Carlo (MCMC) methods. The temporal modification factors for recruitment, survival, and detection probability ($\overline{\phi_R}$, $\overline{\phi_S}$, $\overline{\phi_D}$) were estimated after first initializing the population at the conditional equilibrium abundance and size distributions at the start of the time series, conditional upon the mean baseline values for survival and recruitment. I compare the estimates of modification factors to assess the relative influence of temporal variation in recruitment, survival, and detection probability on the post-2013 changes in observed abundance and size frequency distribution. I evaluated model goodness of fit using graphical posterior predictive checks and by estimating the Bayesian-P values (Gelman 1996), to ensure that out-of-sample distributions were reflective of the observed data distributions. A Bayesian-P value close to 0.5 would indicate similar distributions between the simulated data and real observed data.

Patch level dynamics

I explored patch-level dynamics over a three-year study period (2017-2019) to further examine how sea urchin behavior underpins switching among patch states (forest, barren). The field sampling methods used for this phase of the project are described in detail in Smith et al. 2021. Briefly, I surveyed a total of 236 subtidal sites from May-September in 2017 (n = 71), 2018 (n = 92), and 2019 (n = 73) to determine state transition dynamics and attributes of each state such as sea urchin behavior, density, and the cover of key groups of algae. Survey sites were randomly selected on hard substratum between 5- and 20-meters of water. Each site was sampled using 16 $1m^2$ quadrats randomly stratified across eight 5-meter long transects (two quadrats per transect), and each transect radiated from a fixed central location (Figure 1.1). Therefore, each survey site represents an independent replicate sample.

The state (barrens, forest) of each site was characterized by constructing a linear discriminant analysis (LDA) using urchin behavior, density, and the cover of algae as classifiers. In the field, each site was surveyed using 16 randomly placed $1m^2$ quadrats fixed with a high-resolution GoPro Hero4 camera and two Sola LED video lights. The density of urchins was recorded *in situ* within each quadrat by quantifying visually detectible sea urchins and by searching in cracks and crevices for cryptic individuals. I also recorded site patch state (barrens, forest) based on initial impressions of the site at the start of each dive. In the lab, photoquadrats were analyzed to determine the number of actively foraging (i.e., exposed) sea urchins, and to estimate the cover of key algal groups that are characteristic of forests and barrens

(Filbee-Dexter and Scheibling 2014). Each photoquadrat was assigned 16 universal points using a digital grid in ImageJ. Because many alga are difficult to visually quantify to the species-level in imagery, I used four taxonomic categories that are known indicators of patch state (Filbee-Dexter and Scheibling 2014): articulated coralline algae, encrusting coralline and red algae, brown algae, and foliose red algae. Finally, exposed sea urchins were quantified from photoquadrats by counting only urchins where 50% or more of the test diameter was visible (Smith et al. 2021). I then constructed the LDA by using these variables (sea urchin density, proportion of exposed urchins, cover of algae) as predictors of the field patch-state classification. Out of 284 sites used in training the LDA, only seven were misclassified and the entropy R^2 was 0.89. Therefore, I elected to use the predicted states from the LDA (rather than diver-based site impressions) in subsequent analyses.

To test the hypothesis that shifts in patch state are associated with alternations in sea urchin foraging behavior, I explored transition dynamics across two time-steps (2017 to 2018, and 2018 to 2019). For this analysis, I only used sites that were surveyed at the same spatial location in sequential years to determine whether each site (1) persisted as the same state across the time step, (2) forward-shifted from a forest to barren, or (3) reverse-shifted from a barren to a forest. A logistic regression was used to determine the transition probability based on the natural log-transformed mean density of exposed (i.e., actively foraging) sea urchins, mean number of cryptic urchins, and starting state (barren, forest). I defined the logistic target level based on a positive state shift, where a transition to a different year-following state was classified as ‘1’, and state persistence as ‘0’. Therefore, each of the variables in the model represent starting-year values used to predict the year-following state. Finally, to determine the strength of discontinuity in state-shift thresholds, I examined the logged odds of state transition probabilities from the logistic regression as a function of exposed sea urchin density.

Forest recovery following sea urchin movement

In 2019, I observed a dramatic reduction in counts of sea urchins and an extraordinary recolonization of a kelp forest to an area that was an expansive sea urchin barren just two years prior (2017). Surveys farther inshore (i.e., shallow water) during the recovery year (2019) revealed an abundance of large (>6 cm) sea urchins and a reef devoid of macroalgae. I hypothesized that the observed recovery of kelp was associated with sea urchin movement to shallow water. To test this hypothesis, I examined urchin size-structure and density across three depth zones and three survey years. For this analysis, I categorically assigned a subset of sites (n = 18) near the recovery area to one of three depth zones: shallow (0-6 m), mid (7-13 m), and deep (14-20 m). Sea urchins were categorically assigned to one of three size classes based on test diameter: small (<30 mm), medium (30-38 mm), and large (>38 mm). These size classes were selected based on the first, second, and third quantiles of the entire population size-distribution across all three survey years (n = 6827 individuals).

I used a mixed model with a Restricted Maximum Likelihood (REML) to test for differences in mean sea urchin density across three survey years (2017-2019), three depth zones (shallow, mid, deep), and three size-classes of sea urchins (small, medium, large). The model was constructed as a full factorial with year, depth zone, and size class as fixed effects, and site and transect as random effects. I then used a contrast test to examine the hypothesis that the density of large and medium sized urchins declined over the period 2018-2019 in the deep zone, and simultaneously increased in the shallow zone. After examining the output of the mixed model, it was clear that the density of urchins did not significantly change across the 2017-2018 time period. Therefore, I restricted the subsequent contrast test to the 2018-2019 period.

Finally, I explored changes in the algal assemblage across each depth zone in relation to sea urchin movement. To test for changes in the mean percent cover of foliose red algae, brown algae, and encrusting algae, I used an analysis of variance (ANOVA) test on photoquadrats at each of my survey sites with depth zone and algae type as predictors of percent cover. I then used PISCO data on kelp density from an adjacent site located near the recovery area (Pt. Piños) to examine whether kelp recovery at deep reefs was associated with sea urchin movement to shallow water.

Results

Urchin behavioral shifts at the regional scale

I found a pronounced increase in total counts of visually detectible purple sea urchins that occurred between 2013 and 2014. Variation in the sum of squares of the differences in counts of urchins were best minimized using two breakpoints, with one at 2014 and one at 2017 ($R^2 = 0.96$, DF = 10, Residuals S.E. = 719). Bayesian regression using multiple change points revealed a sharp uptick in urchins that initiated in 2014 and continued for at least four years (2017) before reaching an apparent deceleration (Figure 1.2). Prior to 2014, the mean fitted counts of visually detectible sea urchins was 152 individuals (± 60 SE). However, total counts of urchins in the 2017 to 2020 period increased by roughly 4000% to 6092 individuals (± 764 SE).

Size-frequency analyses revealed that counts of 3 cm to 10 cm urchins uniformly increased over a magnitude of 600% between 2013 and 2014 (Figure 1.3). A Kolmogorov-Smirnov (KS) two-sample test of equality revealed no significant difference in the size distribution of urchins between these two years. Moreover, I did not find evidence of an anomalous pulse in urchins at the lower end of the size distribution (< 4 cm) in the years prior to 2014.

The size-structured population dynamics model fit to survey data converged relatively well and satisfied posterior predictive checks (all psrf values < 1.3; Appendix 1 Table T2). The simulated model reproduced similar annual size-frequency distributions comparable to the field survey estimates (Bayesian P = 0.42, Figure 1.4). After analyzing the parameter posterior distributions, detection probability emerged as the most influential demographic process driving observed population dynamics (Figure 1.5). The mean logit for the detection parameter was 5, indicating over a 148% increase in the likelihood that divers encountered visually detectible sea urchins. Moreover, these sea urchins (> 5 cm) are too large to have settled from the plankton later than 2012, based on the model predicted growth rates (Appendix 1 Table T2). Therefore, the dramatic increase in counts of purple sea urchins in 2014 is explained almost entirely by the emergence of large (adult) sea urchins from refuge.

Patch level dynamics

I found support for the hypothesis that patch state transitions are explained by shifts in sea urchin behavior. The linear discriminant analysis revealed that 113 sites persisted as the same starting and ending state across time steps, 11 forward-shifted from a forest state to barren, and 12 reverse-shifted from a barren state to forest. Model selection for the full logistic regression with behavior (active, passive) as a predictor of the year-following state showed that the density of actively foraging (i.e., exposed) urchins was the strongest determinant of transition probability ($R^2 = 0.18$, $P < 0.0001$, AICc = 112).

An analysis of the logged odds from the logistic regression revealed evidence of a strong discontinuous state shift (Figure 1.6). The 50% probability transition threshold for a forward-shift from a kelp forest to a sea urchin barren was 2.71 exposed urchins/m^2. However, the 50% probability transition threshold for a reverse-shift from a barren to a forest was 0.03 exposed urchins/m^2.

Forest recovery following sea urchin movement

In 2019, I observed a remarkable recovery of forests at a subset of deep (14-20m) survey sites that were expansive sea urchin barrens just two years prior (2017). Long term subtidal monitoring data revealed a rapid decline in kelp density across all depth zones in 2014 that coincided with the onset of sea urchin barrens. Starting in 2018, bull kelp (*Nereocystis luetkeana*) recolonized the deep depth zone, with a sharp and pronounced recovery in 2019 (Figure 1.7).

I found that the total density of sea urchins significantly decreased in the deep zone between the 2018 and 2019 sampling seasons, with the most pronounced effects occurring in the large and medium urchin size-classes ($R^2 = 0.53$, $P < 0.0001$; Figure 1.8A). A less dramatic but similar decline in medium and large urchins was observed across the same time step at mid depths (7-13m). In the shallow zone, the total mean sea urchin density increased from 1.58 urchins/m^2 (±0.34 S.E.) to 14.17 urchins/m^2 (±1.19 S.E.). All size classes of urchins significantly increased in the shallow zone in the 2019 survey year ($P < 0.0001$). The contrast test revealed that the density of large and medium sized urchins significantly declined within the deep zone between 2018 and 2019 (t-ratio = 2.77, $P < 0.005$) and increased within the shallow zone during this same time period (t-ratio = -5.69, $P < 0.0001$). Finally, a comparison of slopes between the deep and shallow zones across the 2018 and 2019 period revealed that they were significantly different (DenDF = 2765, F = 20.16, $P < 0.0001$).

Results from analyses on the percent cover of foliose red algae, brown algae, and encrusting algae further support the hypothesis of mass sea urchin movement to shallow water. Starting in 2019, the cover of encrusting coralline algae significantly decreased in the deep zone, along with a simultaneous increase in the cover of foliose red and brown algae ($R^2 = 0.79$, DF = 2, $P < 0.0001$; Figure 1.8B). In the shallow zone, the cover of foliose red algae significantly decreased, with a pronounced spike in the cover of encrusting coralline algae ($R^2 = 0.48$, DF = 2, $P < 0.0001$).

Discussion

This study demonstrates the important role of grazer behavior in mediating alternative state dynamics. The patchy kelp forest-urchin barrens mosaic that developed following the extirpation of *Pycnopodia* and the marine heatwave revealed how grazer behavior shapes alternations between kelp-dominated and urchin-dominated states. These findings suggest that the initial 2014 sea urchin outbreak along the central coast of California was primarily driven by the emergence of adult sea urchins from refuge, not by a demographic response (i.e., recruitment or survival). Behaviorally driven alternations among patch states across the mosaic further demonstrate the role of grazer behavior in facilitating transition dynamics.

In many systems, behavior is a primary mechanism for the organization of ecological communities (Lima and Zollner 1996, Werner and Peacor 2003). The vast majority of studies that demonstrate behavior-induced community patterning often result from demographic (i.e., recruitment) or density-dependent responses of predators and their prey (Levin 1976). This study suggests how both predatory release and starvation-induced behavioral switching can facilitate persistent patterning of community states. The uniform increase in the density of adult sea urchins recorded on long-term monitoring surveys revealed a clear and rapid behavioral shift that resulted in the formation of the spatial mosaic of kelp forests interspersed with sea urchin barrens. The initial sea urchin outbreak observed in 2014 is likely reflective of a shift in grazing modality (from passive, to active grazing) in response to reduced food availability and from a reduction in the abundance of an important benthic mesopredator (Cowen 1983, Harrold and Reed 1985, Burt et al. 2018). However, the relatively low abundance of *Pycnopodia* prior to the sea star wasting syndrome suggests that predator-induced sheltering behavior was likely a strong mechanism for suppressing active sea urchin grazing (Spyksma 2017).

While I did not find evidence of a demographic response coinciding with the 2014 sea urchin outbreak, recruitment facilitation is a known driver of alternative state dynamics (Baskett and Salomon 2010). Sea urchin recruitment dynamics are often episodic, with considerable geographic variation (Pearse and Hines 1987, Ebert and Russell 1988). Moreover, grazing of macroalgae by adults can maintain patches of suitable habitat that enhance settlement of pelagic urchin larvae, creating feedback loops that expand the spatial extent of barrens (Baskett and Salomon 2010, Karatayev and Baskett 2020). Following the initial sea urchin behavioral shift in 2014, it is possible that the formation of barren patches enhanced sea urchin recruitment to barrens within the mosaic. Additionally, recruitment may have occurred prior to 2012 in this system, or with variable timing and magnitude at other locations along the northeastern Pacific Ocean (Okamoto et al. 2020).

Long-term monitoring observations along the central coast of California, USA indicated that the 2014 sea urchin outbreak continued for at least four years before reaching an apparent deceleration in 2017. During this same period, canopy-forming kelps to the north and south of the study region experienced unprecedented declines resulting from the marine heatwave and even more expansive outbreaks of purple sea urchins (Arafeh-Dalmau et al 2019, Rogers-Bennet and Catton 2019, Beas-Luna et al. 2020, McPherson et al. 2021). One explanation for the persistence of remnant kelp patches in this system (as opposed to adjacent neighboring areas) is the presence of trophically redundant predators. The urchin predator guild along the west coast of North America is comprised of five key species: sea otters (*Enhydra lutris nereis*), lobsters (*Panulirus interruptus*), sheephead (*Semicossyphus pulcher*), sunflower sea stars (*Pycnopodia helianthoides*), and rock crab (*Cancer spp.*; Scheibling and Hamm 1991, Eisaguirre et al. 2020). The abundance of these five species varies geographically along the west coast. In northern California where rock crab and wolf eels are the only alternative predators of urchins, forests were reduced by over 95% with the loss of *Pycnopodia* (McPherson et al. 2021). However, forests in southern California that have a suite of urchin predators (e.g., lobster, sheephead, rock crab) experienced an apparent buffer from kelp decline following the demise of *Pycnopodia* (Eisaguirre et al. 2020). Finally, on the central coast of California, remnant patches of kelp forests are indirectly maintained by sea otters that target energetically profitable sea urchins in patches of forest (Smith et al. 2021). This spatially explicit foraging by sea otters is likely the mechanism responsible for the persistence of kelp patches within the mosaic.

In this study, switching among patch states within the mosaic was explicable by changes in the density of exposed (i.e., active foraging) sea urchins. Behavioral switching within the mosaic across such a short temporal duration is most likely driven by spatial variability in drift kelp. High-levels of drift kelp have been shown to facilitate reef-scale behavioral feedbacks in California, Chile, and New Zealand (Vasquez and Buschmann 1997, Ling et al. 2019, Kriegisch et al. 2019). I also found evidence of strong discontinuous state shift thresholds, with at least two discontinuous thresholds required to facilitate switching among patch states. A number of studies have suggested a critical threshold of a forcing variable that drives state transitions to less productive configurations (Petraitis and Dudgeon 2004, Casini et al. 2009). The strong forward and reverse-shift thresholds identified in this study provides an empirical demonstration of this phenomenon.

The isolated recovery of kelp forest patches in 2019 was associated with sea urchin movement to shallow water. This is evidenced by the dramatic reduction in medium- and large-sized urchins at deep reefs, simultaneous increase of those size classes inshore, and the pronounced reduction of foliose red macroalgae in shallow water. It is important to note that the kelp species that repatriated the once barren grounds was the bull kelp (*Nereocystis luetkeana*, an annual species), not the giant kelp (*Macrocystis pyrifera*, a perennial species). Prior to the 2014 sea urchin outbreak, kelp forests along the Monterey Peninsula were dominated by the giant kelp

(Foster and Schiel 1985, Graham et al. 1997). It is well established that shading by giant kelp limits algal recruitment and the growth of other noncalcareous species (Reed and Foster 1984, Kennelly 1989). The removal of long-standing giant kelp forests by purple sea urchin grazing may have released the annual-growing species *Nereocystis* from light limitation, thereby enabling the rapid recolonization and growth of *Nereocystis* following sea urchin movement inshore to shallow water.

The results presented in this study highlight the role of behaviorally mediated effects in structuring ecological communities. One of the most unusual aspects of this system is the ability for sea urchins to persist in low resource environments for extended periods of time (Ebert 1967, Ebert 1982, Smith and Garcia 2021), which may contribute to the longevity of the alternative barrens state of the ecosystem. However, many other small consumers switch between sit-and-wait foraging and open roaming (Higginson and Ruxton 2015). Therefore, the degree to which behavior of grazers, especially of ecosystem engineers, is affected both directly and indirectly by resource abundance and predatory cues is fundamental to community dynamics.

Figures

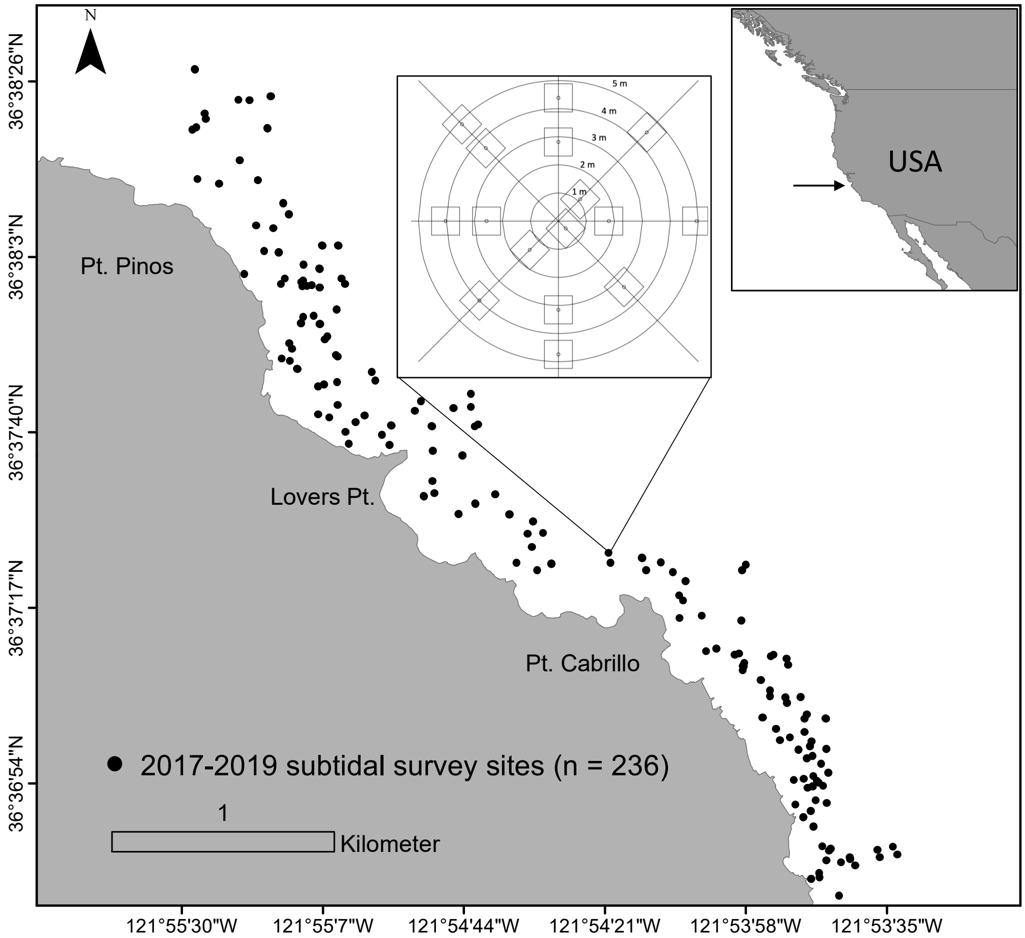

Figure 1.1. Study area along the Monterey Peninsula, California, USA. Each point represents an independent survey site. The inset diagram depicts the sampling design used to survey each site using eight 5-meter-long transects (lines) radiating from a fixed central position, with two 1m^2 quadrats (squares) sampled per transect.

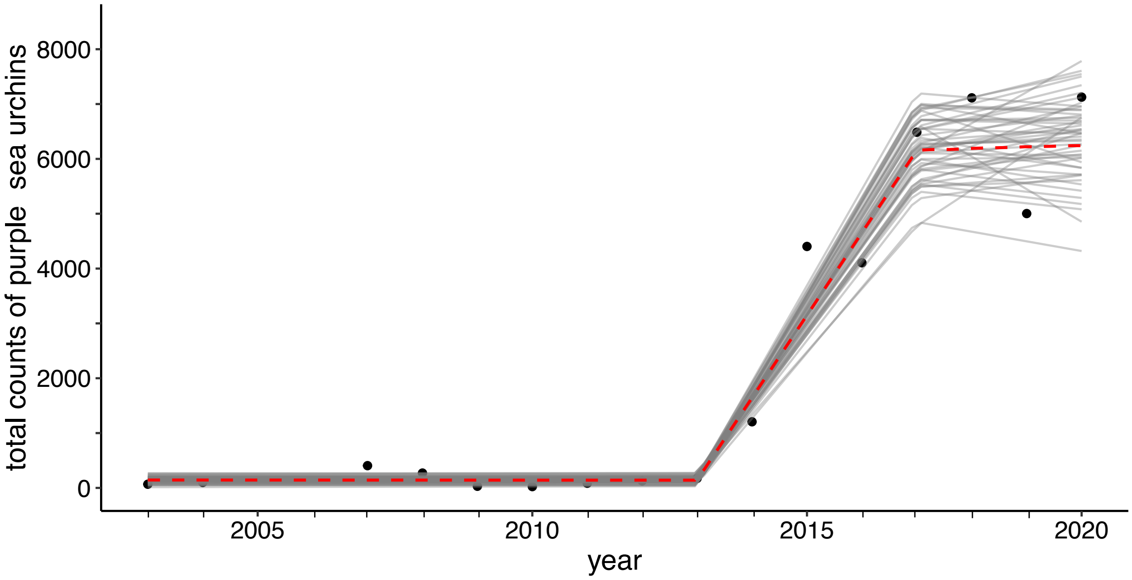

Figure 1.2. Annual counts of purple sea urchins at long-term subtidal monitoring sites in Monterey Bay, California, USA. Each point represents the total counts of purple sea urchins in a given year. The grey lines represent 50 simulations of multiple change points using Bayesian inference and the red dashed line indicates the median across three segments.

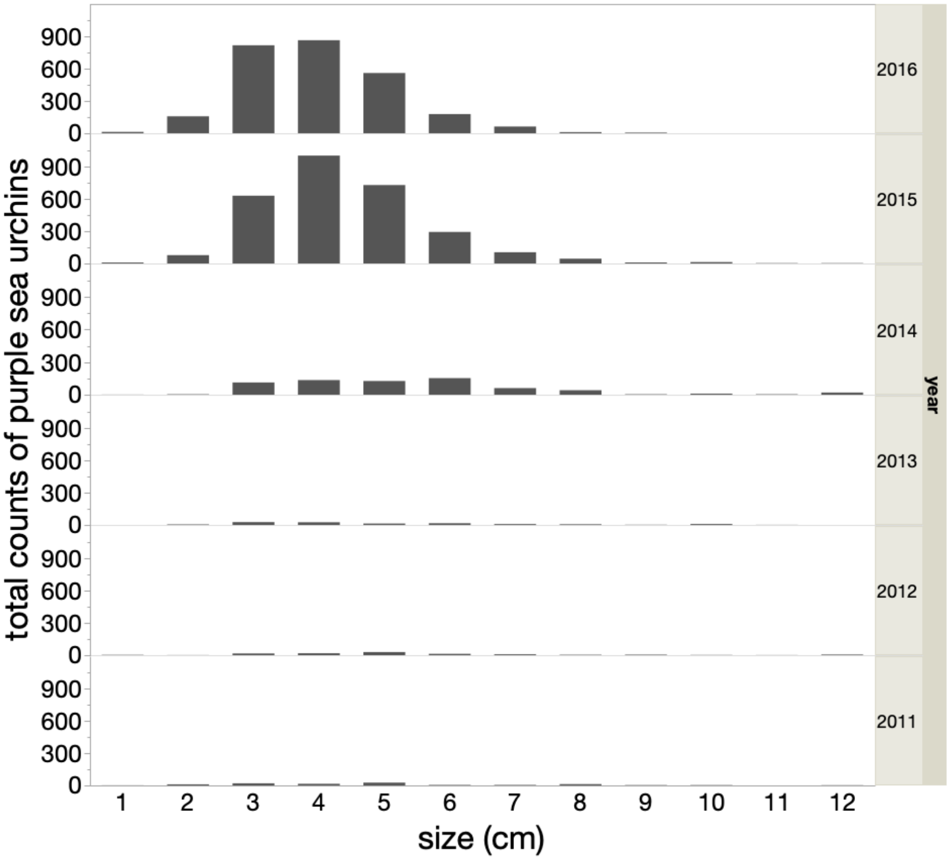

Figure 1.3. Size frequency distribution of purple sea urchins (*Strongylocentrotus purpuratus*) in Monterey, CA recorded on long term subtidal monitoring surveys by PISCO. Each bar depicts the annual total counts of purple sea urchins across 12 discrete size-classes.

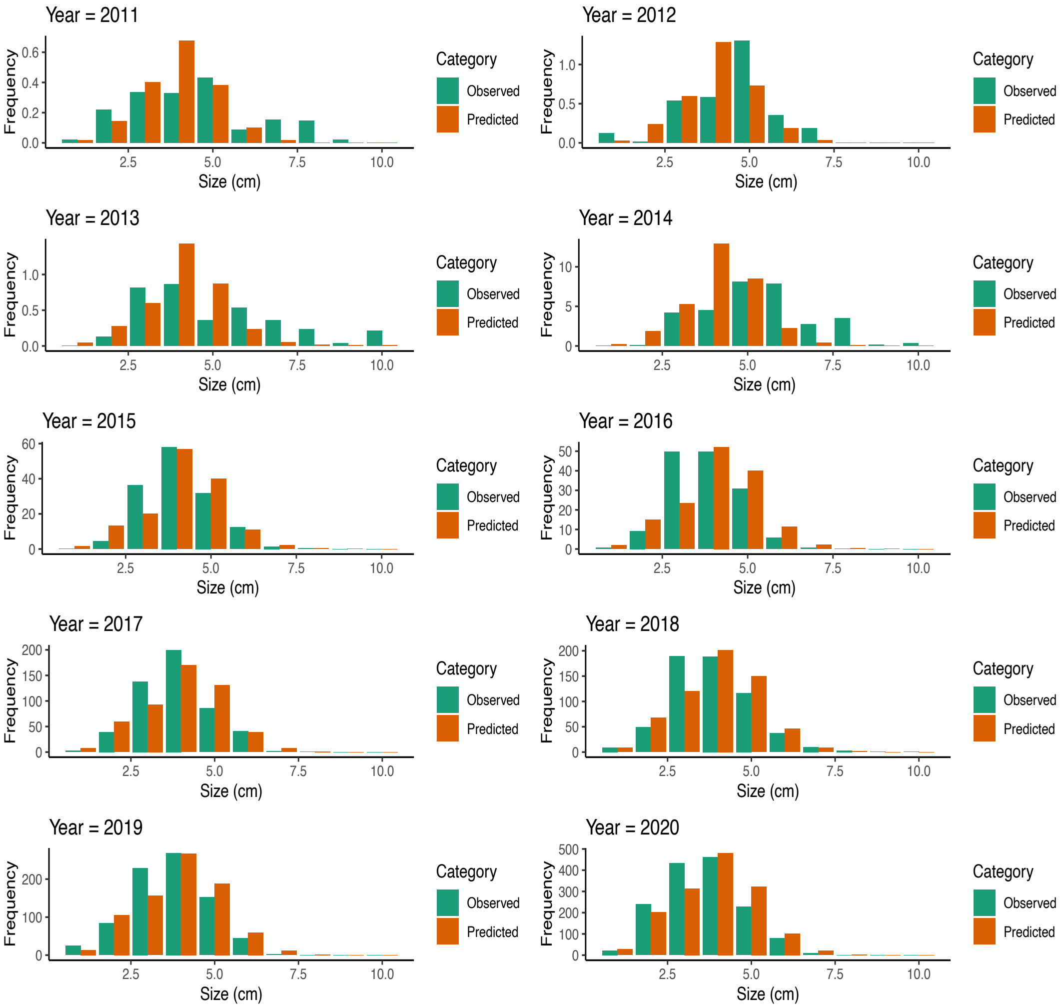

Figure 1.4. Observed (green) and model-predicted (orange) mean size frequency distributions across 10 sampling years.

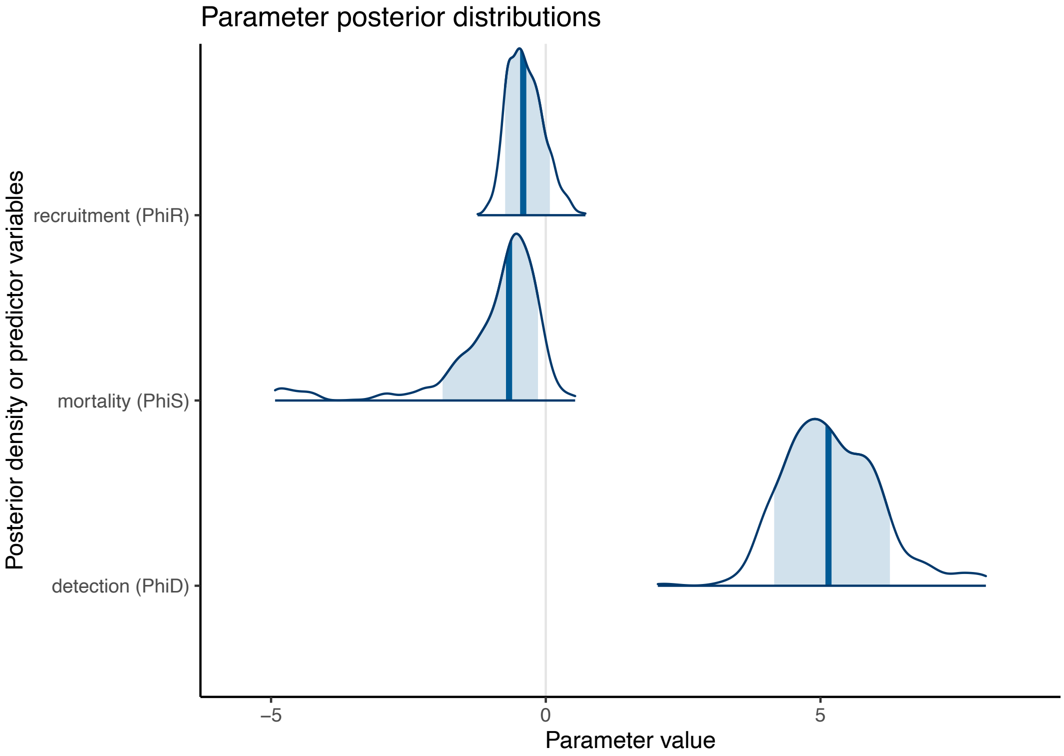

Figure 1.5. Posterior distributions for δ parameters estimated by a hierarchical Bayesian state space model fit to field survey data. Each ***δ*** value depicts the difference between log hazard rates for each of the three demographic processes of interest (recruitment, mortality, and detection).

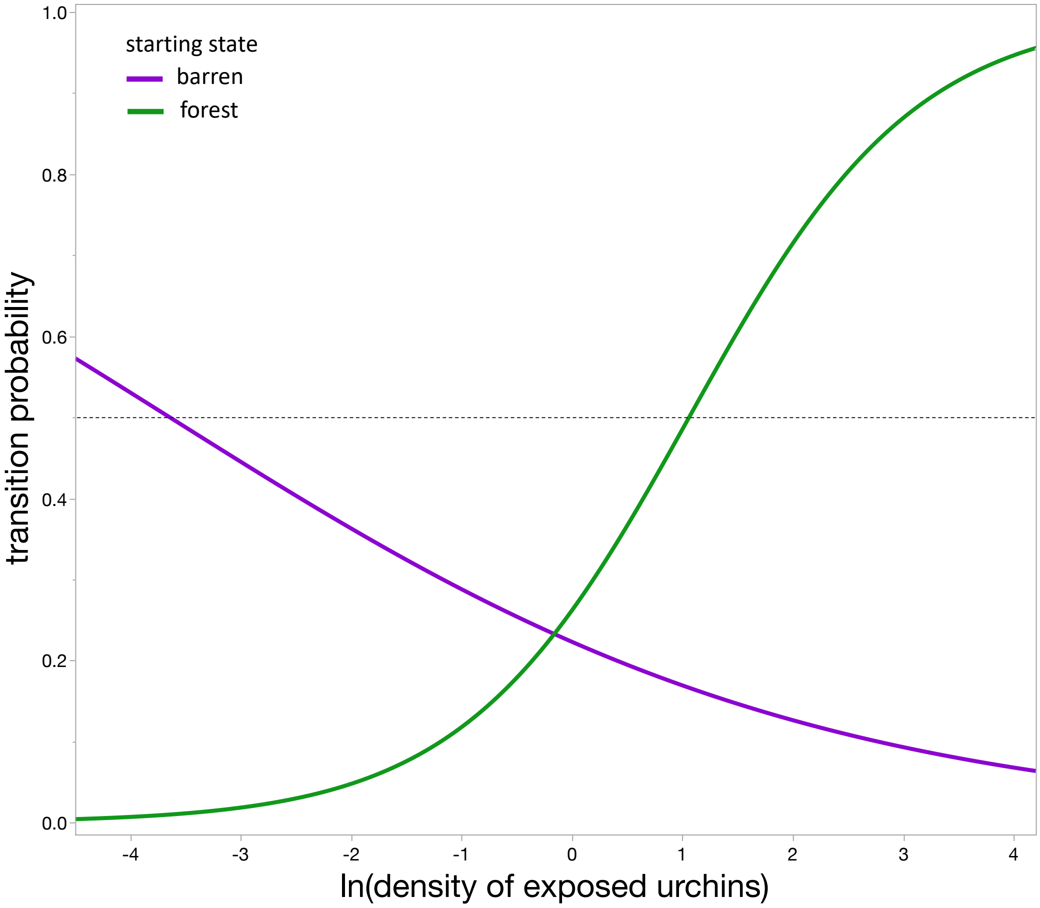

Figure 1.6. Transition probabilities depicting simulated logged odds for each starting state based on the log-transformed density of exposed sea urchins. The green line indicates the probability of a forest patch transitioning to a sea urchin barren in the following year, and the purple line indicates the probability of a barren becoming a forest in the following year. The dashed line indicates the 50% probability transition threshold.

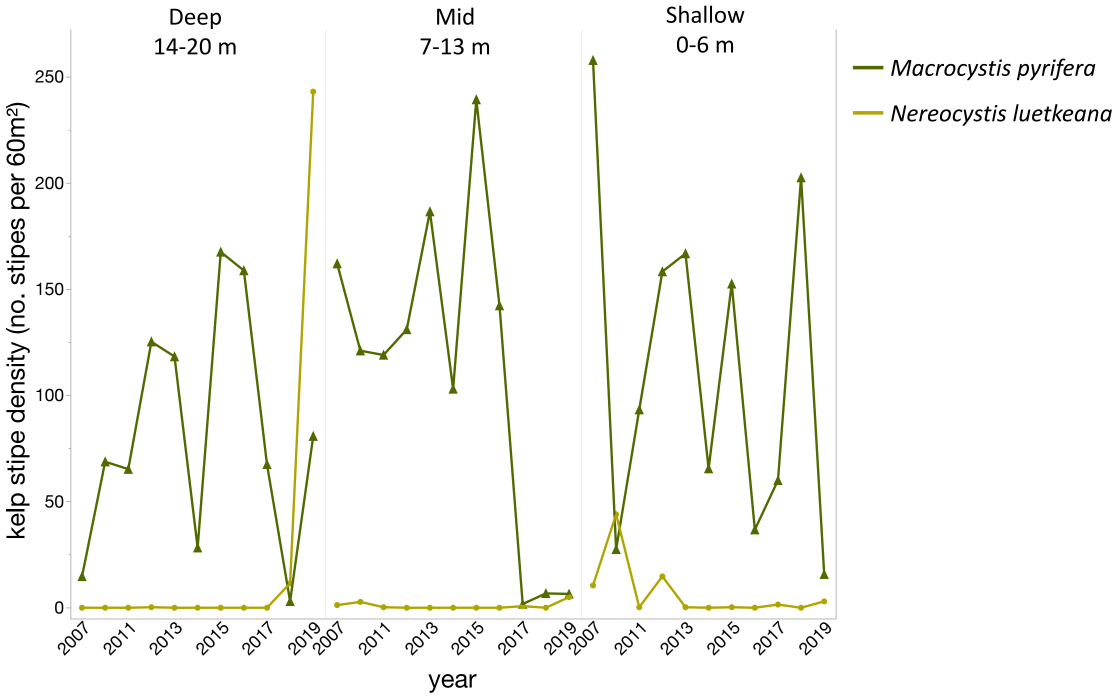

Figure 1.7. Density of giant kelp (*Macrocystis pyrifera*, green) and bull kelp (*Nereocystis luetkeana*, brown) across three depth zones at Pt. Piños, recorded by PISCO.

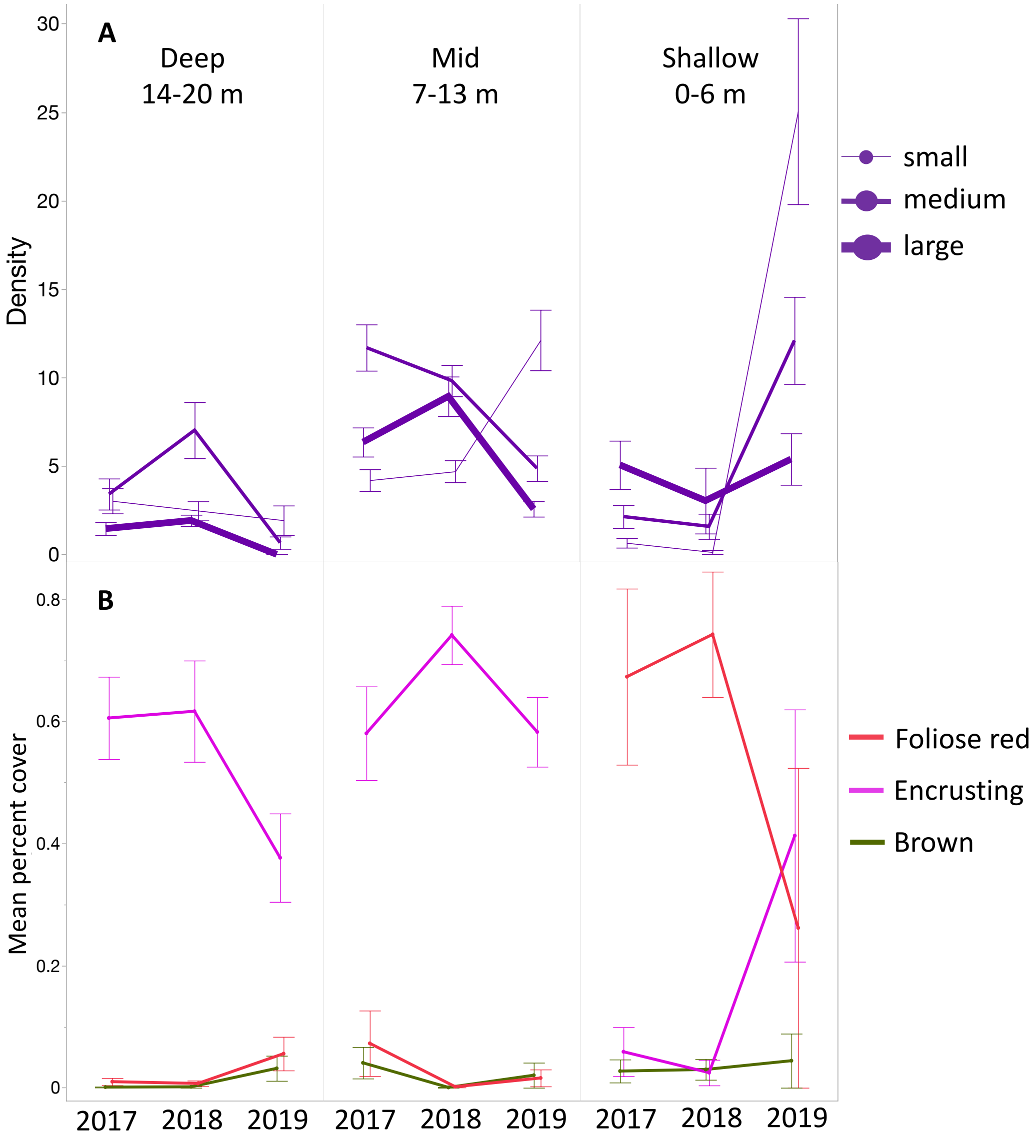

Figure 1.8. Urchin movement dynamics across three depth zones at survey sites located near Pt. Piños with 95% confidence intervals. Panel A depicts the mean density of small (< 30 mm), medium (30-38 mm), and large (> 38 mm) purple sea urchins. Panel B depicts the mean cover of foliose red algae (red), encrusting red and crustose coralline algae (pink), and brown algae (green).

CHAPTER TWO

BEHAVIORAL RESPONSES ACROSS A MOSAIC OF ECOSYSTEM STATES RESTRUCTURE A SEA OTTER-URCHIN TROPHIC CASCADE

Chapter 2: Behavioral responses across a mosaic of ecosystem states restructure a sea otter-urchin trophic cascade.

This chapter was originally published in a peer-reviewed journal. It is reproduced here in its entirety for this dissertation. The original citation is:

Smith JG, J Tomoleoni, M Staedler, S Lyon, J Fujii, T Tinker. 2021. Behavioral responses across a mosaic of ecosystem states restructure a sea otter-urchin trophic cascade. *Proceedings of the National Academy of Sciences* 118(11) DOI: 10.1073/pnas.2012493118.

Abstract

Consumer and predator foraging behavior can impart profound trait-mediated constraints on community regulation that scale-up to influence the structure and stability of ecosystems. Here I demonstrate how the behavioral response of an apex predator to changes in prey behavior and condition can dramatically alter the role and relative contribution of top-down forcing, depending on the spatial organization of ecosystem states. In 2014, a rapid and dramatic decline in the abundance of a meso-predator (*Pycnopodia helianthoides*) and primary producer (*Macrocystis pyrifera*) coincided with a fundamental change in purple sea urchin (*Strongylocentrotus purpuratus*) foraging behavior and condition, resulting in a spatial mosaic of kelp forests interspersed with patches of sea urchin barrens. I show that this mosaic of adjacent alternative ecosystem states led to an increase in the number of sea otters (*Enhydra lutris nereis*) specializing on urchin prey, a population-level increase in urchin consumption, and an increase in sea otter survivorship. I further show that the spatial distribution of sea otter foraging effort for urchin prey was not directly linked to high prey density, but rather was predicted by the distribution of energetically

profitable prey. Therefore, I infer that spatially explicit sea otter foraging enhances the resistance of remnant forests to overgrazing but does not directly contribute to the resilience (recovery) of forests. These results highlight the role of consumer and predator trait-mediated responses to resource mosaics that are common throughout natural ecosystems and enhance understanding of reciprocal feedbacks between top-down and bottom-up forcing on the regional stability of ecosystems.

Introduction

The role of trophic interactions in creating and maintaining the structure and functioning of natural communities remains a central issue in ecology. There are now many examples of the importance of top-down (i.e., predator-driven) and bottom-up (i.e., resource driven) processes that determine the structure and stability of communities (Estes et al. 1998, Schmitz 1998, Eldred 2019). Although odd or even numbers of trophic levels can define the relative importance of top-down versus bottom-up community regulation, the addition or loss of entire trophic levels is uncommon relative to changes in the strength of interactions between trophic levels. Such changes can result from environmental disturbances (e.g., severe storms, drought), or from shifts in the abundance or traits (e.g., foraging behavior, size structure) of populations (Pace et al. 1999, Hopcraft et al. 2005, Eldred 2019). Therefore, empirical evaluations of ecological processes that enhance or dampen the likelihood of shifts between top-down and bottom-up forcing are essential to understanding the potential for cascading effects that can underpin community structure, functioning, and stability (Estes et al. 1998, Christianou and Ebenman 2005, Nichols et al. 2015). Moreover, the processes that facilitate these alternations at ecologically relevant scales may only be revealed through opportunistic and significant disturbance events, especially in the form of herbivore outbreaks (Power et al. 1985, Hunter and Price 1992, Terborgh and Estes 2013).

While trophic cascades have traditionally focused on the direct role of apex predators on lower trophic level species, it is now clear that both predator foraging behavior and prey attributes (e.g., morphological, physiological, behavioral) can impart profound trait-mediated constraints on community regulation (Werner and Peacor 2003). For example, prey condition (e.g., age, health) may influence the strength of top-down control by altering predator foraging strategies and the capacity for predators to optimize prey acquisition (Hopcraft et al. 2005). Prey may also respond to the mere presence of predators by reducing their grazing activity, thereby enhancing the productivity of primary producers (Schmitz 1998). However, bottom-up trait-mediated interactions can also dictate community dynamics through changes in energy transfer between primary producers and higher trophic level consumers (Eldred 2019, Lynam et al. 2017). Therefore, understanding how shifts in prey condition and behavior resulting from changes in primary production reciprocally influence the foraging preferences of predators is essential to predicting when, where, and under what conditions communities vary in the relative influence of top-down or bottom-up processes, and how such interactions influence the state of communities and ecosystems.

In kelp forest ecosystems around the world, active sea urchin grazing has repeatedly transformed forested reefs to sea urchin ‘barrens’ that are void of macroalgae (Filbee-Dexter and Scheibling 2014). Fundamental changes in sea urchin foraging behavior (from passive foraging on drift algae, to active foraging on live kelp and other macroalgae) have been attributed to the loss of sea urchin predators (Estes and Palmisano 1974, Mann 1982, Cowen 1983, Scheibling 1996, Burt et al. 2018), or a reduction in food availability (Harrold and Reed 1985). In kelp forests along the northeastern Pacific, sea urchins reside in the refuge of cracks and crevices, primarily forage on drift algae, and invest energy into reproductive gonad production (Conor 1972). However, when sea urchins shift to an active foraging modality and emerge from the refuge of cracks and crevices, they have the capacity to drastically reduce kelp abundance, at which point gonad condition can decline due to reduced food availability (Conor 1972). While many studies have focused on the role of apex predators in sea urchin population control, less attention is given to how predators respond to variation in both the behavior (i.e., cryptic or exposed) and gonad condition (i.e., energetic profitability) of sea urchin prey resulting from changes in the abundance of macroalgae.

In this chapter, I examine how a shift in grazer behavior and energetic profitability led to a fundamental change in predator foraging behavior, thereby altering both the role and contribution of top-down forcing on the system. Along the central coast of California, USA, forests of giant kelp (*Macrocystis pyrifera*, hereafter ‘kelp’) had persisted for decades because purple sea urchins (*Strongylocentrotus purpuratus*, hereafter ‘urchins’) were controlled by the top predator, the southern sea otter (*Enhydra lutris nereis*, hereafter ‘sea otter’), and various meso-predators. However, in 2014 an unprecedented decline in kelp resulted from a series of climatic stressors similar to those observed farther north (Rogers-Bennett and Catton 2019). This decline in kelp production coincided with a widespread sea star wasting disease that decimated local populations of the urchin predator, *Pycnopodia helianthoides* (hereafter, ‘*Pycnopodia’*; Harvell et al. 2019). Both of these factors likely contributed to a shift in sea urchin foraging behavior from cryptic passive-grazing to active-grazing of live macroalgae, transforming a once expansive kelp forest to a patchy-mosaic landscape of remnant kelp forests interspersed with sea urchin barrens.

Here I examine how sea otters (predator) respond to changes in urchin (prey) behavior and condition (i.e., gonad index) to better understand how the contribution and role of predator-driven impacts (top-down forcing) and resource abundance (bottom-up forcing) drive the spatial dynamics of community structure. First, I test two hypotheses related to prey behavior and condition as a function of resource availability: (1) a shift in sea urchin behavior from passive to active foraging is associated with a decline in kelp availability, and (2) active sea urchin foraging behavior is associated with a decline in prey condition (gonad volume). I build on these hypotheses by exploring whether a top predator responds numerically and functionally to changes in sea urchin behavior and condition. Specifically, I test for a numerical response by exploring whether (3) a population-level increase in sea otter abundance is explained by an increase in the density of exposed prey (purple sea urchin). I then explore the functional response of sea otters by testing for (4) an increase in the dietary contribution of urchins. Finally, I test the hypothesis that (5) the spatial distribution of sea otter foraging effort for urchin prey is not directly linked to high prey density, but rather is predicted by the distribution of energetically profitable (gonad rich) prey.

Methods

To address my five hypotheses, I combine spatially explicit observations of numerical and functional responses of sea otters with changes in sea urchin behavior and condition to reveal the relative contribution of top-down and bottom-up control in the structure of kelp forest communities.

Study area

This study was conducted along the Monterey Peninsula, California (Appendix 2 Figure S1). The study region is approximately 300 ha and all marine mammals, algae, and invertebrates are protected from harvest (since 2007) within marine protected areas. The subtidal habitat covers a range of low to high topographic relief comprised of continuous igneous rock that extends from the shore to approximately 23 meters depth, where it becomes expansive sandy bottom strewn with small rocky outcrops. In the 19th century, the southern sea otter (*Enhydra lutris nereis*) was locally hunted to near extinction, but a recovering sea otter population repatriated the area in the early 1960s. The local sea otter population increased rapidly over the course of the following 30 years, reaching an apparent equilibrium by the late 1990s (Hatfield et al.

2019, Tinker et al. 2021). In 2014, the region shifted from a once expansive kelp forest to a mosaic of remnant forests interspersed with patches of sea urchin barrens that range in size from approximately 30-60 ha (Appendix 2 Figure S2). The formation of the mosaic was initiated in-part by the loss of a sea urchin meso-predator (*Pycnopodia helianthoides*) that coincided with an unprecedented marine heatwave (resulting in reduced kelp productivity), an outbreak of purple sea urchins (*Strongylocentrotus purpuratus*), and an increase in the abundance of sea otters well beyond levels recorded since the early 1960s.

Shifts in urchin behavior and condition

A total of 236 underwater surveys (hereafter, 'reference sites') were conducted from May-September in 2017 (n = 71), 2018 (n = 92), and 2019 (n = 73) to evaluate the spatial extent and temporal dynamics of kelp forests and urchin barren patches across the study area, and to determine urchin foraging behavior and condition. Survey sites were randomly selected on hard substratum between 5 and 20 meters of water (based on diving limitations). All surveys were conducted between the hours of 9am and 1pm. Each site was sampled using eight 5 meter-long transects with two randomly placed 1 m^2 quadrats (16 quadrats per site) fixed with a high-resolution camera. A single transect was assigned to each cardinal (N, E, S, W) and inter-cardinal (NE, NW, SE, SW) direction around the survey site (eight total transects). The positions of the quadrats along each transect were weighted using a randomly stratified design so that the quadrats were not biased towards either the center or outer edge of the sampling circle (Appendix 2 Figure S9). Therefore, each survey site represents an independent replicate sample.

The density of purple urchins was recorded *in situ* within each 1 m^2 quadrat by carefully searching for urchins, including those seeking refuge in cracks and crevices. Still photos were taken of each quadrat for estimates of urchin behavior. In the lab, photos were analyzed for the presence of exposed, actively foraging urchins. Urchins with a test diameter visible by 50% or more were quantified as *exposed*. I selected the 50% visibility threshold to account for actively foraging urchins at intermediate ranges of exposure, and because a subsample of urchins from a representative sample of 505 quadrats quantified at the 100% exposure level was not statistically different from the 50% level. The ratio between the number of urchins quantified as *exposed* and the total number of urchins quantified *in situ* represents a proportional estimate of urchins employing active foraging behavior. At each site, kelp density was quantified as the number of stipes in the entire survey area (per 78 m^2).

To test the hypothesis that a shift in urchin behavior from passive to active foraging is associated with a decline in kelp availability, I used a sequential model fitting approach to assess whether the mean proportion of exposed urchins was related to kelp density. First, I conducted a linear regression with the proportion of exposed urchins as a function of the log-transformed urchin density to control for the positive effect of urchin density on foraging behavior (i.e., urchins are more likely to be exposed at higher densities). I then regressed the residuals from that model against kelp stipe density to determine the relationship between the proportion of exposed urchins and kelp density. I took the sequential approach instead of using multiple regressions because it was clear from initial analyses that both relationships (proportion vs urchin density and proportion vs kelp density) were non-linear such that a simultaneous (and linear) approach would mask the actual relationships. Finally, to rule out refuge availability as a confounding effect of behavior, I regressed field estimates of rugosity collected using Risk's chain-and-tape method (Risk 1972) against site location, kelp density, and the proportion of exposed urchins, for which I found no effect (i.e., rugosity was relatively uniform across all sites).

Gonadal indices were constructed to comparatively evaluate the hypothesis that active urchin foraging behavior is associated with a decline in condition (i.e., gonad quality). At each of the survey sites above, a maximum of 32 urchins were randomly collected (two per quadrat from adjacent fixed positions) and brought to the lab for dissection ($n = 4408$). Urchins were placed on ice immediately after collection to slow digestive and reproductive processes. Soon after returning to the lab, urchins were injected with 2 – 12 mL of 10% neutral buffered formalin (depending on the size of urchin). Urchins were injected through the peristomial membrane and placed in a venting room for a minimum of 24 hours to allow fixation of tissues and gonads. After fixation, gonads were blotted dry and weighed to the nearest 0.01 g. To compare gonad mass across individuals, gonad indices were calculated as,

$$\text{Eq. 1} \quad Gonad\ Index = \frac{Gonad\ mass\ (g)}{Urchin\ mass\ (g)} * 100$$

Because the fixation process results in variable amounts of perivisceral fluid loss, an equation relating wet mass to test diameter was generated following the methods of Harrold and Reed (1985). A biomass equation was fitted to a previous sample of over 400 purple sea urchins. The r^2 for Eq. 2 was 0.97 and the partitioned sum of squares gave $P < 0.0001$.

$$\text{Eq. 2} \quad \textit{Urchin Mass (g)} = -22.45 + 12.23e^{0.0394 * \textit{Test Diameter (mm)}}$$

Sea otter numerical response to density of exposed prey

I examined support for a numerical response by testing for a temporal change in the mean annual sea otter abundance within the focal study area (Monterey) before (2000-2013) and after (2014-2018) the 2014 urchin outbreak. I used published annual abundance surveys for southern sea otters (Hatfield et al. 2019) to test for variation in abundance over time. Specifically, I evaluated support for a temporal change in sea otter abundance within the focal study area (Monterey) by comparing the mean annual abundances for two time periods (2000-2013, 2014-2018). In order to distinguish a numerical response due to increased survivorship (as opposed to a redistribution or migration), I compared sea otter abundance dynamics in the regions immediately to the north (Pigeon Pt. to Seaside, hereafter ‘Santa Cruz’) and south (Pt. Sur to San Simeon, hereafter ‘Big Sur’) of the study area (Appendix 2 Figure S10). Abundance dynamics were evaluated between regions and across time periods using a generalized mixed model, treating abundance estimates as a gamma-distributed response variable and with time period, region, and their interaction as fixed effects and segment (repeated annual survey area) as a random effect.

To assess whether the observed changes in abundance were explicable by biologically feasible changes in vital rates, and to generate estimates of regional trends that reduce the effects of observer error in the raw counts (Tinker and Hatfield 2016), I fit a Bayesian state space model to the time series of survey counts for pups and independent otters (see Appendix 2 *Methods*). The model structure followed previously described age-structured models of sea otter demographics (Gerber et al. 2004, Thometz et al. 2014) and allowed me to infer the underlying changes in survival rates that explained population trends over the study period.

Prevalence of urchins in sea otter diets

To test for a sea otter functional response to increases in prey abundance, I evaluated the dietary prevalence of urchins in sea otter diets before and after the 2014 increase in the abundance of exposed urchins. Long-term sea otter observational foraging data were collected from 2000-2018 to determine diet composition and the spatial extent and frequency of urchin captures. Observational foraging data were collected primarily from radio-tagged sea otters that were captured and monitored as part of long-term population studies (Gerber et al. 2004, Tinker et al. 2019). Observation sessions were conducted from shore to collect foraging data and were somewhat opportunistic and haphazard (i.e. based on availability of candidate animals foraging within visible distance of shore), although consistent efforts were made to obtain balanced sample sizes of foraging observations from each tagged study animal in each season (target = 200 observed dives per otter, per season), and to distribute observations for each animal throughout its home range, to avoid spatial biases. Once a feeding sea otter was selected for observation, the observing team used a high powered telescope, stop-watch, GPS, compass and laser range finders to record the following variables for each dive in the feeding bout (contiguous series of dives made by a single otter): geolocation (computed based on observer's location and direction/distance to otter), dive duration, inter-dive interval, dive outcome (success or no prey), prey type (to the lowest taxonomic level possible), prey size, number of prey items, prey handling time, and various other fields (Tinker et al. 2006, Tinker et al. 2008).

For purposes of analyzing individual sea otter diets, I restricted analysis to tagged sea otters for which we recorded a minimum of 10 bouts comprising 300 or more feeding dives over a 1-3 year period. I assembled information on diameter-biomass relationships and calorific densities for each of the most common prey types (Tinker et al. 2012). For the population as a whole, and for each tagged study animal, I then estimated diet composition on the basis of consumed wet edible biomass using a Monte Carlo, re-sampling algorithm designed to account for uncertainty and potential biases inherent in the raw data (Tinker et al. 2006, Tinker et al. 2008). Briefly, the analysis utilizes empirically derived relationships between recorded variables (prey handling time, prey size, number of items per dive) to correct for those dives with missed data points. The Monte Carlo analysis results in bias-corrected estimates of consumption rates (g/minute) for each prey type, and thus proportional contribution of each prey type to individual diets and to the population-level diet. I then used K-means cluster analysis to test for natural groupings in the diet composition data for individual sea otters, as previous analyses of sea otter diets on the central coast of California have found strong evidence for individual diet specialization (Tinker et al. 2006, Tinker et al. 2008, Tinker et al. 2012). I used the silhouette method combined with examination of elbow plots (Newsome et al. 2009) to determine the optimal number of clusters. To interpret cluster assignments, I identified the most common prey type for sea otters assigned to each cluster (previous analyses have found that a single prey type generally comprises 35% or more of the diets of individuals assigned to a given cluster; Kaufman and Rousseeuw 2009). Urchin specialists were identified as sea otters belonging to the cluster where urchins were the most common prey type.

The dietary prevalence of urchins was compared using the proportional contribution of urchins to individual sea otter diets across two time periods: 2000-2013, and 2014-2018 (one period before and one after the increase in the abundance of exposed urchins). I used beta regression to account for the proportional (0-1) response variable (Fujii et al. 2017, Cribari-Neto and Zeileis 2010), with time period and diet specialization (urchin specialists vs. all other diet types) as categorical predictor variables and allowing for an interaction between these main effects. I then used Fisher's exact test (Mehta and Patel 1983) to evaluate whether there were differences across time periods in the relative frequency of urchin specialists in the population.

Urchin condition and sea otter selectivity

To test the hypothesis that the spatial distribution of sea otter foraging effort for urchin prey is predicted by the distribution of energetically profitable sea urchins, I compared patterns in sea otter foraging behavior with spatially-explicit urchin gonadal indices. For this analysis, a sea otter foraging sub-bout is considered any number of dives made within a 10-meter diameter zone of the starting dive's geolocation. Sub-bouts where three or more consecutive feeding dives resulting in successful capture and consumption of urchins were identified as "non-random urchin foraging patches" (hereafter, 'focal patch').

Additional underwater surveys were conducted at each focal patch in 2017 (*n* = 22) and 2018 (*n* = 29) following the sampling protocol above to construct spatially explicit gonadal indices. These surveys were conducted within a two-week interval from the initial shore observation of sea otter foraging to link urchin gonad condition with sea otter foraging behavior in near-to-real time. Because a sub-bout includes dives made by an otter within a 10-meter diameter zone, an underwater radial sampling design allowed for seamless integration between the underwater surveys and the shore observations of sea otter foraging behavior (Appendix 2 Figure S9).

A stepwise conditional logistic regression was used to test whether sea otter focal patches are predicted by the spatial distribution of energetically profitable urchins. I examined population-level preferences using a binary categorical response variable (defined as 0 [non-focal patch] or 1 [focal patch]) for patch selection across 51 focal patches (where otters were foraging on urchins) and 163 randomly sampled reference sites (where otters were not foraging on urchins). The model terms included gonad index, urchin density, rugosity, temperature, depth, kelp density, and a categorical assignment of patch type (barren or kelp forest). Models were forward-selected and evaluated using Akaike's Information Criterion (AIC).

Results

Variation in the relative density of *Pycnopodia,* exposed purple sea urchins (*Strongylocentrotus purpuratus*), kelp (*Macrocystis pyrifera*), and sea otter (*Enhydra lutris nereis*) abundance were tightly coupled, with evidence of a synchronous increase in urchins and otters, and a sharp decline in kelp and *Pycnopodia,* beginning in 2014 (Figure 2.1). These dynamics initiated the transformation of a once expansive kelp forest to a patchy mosaic of remnant forests interspersed with sea urchin barrens (Appendix 2 Figure S1 and S2).

Shift in urchin behavior and condition

The log-transformed proportion of exposed urchins was positively associated with urchin density ($P < 0.0001$, $DF = 1$, $R^2 = 0.40$). After controlling for the positive effect of density on urchin exposure, variation in the residuals was further explained by a negative exponential relationship with kelp stipe density ($P < 0.0001$, $R^2 = 0.33$; Figure 2.2A). The proportion of exposed urchins was greatest in areas with no kelp, and crevice occupancy increased with increasing kelp density to the point where most individuals were concealed. The asymptotic projection of the model indicated that most urchins were concealed where the mean kelp stipe density was greater than one stipe per m^2.

A linear regression on mean urchin gonad index as a function of the proportion of exposed urchins suggests that gonad index declines with increasing urchin exposure (i.e., active foraging behavior). Gonad index was greatest in areas with high kelp density, where urchins were mainly occupying crevices and assumed to be passively-foraging on drift kelp, but gonad index declined linearly with increasing urchin exposure ($P < 0.0001$, $R^2 = 0.31$; Figure 2.2B).

Sea otter numerical response to density of exposed prey

I found strong support at the population level for a positive numerical response in sea otter abundance that coincided with the onset of an increase in the density of exposed purple urchins. Sea otter numbers around the Monterey Peninsula were relatively stable over the period 2000-2013 (Figure 2.1A; Tinker et al. 2021), a pattern that has been interpreted as being reflective of a population that had reached local carrying capacity (Thometz et al. 2016). However, results from the mixed model suggest that otter abundance increased significantly in the Monterey region (Seaside to Pt. Sur; $P < 0.001$) following the 2014 urchin outbreak, from 269 (SD ± 77) individuals to 432 (SD ± 123) individuals (mixed model $P < 0.001$). Increased abundance in Monterey during this latter period was associated with an initial spike in the ratio of pups to independent otters, followed by a rapid increase in the number of independent otters (Appendix 2 Figure S3). A demographic model fit to the survey data suggests a sharp uptick in survival of both pups and sub-adults after 2013 (Appendix 2 Figure S4), a pattern consistent with greater prey availability (Tinker et al. 2021). The decline in pup ratio after 2015 reflects the dramatic increase in the number of surviving subadults (i.e., pre-reproductive animals) and thus a decrease in the proportional representation of reproductive-age females.

To rule out the potentially confounding effects of an aggregative response (i.e., sea otter movement between regions) on sea otter abundance, I compared abundance dynamics in adjacent neighboring regions to the north and south of the Monterey study area. A contrast test on the region and time period interaction term revealed a less dramatic but significant increase in sea otter abundance in the region to the south (Big Sur, $P < 0.0001$, $F = 17$, $DenDF = 105$), and no significant change in abundance in Santa Cruz (although there appeared to be a declining trend after 2012). Considering both neighboring areas together there was almost no net change in abundance after versus before 2014, suggesting that sea otters were not simply re-distributing into the study area (Appendix 2 Figure S5).

Prevalence of urchins in sea otter diets

A k-means cluster analysis on the diet composition of sea otters revealed an urchin specialist cluster defined by a high composition of urchin prey (>40%). While there were no detectable changes in the mean proportion of urchins in the diets of individual sea otters that specialize on urchins, the overall proportion of consumed urchins significantly increased both at the population-level and in sea otters specializing on all other prey types (Appendix 2 Figure S6; $P < 0.0001$, DF = 7). At the population level, there was a significant increase in the frequency of sea otters specializing on urchin prey following the 2014 increase in the density of exposed sea urchins (Appendix 2 Figure S7; $P < 0.01$, DF = 4).

Urchin condition and sea otter selectivity

I found support for the hypothesis that the spatial distribution of sea otter foraging effort on urchin prey is best predicted by energetically profitable prey patches, indicating a strong level of spatially explicit foraging selectivity (Figure 2.3). Model selection for the full population-level logistic regression revealed gonad index, depth, and patch type (barren, forest) as the three most influential factors driving patch selection by sea otters ($R^2 = 0.47$, $P < 0.0001$, $AIC_c = 73$). The resulting logit-transformed probability coefficients indicated that gonad index was the only positive predictor of selection probability ($\beta_{GI} = 0.14$), while depth ($\beta_{Depth} = -0.32$) and the urchin barren patch type ($\beta_{Patch} = -0.66$) were negatively associated with the likelihood of focal patch choice. The threshold estimate of gonad index required to affect a positive selection of a sea otter focal patch was 12% per m^2 (Figure 2.4).

Discussion

This study is the first to demonstrate how the behavioral response of an apex predator to changes in prey behavior and condition can erode the strength of top-down forcing and enhance the role of bottom-up community regulation, depending on the spatial organization of diverse ecosystem states. In 2014, a rapid and dramatic decline in the abundance of a meso-predator (*Pycnopodia helianthoides*) and primary producer (*Macrocystis pyrifera*) coincided with a fundamental change in urchin foraging behavior and condition. This trait-mediated response of urchins to a decline in a primary resource (kelp) and an important benthic mesopredator (*Pycnopodi*a) initiated further declines in kelp abundance, resulting in a spatial mosaic of remnant kelp forests interspersed with patches of sea urchin barrens. The mosaic of forests and barrens provided us a unique opportunity to explore the numerical and functional responses of sea otters when given the choice to forage in adjacent alternative states of the ecosystem, and to evaluate the relative contribution and reciprocal dynamics of top-down or bottom-up control across the landscape. These findings add to a growing body of literature surrounding trait-mediated trophic cascades by revealing that predator and prey behavioral responses to spatially distributed mosaics of resources can underpin community functioning and regional stability.

Long-term monitoring observations around the study area on the central coast of California indicate a simultaneous decline in the giant kelp and an increase in the density of exposed purple sea urchins well beyond historic records (Hatfield et al. 2019). These changes coincided with the 2014 onset of a marine heatwave and decline in the sea urchin predator, *Pycnopodia*. Similarly, in 2014 an unprecedented decline in bull kelp (*Nereocystis luetkeana*) along the northern coast of California coincided with the marine heatwave event and the decline of *Pycnopodia* (Rogers-Bennet and Catton 2019, Harvell et al. 2019, McPherson et al. 2021). Despite a region-wide increase in the density of exposed sea urchins, I found that urchins in patches of forests were more cryptic and had higher gonadal indices than those in barrens. This pattern is consistent with other studies that identified the abundance of predators (Cowen 1983, Lafferty 2004, Hamilton and Caselle 2015, Selden et al. 2017) and food availability (Harrold and Reed 1985, Selden et al. 2017) as drivers of urchin behavior and nourishment.

While predator control of herbivores is widely cited as a fundamental mechanism driving community stability (Power et al. 1985, Pace et al. 1999, Terborgh and Estes 2010), far less is known about predator behavioral responses resulting from resource-driven variability in herbivore condition and behavior. The sea otter-sea urchin-kelp forest trophic cascade in the northern Pacific is perhaps the most well-known example of predator-driven recovery, where the reclamation of historical range by sea otters reduced the abundance of herbivorous sea urchins, thereby enhancing the recovery of kelp forests (Estes and Palmisano 1974). This study is the first documented example of where a sea urchin outbreak occurred in an area where sea otters were near their projected local carrying capacity (Raymond et al. 2019, Tinker et al. 2021), although a broadly similar urchin increase was reported in the 1980s prior to the start of sea otter census surveys (Watanabe and Harrold 1991). The unanticipated herbivore outbreak that began in 2014 helped reveal the consequences of predator and prey trait-mediated responses on community regulation. The results presented in this study suggest that because sea otters mostly ignore urchins in barrens, they are unlikely to directly contribute to the recovery of forests in barren areas. However, spatially explicit sea otter foraging for energetically profitable urchins in forested areas enhances patch resistance to overgrazing. This latter response has important implications for the recovery of barrens to the forested state because these remnant forests protected by sea otters are the spore sources to ultimately replenish and facilitate recovery of forests in barren areas.

Concurrent with the 2014 increase in the density of exposed urchins, sea otter abundance increased well beyond levels seen since the repatriation of otters to the Monterey region in the early 1960s (Tinker et al. 2021). Given the large area of each of the three survey regions (Big Sur, Monterey, Santa Cruz), population-level dynamics within each region are expected to be primarily driven by demographic processes rather than by immigration or emigration (Tinker et al. 2008, Raymond et al. 2019). Because sea otter birth rates do not vary over time (Tinker et al. 2008, Thometz et al. 2014), higher pup recruitment and higher survival of juvenile and sub-adult sea otters are the most likely demographic mechanisms for the observed numerical response, a scenario consistent with the sequential spikes in pup ratio and numbers of independents, and supported by the results of a state-space model fit to these data (see Appendix 2 *Methods*; Riedman et al. 1994). Sea otters have been reported to be food limited in the Monterey region prior to 2014 (Chinn et al. 2016, Thometz et al. 2016, Hatfield et al. 2019), with a net annual growth rate of just 1% per year from 2000-2014 (Figure 2.1A). The demographic analysis suggests that a 60% reduction in the instantaneous mortality rates of pups and subadults, and a smaller reduction in adult mortality, was sufficient to explain an increase in annual growth rate to approximately 15% per year between 2014 and 2016. This growth rate is consistent with trends reported for other areas of California where prey resources are more abundant (Tinker et al. 2017). However, urchins are not the only prey type to have increased after 2014; we also observed a sharp uptick in the intake of mussels at this time, which may also have contributed to increased otter survivorship (Appendix 2 Figure S8). Finally, concurrent studies of tagged otters during this time period showed no evidence of significant movements of animals between regions (Tinker et al. 2019), and combined with the lack of a net decline in numbers in neighboring regions this would argue against re-distribution (i.e., an aggregative response) as a plausible explanation for the increase in numbers around Monterey.

Asynchronous trends in sea otter dynamics between the southerly regions (Monterey, Big Sur) and the northern Santa Cruz region may be explained by differences in sea otter mortality factors. Santa Cruz is located within 8 km of Point Año Nuevo, which is a white shark hunting location (Klimley et al. 2001). Sea otter shark-bite mortality has increased substantially over the past 15 years (Tinker et al. 2016), but this increase has been less pronounced in Monterey than in regions to the north and the south (Nicholson et al. 2018, Hatfield et al. 2019). There has also been a reduction in protozoal encephalitis since the earlier 2000s, possibly driven in-part by drier years and reduced runoff input of pathogens from watersheds (Burgess et al. 2018). Thus, spatial differences in several mortality factors likely contribute to variation in observed sea otter trends across the surveyed regions (Miller et al. 2020).

At the community level, this study demonstrates strong functional responses in a top predator as a result of changes in prey behavior and condition. Many studies have quantified functional responses of predators (Holling 1966, Real 1979); however, fewer have examined the multiple pathways by which trait-mediated interactions can erode or amplify trophic cascades (Trussel et al. 2017, Witman et al. 2017). The analysis of long-term sea otter diet composition across the study area revealed a clear and rapid increase in population level specialization and selectivity in response to increases in prey density and variation in prey energetic profitability. In particular, as the density of exposed sea urchins increased, the prevalence of sea urchin prey in sea otter diets also increased, indicating a rapid population-level functional response. This response reflected in part an increase in the relative numbers of urchin specialists within the population, and in part an increase in the numbers of urchins consumed by non-urchin specialists. However, the spatial distribution of foraging effort for urchin prey was not directly linked to the density of exposed prey, but rather was predicted by the distribution of energetically profitable (gonad rich) prey. As such, both the role and contribution of top-down control of community structure was dramatically altered by these trait-mediated interactions.

The results presented in this study have far-reaching implications to the field of community ecology that enhance understanding of how the strengths of trait-mediated interactions can reorganize community regulation. While shifts in density-mediated interactions are a mechanism for trophic cascades (Rosenzweig 1973, Oksanen et al. 1981, Schmitz 1998), this study suggests that community dynamics also depend on the relative magnitude of behaviorally mediated interactions, as well as the temporal and spatial scales over which population responses occur. This study demonstrates that the barrens ecosystem state is maintained by bottom-up processes driven by intense grazing pressure as a result of a reduction in the availability of a primary producer and a shift in sea urchin behavior to active foraging. In contrast, abundant stands of macroalgae in kelp forest patches promote cryptic and passive-foraging behavior in sea urchins that translates to higher energetic profitability. In a patchy mosaic landscape of kelp forests interspersed with sea urchin barrens, spatially explicit top-down control by sea otter foraging on energetically profitable sea urchins may indirectly maintain the kelp forest state of the ecosystem by promoting stability of kelp forest patches within the mosaic.

This study highlights the underexplored role of consumer and predator foraging behavior on community functioning and stability. I suspect that the patterns here are not unique to kelp forest ecosystems, but are reflective of how predators and prey respond to mosaics of resources that are common throughout ecosystems around the world. Greater consideration of consumer and predator behavioral responses to resource mosaics may therefore present new ways of understanding how trait-mediated interactions and reciprocal feedbacks between top-down and bottom-up forcing affect community dynamics and ultimately underpin the regional stability of ecosystems.

Acknowledgements

I am indebted to C. de Jong, S. Garcia, L. Gaspar, T. Gorra, C. Jarman, C. Juliussen, M. Lovos, and dozens of other researchers and volunteers who contributed to fieldwork and laboratory assays. I deeply thank M. Carr, P. Raimondi, A. Salomon, J. Estes, and members of the Raimondi–Carr laboratory for their helpful comments and feedback. I also thank J. Kendall-Bar for illustrations of the study animals. This research was supported by the NSF Grant OCE-1538582, the NSF Graduate Research Internship Program, the Future Leaders in Coastal Science Award at the University of California Santa Cruz, and the United State Geological Survey. Any use of trade, firm, or product names is for descriptive purposes only and does not imply endorsement by the US government. Operational and logistical support for sea otter studies were provided by the US Geological Survey, Monterey Bay Aquarium, and California Department of Fish and Wildlife.

Figures

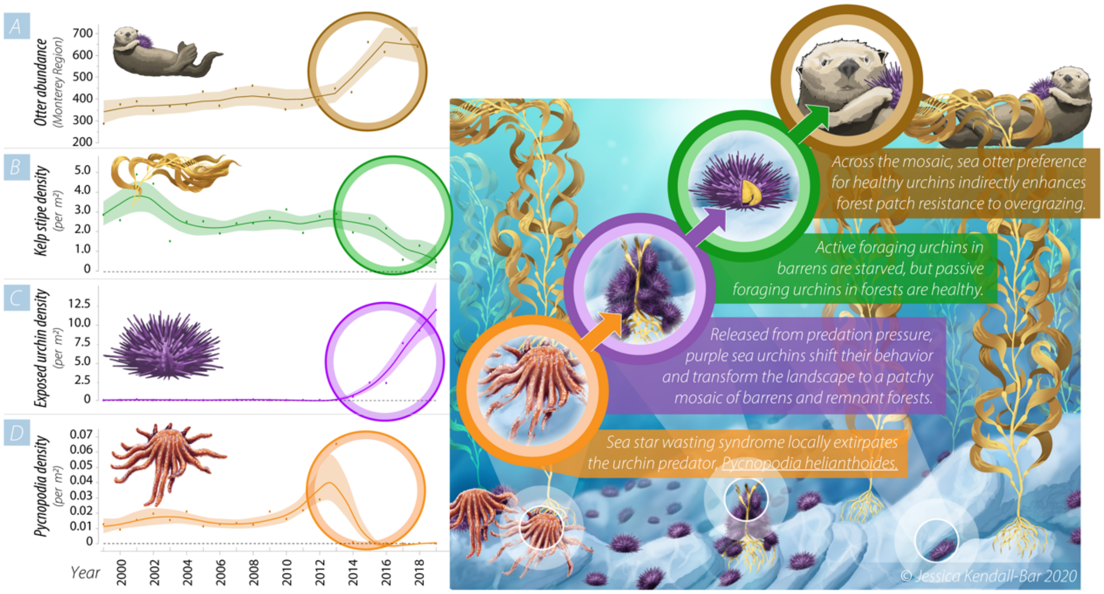

Across the mosaic, sea otter preference for healthy urchins indirectly enhances forest patch resistance to overgrazing.

Active foraging urchins in barrens are starved, but passive foraging urchins in forests are healthy.

Released from predation pressure, purple sea urchins shift their behavior and transform the landscape to a patchy mosaic of barrens and remnant forests.

Sea star wasting syndrome locally extirpates the urchin predator, *Pycnopodia helianthoides.*

Figure 2.1. Temporal dynamics of sea otters, kelp, sea urchins, and *Pycnopodia*. (left) Annual changes in sea otter abundance in the Monterey study region (*A*) and relative density of kelp stipes (*B*), exposed sea urchins (*C*), and *Pycnopodia* (*D*). The trend line in *A* is corrected for observer error and fit with a Bayesian state-space model (Appendix 2) to the time series of raw survey counts of independent sea otters. *B-D* represent annual mean observed densities fit with a cubic spline (λ = 0.05). Each shaded region across *A-D* represents the 95% credible interval. (*Right*) A conceptual illustration of the dynamics that initiated the formation of the mosaic of remnant kelp forests interspersed with sea urchin barrens. See Appendix 2 for expanded time series analyses. I used published data for *A* from the US Geological Survey (available at https://doi.org/10.3133/ds1097) and subtidal data for B–D from the Partnership for Interdisciplinary Studies of Coastal Oceans subtidal surveys (available at https://doi.org/10.6085/AA/PISCO_SUBTIDAL.151.2).

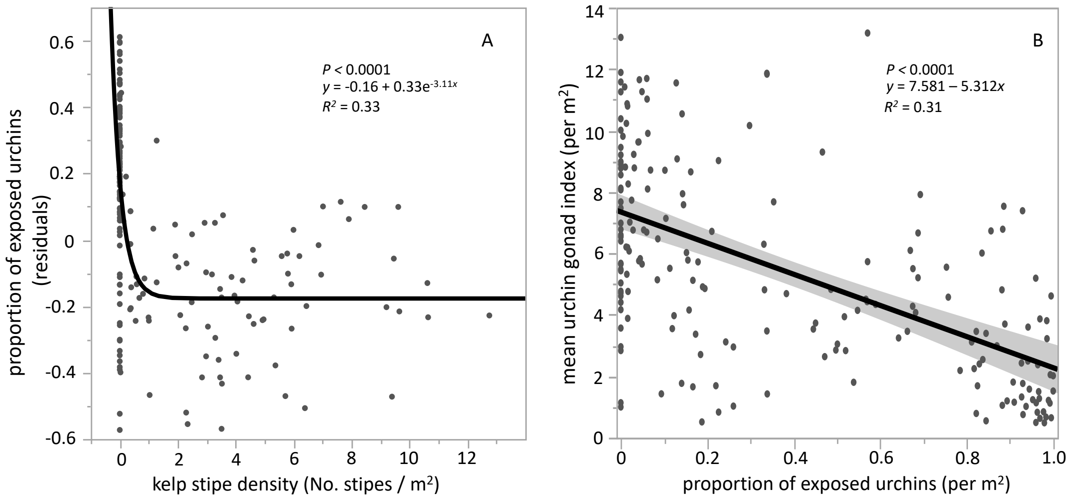

Figure 2.2. Sea urchin foraging behavior (exposed, concealed) and condition (gonad index) as a function of kelp density. (*A*) Residuals from a linear regression on the log-transformed proportion of exposed urchins (to account for urchin density) fit with a negative exponential decay function with kelp stipe density. (*B*) The relationship between mean gonad index (per square meter) and the proportion of exposed sea urchins. The gray shaded area represents the 95% confidence of fit.

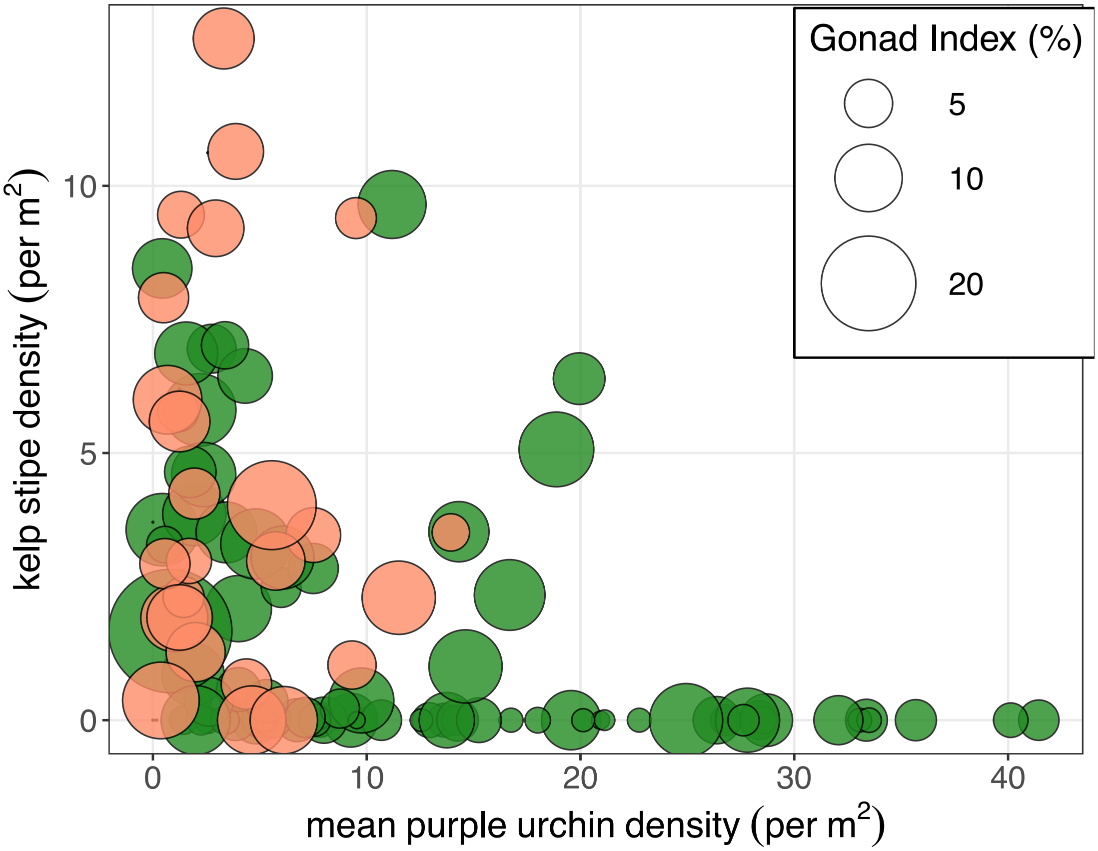

Figure 2.3. Gonad index of sea urchins in focal patches where sea otters were actively foraging on sea urchins (orange circles) and references sites (green circles) where otters were not foraging on sea urchins. Also depicted is the density of urchins and kelp at each patch.

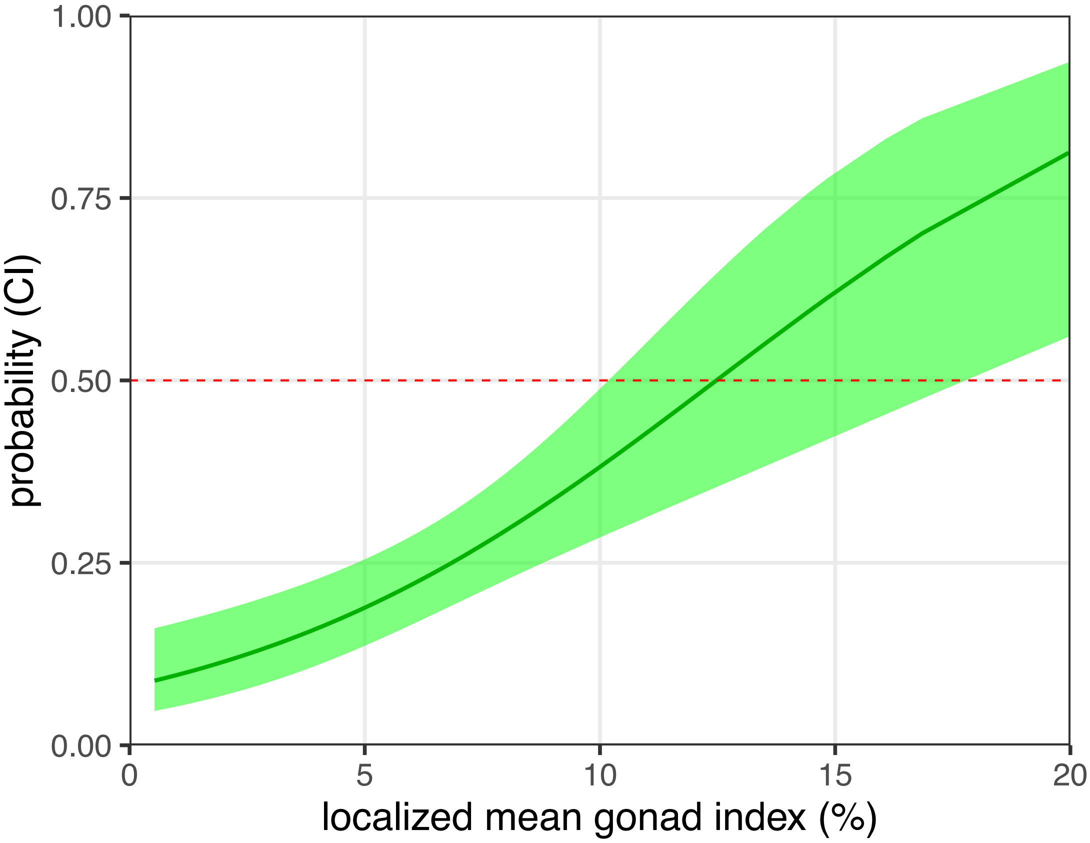

Figure 2.4. Probability of sea otter focal patch selection by urchin gonad index. Model predicted foraging preference (with 95% CIs shaded in green) using the localized mean urchin gonad index (mean gonad index/square meter). Probability values (green line) are translated from the logit-transformed logged odds. The red dashed line indicates the 50% transition threshold.

CHAPTER THREE

SPATIAL COHESION IN COMMUNITY STRUCTURE DESTABLIZATION FOLLOWING THE OUTBREAK OF A DOMINANT REEF GRAZER

Chapter 3: Spatial cohesion in community structure destabilization following the outbreak of a dominant reef grazer.

Abstract

Ecological communities can be stable over multiple generations, or rapidly shift into structurally and functionally different configurations. In kelp forest ecosystems, overgrazing by sea urchins can abruptly shift forests into alternative states that are void of macroalgae and primarily dominated by actively grazing sea urchins. Beginning in 2013, a series of biotic and environmental perturbations initiated a sea urchin outbreak the central coast of California that resulted in a patchy mosaic of remnant forests interspersed with sea urchin barrens. In this study, I used a 14-year subtidal monitoring dataset of invertebrates, algae, and fishes to explore changes in community structure associated with the loss of forests at 23 sampling sites in central California (Carmel Bay and southern Monterey Bay) and to determine: (1) whether the spatial mosaic of barrens and forests resulted in a shift in community structure relative to the years preceding the formation of the mosaic, (2) how the spatial dynamics of community structure trajectory vary across the mosaic (and which species align well with observed dynamics), and (3) whether community structure dynamics were spatially cohesive among sample sites and regions (Monterey and Carmel Bay). I found that beginning in 2013, many sites across the study region departed from a common multivariate ("forested") state, which had persisted for the previous six-years, and drifted into a new multivariate configuration ("urchin barrens"). Although sites trended toward a common reconfiguration, community

trajectories were highly variable, and sites exhibited regional cohesion in their trajectories (Carmel, Monterey Bay). These results suggest that outbreaks of grazers associated with punctuated environmental (e.g., marine heatwaves) and biotic (loss of predators, sea urchin outbreaks) perturbations can drive apparently stable kelp forest communities to alternative potentially stable states.

Introduction

Ecological communities can be stable over multiple generations, or rapidly shift into structurally and functionally different configurations (Holling 1973, Connell and Sousa 1983, Tilman 1996, Scheffer and Carpenter 2003). One of the most pressing challenges in the field of ecology is to identify and understand the mechanisms that facilitate community stability (i.e., resistance and resilience), that drive alternations between states, or that enhance the ability for a system to return from a perturbation (Hooper et al. 2005, Dudgeon et al. 2010). However, the capacity to predict when, where, and under what conditions ecosystems are subject to change requires understanding how and why the structural integrity (i.e., species composition, diversity, interactions, trophic structure) of ecological communities varies across time and space (Estes et al. 1998, Beisner et al. 2003, Dudgeon et al. 2010, Staver et al. 2011).

State shifts in both terrestrial and marine environments can markedly alter the structure and functioning of ecosystems and can impart rapid changes to ecosystem services (Mann 1982, Dayton et al. 1998, Scheffer and Carpenter 2003, Worm et al.

2006). However, theoretical and empirical advances on the processes (i.e., environmental or biotic) that initiate state shifts are often constrained to opportunistic events in space and time that expose the boundaries at which shifts occur (Tilman 1996, Loreau and De Mazancourt 2013). Events that erode (either punctuated or continuous) persistent community configurations may elucidate causal mechanisms that facilitate state shifts, including factors that reduce resilience, and the ecosystem-wide consequences that follow destabilization (Scheffer et al. 2001, Schröder et al. 2005, Loreau and De Mazancourt 2013). Like many terrestrial and aquatic ecosystems, herbivore outbreaks in coastal marine ecosystems can drive population and community dynamics that scale-up to influence ecosystem stability and resilience.

In coral reef, rocky intertidal, and kelp forest ecosystems around the world, outbreaks in populations of herbivorous sea urchins have led to abrupt state transitions from macroalgae dominated communities to alternative sea urchin 'barrens' (Pearse 2006, Baskett and Salomon 2010, Filbee-Dexter and Scheibling 2014). Sea urchin barrens are characterized by an abundance of exposed actively foraging sea urchins, are primarily dominated by encrusting red and coralline algae, and are devoid of macroalgae (Filbee-Dexter and Scheibling 2014). Barrens are generally highly unproductive and can persist for several years because of the ability of sea urchins to survive with minimal resources and consume newly recruited algae (Dean et al. 1984, Graham 2004, Smith and Garcia 2021). As such, sea urchin barrens are often considered a stable alternative ecosystem state because of intrinsic feedback mechanisms (e.g., positive sea urchin settlement reinforcement) that promote the persistence of that particular community configuration (Baskett and Salomon 2010, Filbee-Dexter and Scheibling 2014, Ling et al. 2015).

Although numerous studies have explored changes in algae, invertebrate, and fish assemblages independently between kelp forest and sea urchin barren habitats (e.g., Steneck et el. 2002, Pinna et al. 2020, Gabara et al. 2021), fewer have tracked entire community and ecosystem-level responses through the formation, expansion, and persistence of sea urchin barrens over time. Such long-term studies are important for disentangling the spatial and temporal scales over which state shifts occur, including identifying the relative contributions of individual species responsible for community destabilization, and estimating the magnitude to which changes in community structure permeate entire trophic networks (Ebeling et al. 1985, Reed et al. 2006, Duffy et al. 2007).

In 2014, kelp forests along the west coast of North America experienced a rapid and pronounced shift from highly expansive forests to large swaths of unproductive sea urchin barrens (Beas-Luna et al. 2020, McPherson et al. 2021, Smith et al. 2021). Of particular concern is whether (and how) this widespread kelp deforestation resulted in a marked shift in the predominant source of primary production (from macroalgae to plankton) and decreased food web complexity. Recent studies have identified considerable geographic variation in species responses and key functional groups to a marine heatwave and decline in kelp, most notably in Mexico and northern California kelp forests, where the extent of forest loss was region-wide

(Beas-Luna et al. 2020, McPherson 2021). In contrast to these region-wide shifts in system state, forest loss in central California was spatially heterogenous resulting in mosaics of forests and barrens (Smith et al. 2021). These mosaics allow for concurrent comparison of community structure in forest and barrens subjected to similar past and present environmental (oceanographic, geomorphological) conditions.

Here I examine the community-wide consequences of kelp deforestation along the central coast of California, where outbreaks of purple sea urchin (*Strongylocentrotus purpuratus*) grazers shifted a once expansive kelp forest to a mosaic landscape of sea urchin barrens interspersed with remnant patches of kelp (Smith et al. 2021). The purpose of this study was to explore changes in community structure associated with the loss of forests as a result of overgrazing by sea urchins to determine: (1) whether the spatial mosaic of barrens and forests resulted in a shift in community structure relative to the years preceding the formation of the mosaic, (2) how the spatial dynamics of community structure trajectory vary across the mosaic (and which species align well with observed dynamics), and (3) whether community structure dynamics were spatially cohesive among sample sites and regions (Monterey and Carmel Bay).

Methods

Using the mosaic landscape of sea urchin barrens interspersed with remnant patches of kelp forests and a 14-year kelp forest community monitoring dataset that spanned the 2014 shift in forest states, I evaluated the consequences of sea urchin grazing and forest loss on community structure within and across sites of diverging ecosystem states.

Study area

This study was conducted along the northern coast of the Monterey Peninsula and along the coast of Carmel Bay, California, USA (Figure 3.1). All marine algae and invertebrates are protected from harvest (full protection established in 2007) within marine protected areas. As an eastern boundary system, coastal upwelling is the predominant driver of productivity on both sides of the Monterey Peninsula. However, considerable heterogeneity in mixing results from variation in bathymetric features and wind forcing on either side of the peninsula (Lowe 2020). As such, the algal assemblage along the north side of the Monterey Peninsula is comparatively lower in richness than inside Carmel Bay (Malone et al. 2021). In 2014, outbreaks of purple sea urchins shifted forests on both the north side of the Monterey Peninsula (Smith et al. 2021) and Carmel Bay to a patchy mosaic of remnant kelp forests interspersed with sea urchin barrens that are void of macroalgae.

Kelp forest monitoring surveys

To characterize the spatial and temporal patterns of community structure, I used long-term subtidal monitoring data collected by the Partnership for Interdisciplinary Studies of Coastal Oceans (PISCO, Malone et al. 2021). Although PISCO sampling began in 1999, I elected to use 2007-2020 as my study period to standardize relatively equal sampling effort among sites, years, and before and after the sea urchin outbreak (i.e., fewer sites were sampled prior to 2007).

The PISCO subtidal sampling design and protocols are described in detail in Malone et al. 2021. Briefly, I subset a total of 23 PISCO sites surveyed annually between mid-June to mid-October from 2007-2020 in Carmel Bay and southern Monterey Bay, California. Annual surveys at each site consist of visual surveys by SCUBA divers of the density and percent cover of conspicuous benthic algae, invertebrates, and benthic and water column-dwelling fishes. Density and percent cover estimates of conspicuous benthic algae and invertebrates are recorded along six replicate 2 m x 30 m transects stratified across three bottom depths (5 m, 12.5 m 20 m; two transects per depth level). Densities of mobile and individually distinguishable sessile invertebrates and stipitate brown algae (*Laminariales spp*.) are identified to the species-level. Sessile macro-invertebrates and other macroalgae difficult to distinguish individually (e.g., colonial sponges, tunicates, foliose algae) are quantified using uniform point-contact ('UPC') estimates of percent cover every meter along each 30 m long transect (30 total points per transect). Colonial invertebrates (e.g., sponges, tunicates, bryozoans) surveyed along these UPC transects are identified to the Order level and macroalgae are grouped into morphologically distinct categories (e.g., fleshy red algae, articulated coralline, etc.; see Appendix 3 Table T1 for taxonomic list). Fish densities (number per reef area) are estimated along 12 replicate transects stratified across bottom depths (5 m, 10 m, 15 m, 20 m; three transects per depth level) and identified to the species-level. Each fish transect consists of paired 2 m x 2 m x 30 m bottom and water column transects.

Data processing

To analyze multivariate community-level dynamics, I normalized (converted to z-scores) counts of each species or percent cover across sites and years. This approach yields a metric that has identical units (standard deviations) and a similar value range for all species regardless of original units (e.g., counts or percent cover) and therefore allows for broad integration of survey methods to compare community-level dynamics among sites and years. This approach also results in species all having the same potential impact in the multivariate analyses, regardless of whether they are rare or common. While biomass is typically used as a common currency across taxa (Duffy et al. 2017), it is not suitable for my multivariate analyses because of the large number of kelp forest taxa that are difficult to accurately assign biomass estimates. Therefore, I elected to use a z-score normalization of the datasets to compare broad structural changes in the community.

Community analyses

To evaluate whether the spatial mosaic of barrens and forests resulted in a regional shift in community structure (invertebrates, algae, fishes) relative to the years preceding the formation of the mosaic, I calculated a Euclidean based distance matrix (hereafter, ‘base matrix’) for all sites across all years (PRIMER 7, Bray and Curtis

1957, Clarke and Gorley 2015). Using this base matrix, I plotted the centroids for each year (representative of all sites) using non-metric multidimensional scaling (NMDS) to examine community structure trajectory across the entire sample region through time and in multivariate space. I then used a cluster analysis to identify significant groupings (using Euclidean distance) among the centroids. After analyzing the results of the cluster analysis performed on the centroids, it was clear that all annual centroids (representative of all combined sites) grouped into two distinct clusters, except for the years 2013 and 2014 (hereafter, 'transition' years). I used these distinct clusters to define two critical time periods, one before (2007-2012) and one after (2015-2020) the transition years.

I examined how community structure trajectory varied across the mosaic (within individual sampling sites and across the region) by exploring regional and site-level community dynamics. First, I plotted the annual mean NMDS positions (representative of all sites) from the base Euclidean distance matrix for each year, combined with vectors of the species that correlated well with observed community dynamics. The advantage of using the mean NMDS points for each year (as opposed to centroids) is that the resulting NMDS can be plotted on the same scale as species vectors (i.e., correlates), allowing for broad comparison of species that correlate well with observed community dynamics. I then plotted confidence ellipses that demarcate the two critical time periods ('before' and 'after' identified from the cluster analysis) using 90 percent coverage of the overall mean distribution of NMDS nodes for each of the two periods (hereafter, 'domains of attraction').

To examine site-level variation in community structure trajectory relative to the two domains of attraction, I decomposed the NMDS plot of annual means to display the temporal trajectory of the ecological community at each site. I then superimposed the two ellipses on the site-level plots to examine whether sites persisted in the 'before' domain, moved into the 'after' domain, or drifted in multivariate space. While the confidence ellipses do not change in extent (i.e., coverage), it is important to note that their orientation can change when resampling for the site-level analyses. However, this does not negate the regional-level confidence ellipses superimposed on the site-level trajectories because the same ordination was used for both when generating the site-level plots.

One of the key findings from the multivariate community analyses was that the community trajectory rapidly departed from the six-year cluster of points, beginning in 2013. To determine which taxa were most influential in the departure of the community after 2013, I used a permutational analysis of variance (PERMANOVA) with site and year as factors and then calculated similarity percentages (SIMPER) for each species. I then explored the trajectory of the decomposed site-level NMDS plots to determine whether any individual sites returned to a pre-perturbed (i.e., prior to 2013) configuration.

Finally, I evaluated the spatial cohesion of community structure trajectory among sites and sample regions (Monterey, Carmel Bay). First, I decomposed the centroid plot to visualize community structure trajectory between regions (Carmel, Monterey). I then conducted a second stage analysis on the base matrix for all sites across all years to compare cohesion of community structure trajectory. Using the resulting matrix from the second stage analysis, I tested for differences in the trajectories of community structure between the two regions (Carmel, Monterey) and among sites using an analysis of similarities (ANOSIM) test. To visualize the final correlations of community structure trajectory among sites and regions, I conducted a cluster analysis on the same second stage matrix with each site assigned a unique geographic identifier based on its location (northernmost site = 1, southernmost site = 23). I then used SIMPER to determine the species that typified each region in the before (2007-2012) and after (2015-2020) periods.

Results

I found that beginning in 2013, many sites across the study region departed from a common multivariate ("forested") state, which had persisted for the previous six-years, and drifted into a new multivariate configuration ("urchin barrens"). This departure in community structure from the prior configuration coincided with the sea star wasting event, the marine heatwave, sea urchin outbreak, and decline in kelp (Figure 3.2). These dynamics show a rapid destabilization in the regional structure of the community towards a new (at least within the last 14 years) configuration in multivariate space.

Temporal dynamics of kelp and sea urchins

Beginning in 2014, the density of purple sea urchins increased markedly at all 23 sampling locations (Figure 3.2 and Appendix 3 Figure S1). While the density of sea urchins increased over 200-fold (from 0.05 ± 0.06 to 9.93 ± 10.95 urchins per m^2) overall, the magnitude of increase substantially varied substantially among sites (Appendix 3 Figure S1). Following the sea urchin outbreak, mean kelp stipe density across sites declined by 50 percent, from 131 stipes per 60 m^2 (± 69.04 for the 2007-2012 period) to 66.11 stipes per 60 m^2 (± 84.44 for the 2014-2020 period). However, there was a substantial degree of annual and site-level variation in kelp density (Appendix 3 Figure S1), with some sites maintaining kelp densities comparable to historic trends, despite the large increase in sea urchin densities at those sites. The percent cover of crustose coralline algae and encrusting red algae also substantially increased (Figure 3.2).

Structural changes to the kelp forest community

Across the entire region, the multivariate analyses (NMDS) revealed two periods of tight clustering in the mean annual similarity indices of community structure (Figure 3.3). The years preceding 2013 (2007-2012) were tightly clustered in multidimensional space, but with some expected annual variation. The structure of ecological communities is expected to vary over time (Clarke et al. 2006), therefore the observed variation that occurred prior to 2013 is not surprising. However, in 2013 the community rapidly shifted to a new structural configuration as indicated by the relocation in multidimensional space. It is noteworthy that the 2013 community state (structure) was well separated in multidimensional space from the clusters both before (2007-2012) and afterwards (2015-2020). In 2014, community structure was still outside both before and after clusters of years but had move markedly closer to the after cluster. Post 2014 community structure attained a new configuration (ANOSIM $P < 0.01$). This is evidenced by the significant clustering of years 2015-2020 (the after period in Figure 3.3), which likely reflect a new basin of attraction.

Species vector overlays revealed that 13 species aligned well (Figure 3.4) with observed community dynamics (correlated by 40 percent or more). The structure of the entire kelp forest community prior to 2013 was typified by three species of sea stars (*Orthasterias koehleri, Pycnopodia helianthoides, Pisaster giganteus*), one demersal fish species (*Hexagrammus decagrammus*), one juvenile fish complex (olive-yellowtail-black rockfish), giant kelp (*Macrocystis pyrifera*), and one metric of benthic substrate (shell debris). Following the destabilization that began in 2013, the structure of the community became highly influenced by purple (*Strongylocentrotus purpuratus*) and red (*Mesocentrotus franciscanus*) sea urchins, and by encrusting red and crustose coralline algae. One species of sea star (*Henricia leviscula*), one anemone (*Cribrinopsis albopuncta*), and one colonial tube worm (*Dodecaceria fewkesi*) also aligned well with the post-2013 community configuration.

Site level community structure

Community structure was highly variable at the site level. An ANOSIM using the base (site x year) similarity matrix showed a significant degree of separation by site ($P < 0.01$). Although some locations maintained remnant patches of kelp forests over the duration of this study, community structure at all sites shifted away from the pre-2013 configuration (defined as an ellipse covering 90 percent of the mean centroids; Figure 3.5). A total of 20 sites passed through the post-2013 basin of attraction, and 13 of those remained inside the post-2013 ellipse (Figure 3.5). Three highly variable sites did not enter the post-2013 basin of attraction (Cannery UC, Hopkins DC, Bluefish DC), and none of the survey sites returned to the pre-2013 basin of attraction.

Spatial cohesion in community structure trajectory

The decomposed NMDS plot of community structure trajectory showed that the Monterey region clearly departed from a six-year cluster beginning in 2013, while the Carmel Bay region experienced a pronounced shift that began in 2014 (Figure 3.6). The second stage analysis on the Euclidean based distance matrix further revealed that that the trajectory of community structure was asynchronous and significantly different between the Carmel and Monterey regions (ANOSIM $P < 0.01$). However, community structure trajectories among sampling sites within regions were not significantly different, and the cluster analysis further revealed that there was little cohesion along a north-south gradient (Figure 3.7).

The SIMPER analysis on the cumulative top 70 percent most influential species revealed that prior to 2013, separation between the Monterey and Carmel regions was defined by several species of brown algae (*Laminariales spp.*), foliose red algae, demersal fishes, and sea stars (Appendix 3 Table T2). These groups continued to characterize separation between sampling regions in the post-2014 period, but their relative influence changed as a result of the sea star wasting syndrome, the sea urchin outbreak, and decline in kelp. In particular, there were several species of understory stipitates (*Pterygophora californica, Laminaria setchellii, Eisenia arborea*) and other brown algae (*Costaria costata, Pleurophycus gardneri*) characteristic of Carmel in the before-period (2007-2012) that were infrequently found in Monterey. Surprisingly, none of these brown algae were identified in the SIMPER as species that influenced separation between the sampling regions in the after-period (2015-2020; Appendix 3 Table T3).

Discussion

This study reveals how ecological communities can rapidly depart from long-standing configurations in response to abrupt biotic and physical perturbations. I detected a pronounced community destabilization event triggered by the loss of *Pycnopodia*, the episodic marine heatwave event, and loss of kelp forests that shifted the community into a new multivariate configuration. These results add to a growing body of literature surrounding structural and functional changes in coastal marine communities (e.g., Poloczanska et al. 2013, Bruno et al. 2014, Beas-Luna et al. 2020, Smale 2020) by revealing how multiple stressors (such as an episodic marine heatwave, a reduction in the abundance of a foundation species, and loss of a key mesopredator) can initiate shifts in ecosystem states.

The regional cohesion of community structure trajectory between the Monterey and Carmel regions highlights the scale at which mechanisms that facilitate state shifts are ecologically meaningful. Prior to 2013, Monterey and Carmel were separated by differences in community structure, likely from greater upwelling and primary productivity in Carmel Bay that results in a more diverse algal assemblage (Lowe et al. 2020, Malone et al. 2021). However, both regions were formerly expansive forests that shifted into mosaics following coast-wide physical and biotic perturbations that occurred over a much larger spatial scale. Although community structure trajectories within sites across these regional mosaics were highly variable through time, sites experienced regional cohesion. The onset of community destabilization was nearly synchronous in time between regions, and both regions rapidly departed from long-standing configurations into new multivariate configurations. Moreover, both regions are now much more dominated by species reflective of the alternative barrens state (i.e., void of macroalgae and dominated by encrusting red and coralline algae) of the system.

Because the kelp forest community in this study persisted in separate clusters in NMDS space for multiple years, it implies that there are at least two separate, potentially stable, community configurations. The two centroids of tightly clustered points identified in the NMDS ordinations suggests at least two separate states of attraction, with 2013 being a sudden departure from the proceeding long-standing configuration of the community. Therefore, it seems reasonable to characterize these clusters as basins of attraction (Scheffer and Carpenter 2003). Importantly, community structure transitions between basins of attraction were associated with pronounced physical and biotic perturbations.

Several physical and biotic perturbations likely contributed to the community destabilization that initiated in 2013. First, several species of sea stars were strongly informative of the community state in 2013. This is likely a reflection of increased counts of sea stars due to a behavioral shift, where sea stars emerged from cryptic rock crevices in response to the onset of wasting syndrome (Harvell et al. 2019), thereby increasing their detection probability by divers. Second, the sea star catastrophe in 2013 was soon followed by an extreme marine heatwave event that coincided with a reduction in the abundance of kelp, and simultaneous increase in the abundance of purple sea urchins (McPherson et al. 2021, Smith et al. 2021). Of these, the loss of the sea urchin predator persisted through the study period, while the environmental conditions associated with the marine heatwave returned to pre-perturbation conditions around the year 2016. Collectively, the timing of these perturbations with the trajectory of the whole forest community towards a new basin of attraction provides support for the existence of alternative states in this system.

Alternative stable states are defined by a single set of environmental conditions that can support more than one successional end-state or equilibrium point (Lewontin 1969, May 1977, Beisner et al. 2003, Dudgeon 2010). In contrast, phase-shifts are driven by persistent changes in the environment that shift community structure, but with only one state of attraction under a given set of environmental conditions (Dudgeon et al. 2010). In this study, the sudden destabilization of the community was associated synchronously with an episodic marine heatwave, but the environmental conditions have since returned to a pre-2014 state. Therefore, the marine heatwave, reduction in the abundance of a foundation species (kelp), and loss of a key mesopredator (*Pycnopodia*) constitute a suit of sudden perturbations that likely tipped the system into an alternative sea urchin 'barrens' state. This is evidenced by the failure of community structure to return to the pre-2013 basin of attraction, despite the dissipation of the marine heatwave and return of pre-2014 environmental conditions. However, continued long-term sampling is needed is determine whether the seemingly alternative state of the system persists in this new configuration beyond multiple generations of a key interactor (the purple sea urchin), another requirement for alternative stable states of the community (Connell and Sousa 1983).

Although the marine heatwave, loss of *Pycnopodia*, and decline in abundance of a foundation species were identified as the primary perturbations that shifted this system into an alternative state, several other biotic and environmental mechanisms can facilitate state shifts. Forward state shifts (from forests to sea urchin barrens) can result from spatially explicit and episodic sea urchin recruitment (Lafferty and Kushner 2010, Basket and Salomon 2010, Ling et al. 2015, Okamoto et al. 2020), reduction in the availability of drift (Harrold and Reed 1985), declines in predator abundance (Cowen 1983, Hamilton and Caselle 2015), or from severe storms that result in the rapid loss of kelp biomass (Ebeling 1985). Reverse state shifts (from barrens to forests) can result from sea urchin disease epidemics (Carpenter 1988, Feehan and Scheibling 2014) and from severe storms that physically dislodge exposed sea urchins (Ebeling et al. 1985). Changes in predator diversity or abundance are also widely cited as mechanisms that facilitate transition dynamics.

Sea urchin predators can serve as highly influential mechanisms of stability (Steneck 2002, Hamilton and Caselle 2015) and are frequently cited for their role in reversing sea urchin barrens to a kelp-dominated state (Estes and Palmisano 1974, McClanahan 2000, Hamilton and Caselle 2015). The sunflower sea star (*Pycnopodia helianthoides*) was identified in this study as a highly influential species of the 2013 (and prior) community configuration, despite their relatively low numbers (Malone et al. 2021). Other studies have identified *Pycnopodia* as an important predator for maintaining stability (Byrnes et al. 2006, Burt et al. 2019,), and therefore the collapse of this predator is consistent with the timing of observed community structure destabilization. Moreover, Smith et al. (2021) demonstrated the role of sea otters in maintaining remnant patches of kelp forests in this study system. Therefore, it is likely that the combined role of *Pycnopodia* (either as a direct predator of sea urchins, or as a non-consumptive shelter-response agent) and sea otters provide an important mechanism of stability through complementary predatory control of sea urchins (Burt et al. 2019).

This study provides support for the hypothesis that kelp forest community structure can persist in a stable state for decades, but that episodic physical (e.g., marine heatwaves) and biotic (loss of predators, sea urchin outbreaks) perturbations can rapidly shift the community to alternative stable states. The failure of community structure to return to the pre-perturbed state after the episodic marine heatwave provides support for the existence of multiple stable states and suggests that departures from long-term community configurations may be difficult to reverse (Knowlton 2004). Finally, this study highlights that the spatial extent to which changes in community structure are manifest as alternative stable states should be carefully interpreted with respect to the scales over which environmental and biotic perturbations occur.

Figures

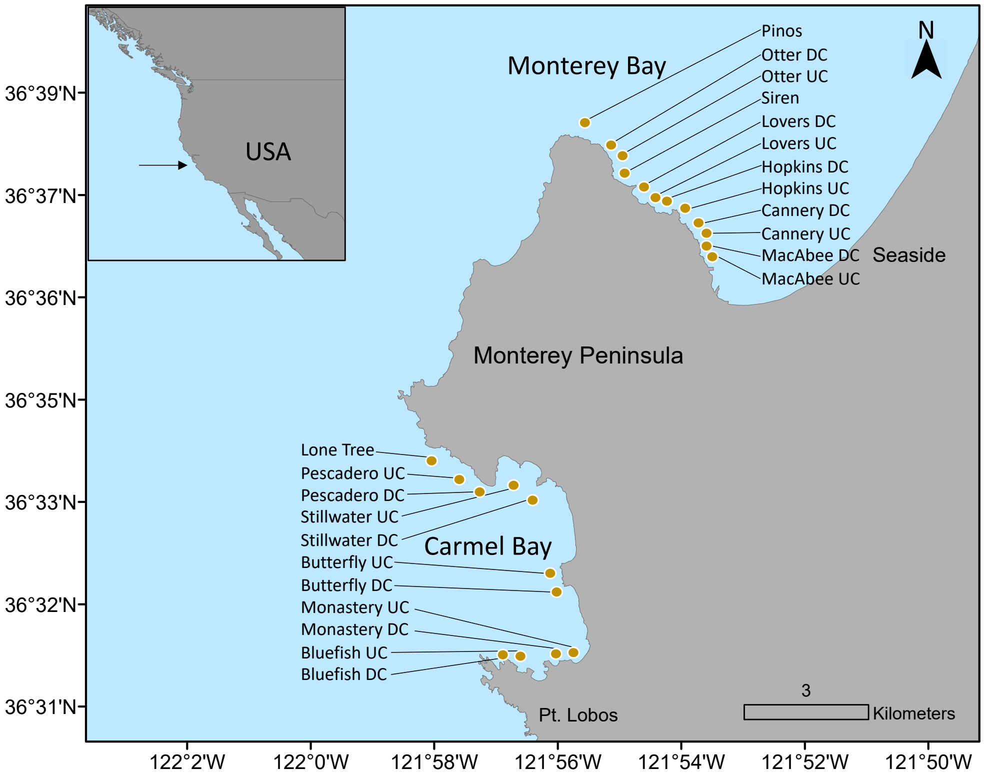

Figure 3.1. Study area in Carmel and Monterey Bay, California, USA. Points depict the approximate locations of 23 long-term benthic subtidal survey sites monitored by the Partnership for Interdisciplinary Studies of Coastal Oceans (Malone et al. 2021).

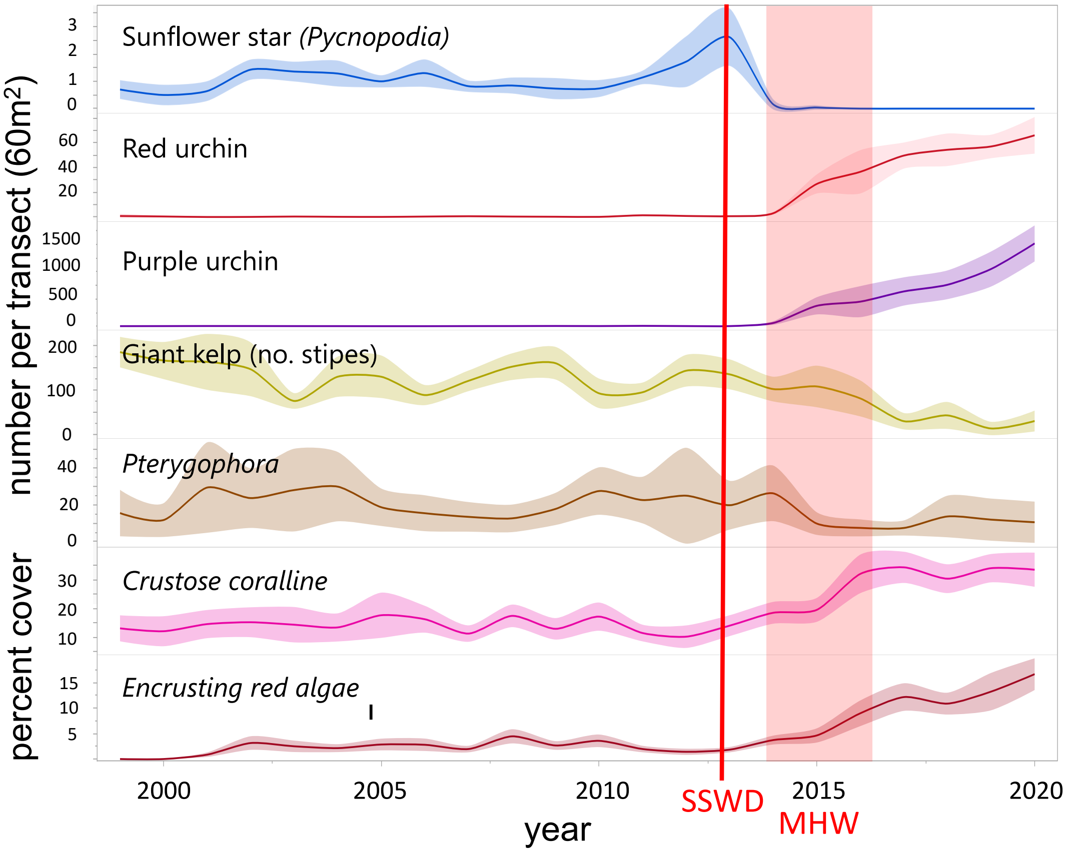

Figure 3.2. Temporal changes in the sunflower sea star (*Pycnopodia helianthoides*), red sea urchins (*Mesocentrotus franciscanus*), purple sea urchins (*Strongylocentrotus purpuratus*), giant kelp (*Macrocystis pyrifera*), the stipitate brown alga *Pterygophora californica*, crustose coralline algae, and encrusting red algae across all 23 sampling sites from 2007-2020. Each line depicts the annual mean density or percent cover (crustose coralline and encrusting red algae) across all sites fit with a cubic spline ($\lambda = 0.05$), and each shaded region depicts the 95% confidence interval. The onset of the 2013 sea star wasting syndrome is depicted as a red vertical bar, and the red band indicates the approximate duration of the episodic marine heatwave event.

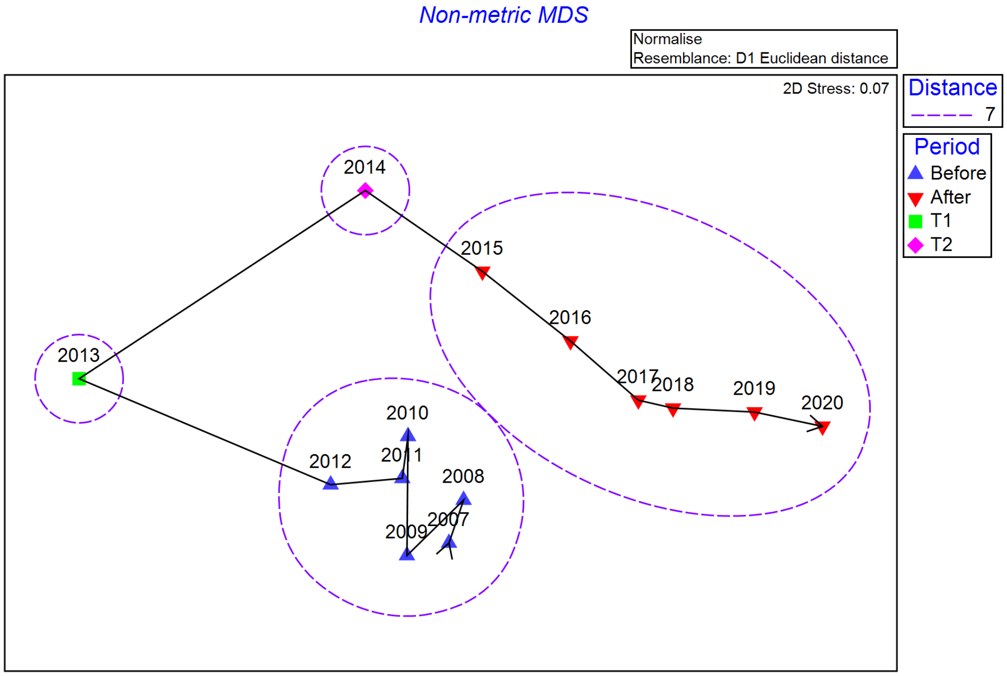

Figure 3.3. NMDS 2D centroid plot depicting community structure trajectory across all 23 sample locations. Each point represents the centroid for a given year and the purple dashed line denotes significant clusters (based on Euclidean distance).

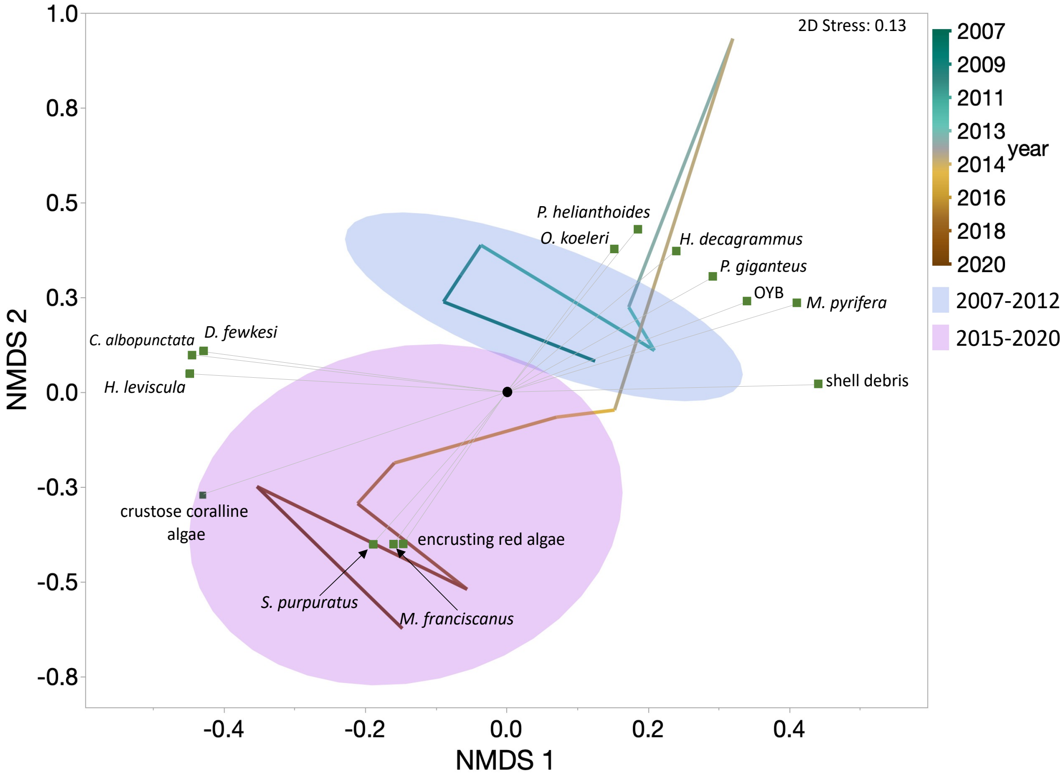

Figure 3.4. NMDS 2D plot of community structure trajectory in Carmel Bay and southern Monterey Bay, California. The gradient line represents the annual mean NMDS position across all sampling locations over the 14-year study period. The blue ellipse denotes the 90% confidence region of community structure for all sites combined during the 2007-2012 period, and the purple ellipse denotes the 90% confidence region of community structure for all sites combined during the 2015-2020 period. Finally, species that aligned well (greater than 40% correlation) with community structure trajectory are depicted as vectors ending in green squares, where the length of each vector corresponds to the strength of influence with community structure in multidimensional space. Species are described in the text and Appendix 3 Table T1.

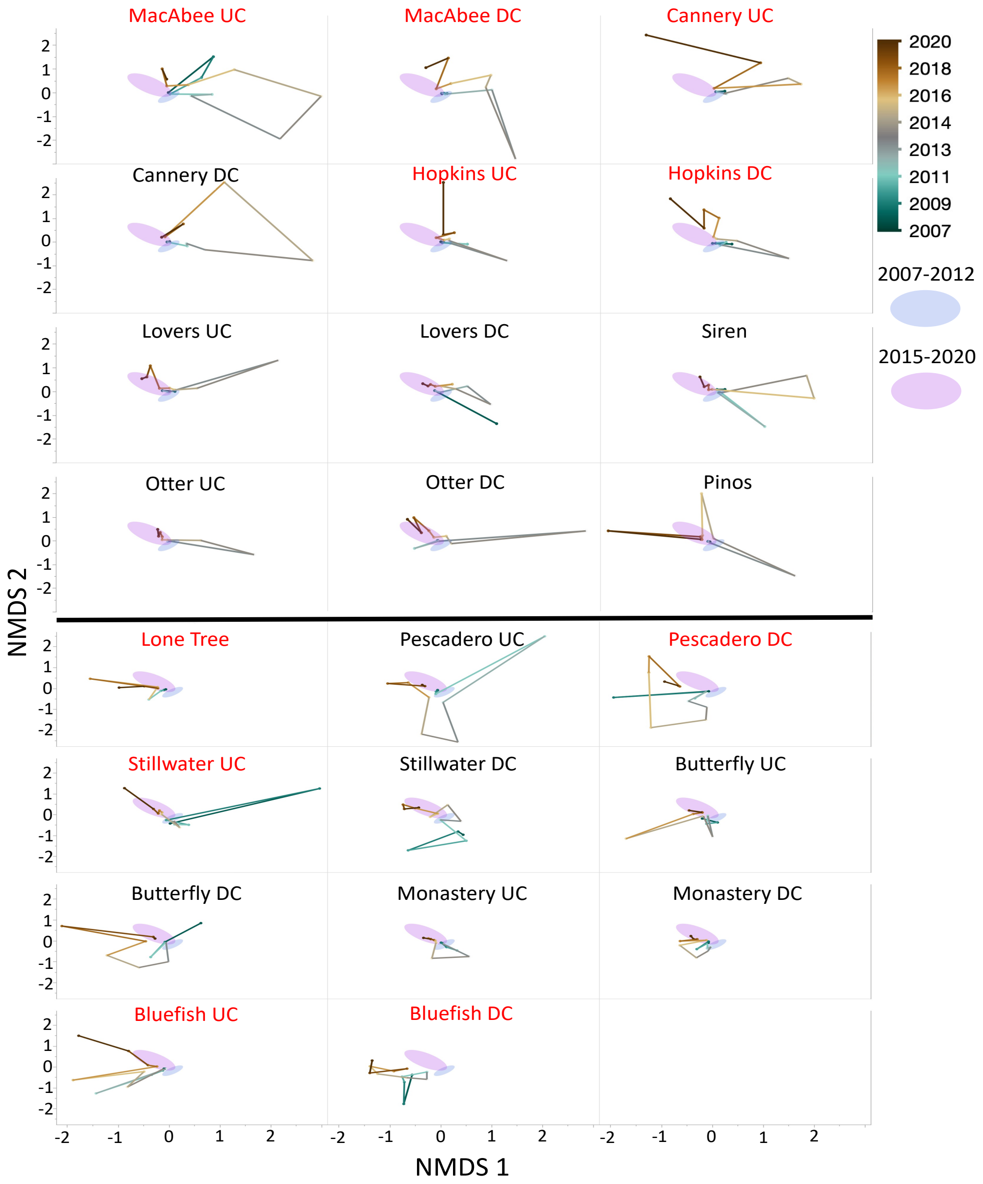

Figure 3.5. NMDS 2D plots for 23 sampling sites in Carmel Bay and southern Monterey Bay, California. Panels are ordered along a latitudinal gradient (MacAbee DC = northernmost site, Bluefish DC = southernmost site) and the horizontal black bar demarcates separation between the Monterey (panels above bar) and Carmel (panels below bar) sampling sites. The gradient line within each panel represents the trajectory of the community over the 14-year study period. The blue ellipse denotes the 90% confidence region of community structure for all sites combined during the 2007-12 period, and the purple ellipse denotes the 90% confidence region of community structure for all sites combined during the 2015-2020 period. Finally, panels labeled in red indicate sites that did not persist in the 2015-2020 basin of attraction (purple ellipse) and continued to drift in multivariate space.

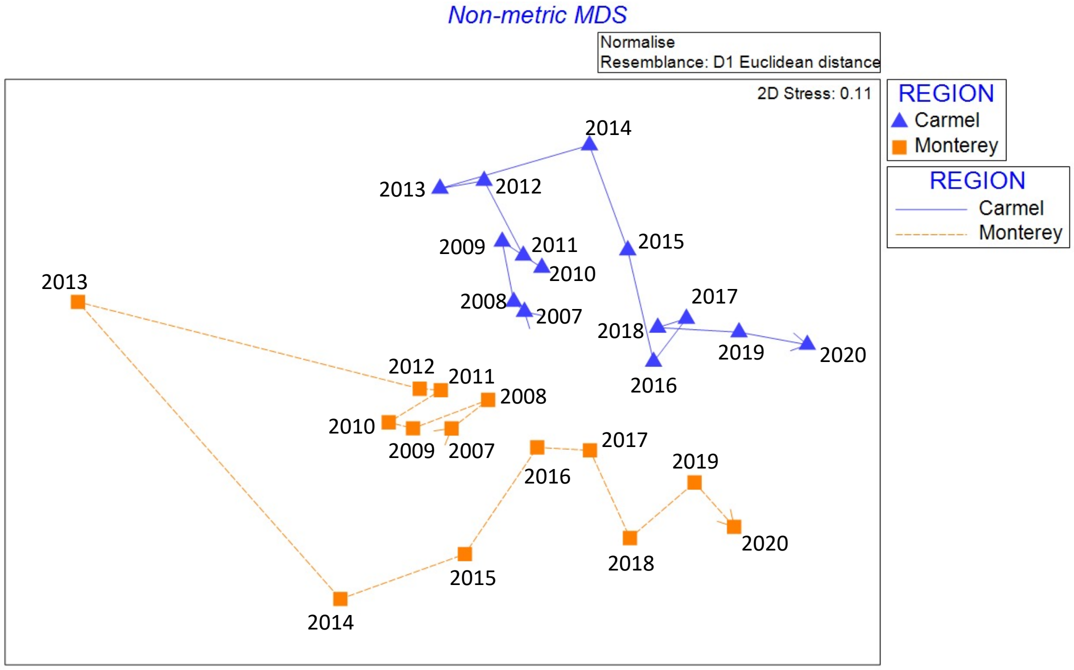

Figure 3.6. NMDS 2D plot depicting community structure trajectory between sample regions (Monterey, Carmel Bay). Each point represents the centroid for a given year and the purple dashed line denotes significant clusters (based on Euclidean distance).

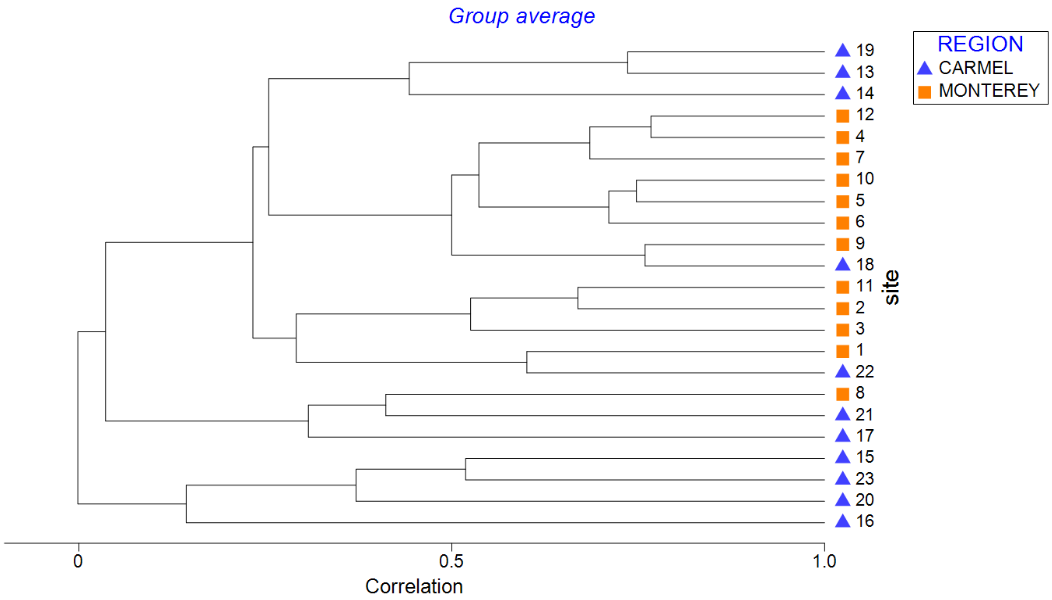

Figure 3.7. Dendrogram from a cluster analysis on the second stage Euclidean distance matrix depicting the spatial cohesion of community structure cross 23 sampling locations in Carmel (blue triangles) and Monterey (orange squares). Each link in the dendrogram corresponds to a single site numbered along a north-south gradient (northernmost site = 1, southernmost site = 23).

Synthesis

This research advances understanding of how patch dynamics, grazer and predator foraging behavior, and community regulation underpin reciprocal feedbacks between top-down (i.e., predator-driven) and bottom-up (i.e., resource-driven) forcing on the regional stability of ecosystems. The resource mosaic of sea urchin barrens interspersed with remnant patches of kelp forest that initiated just three years prior to this study provided a unique opportunity to evaluate: (1) how alternations in the foraging behavior of a primary consumer drives state transition dynamics in patches across the mosaic (Chapter 1), (2) whether predation or resource abundance are the predominant drivers of community regulation (Chapter 2), and (3) whether forest community structure departed from a long-standing configuration in response to the onset of sea urchin barrens (Chapter 3). Collectively, the results presented here have far-reaching implications to the field of community and ecosystem ecology that enhance understanding of how sudden biotic and environmental perturbations can erode persistent community configurations and restructure the relative influence of top-down and bottom-up forcing.

One of the most interesting aspects about the behavior and functional role of sea urchins is their ability to switch from sit-and-wait foraging on kelp detritus, to active herbivory on live macroalgae (Harrold and Reed 1985, Parnell et al. 2017, Spyksma et al. 2017). In Chapter 1, I assessed whether alternations between these two fundamentally different foraging modalities (passive or active grazing) explain shifts in the state of patches (forest or barrens) across the mosaic. I found that the initial

2014 sea urchin outbreak was primarily evidenced by a behavioral shift, not by a demographic response (i.e., increased survival or recruitment). Furthermore, shifts in patch state across the mosaic were explicable by changes in sea urchin behavior. I also found that an extraordinary recolonization of forests at a subset of survey sites was associated with sea urchin movement to shallow water. These results provide an important contribution to the ecological literature surrounding sea urchin behavior and movement by revealing how grazing activity can shape local patterning in community states (Steneck 2013, Karatayev et al. 2019).

Ecological processes that enhance or dampen the likelihood of shifts between top-down (predator-driven) and bottom-up (i.e., resource-driven) forcing underpin community regulation, functioning, and stability (Estes et al. 1998, Christianou and Ebenan 2005, Nichols et al. 2015). In Chapter 2, I demonstrate how a sea star catastrophe, episodic marine heatwave, and reduction in the abundance of a primary producer led to a marked shift in community regulation. Specifically, I show how the formation of the kelp forest-urchin barrens mosaic led to spatial variation in sea urchin energetic profitability. Across the mosaic, sea otters preferentially target energetically profitable sea urchins in patches of forest, but mostly ignore those of low profitability in barrens. This response has important implications for the recovery of barrens to the forested state because the remnant forests maintained by sea otters are the ultimate spore sources to replenish and facilitate recover of forests in barren areas. These findings add to a growing body of literature surrounding behaviorally mediated trophic cascades by revealing that predator and prey responses to spatially distributed mosaics of resources can underpin community functioning and regional stability (Wiens 1995, Scheffer 2004, Breshears 2006, Sheaves 2009).

Ecological communities can be stable over multiple generations, or rapidly shift into structurally and functionally different configurations (Holling 1973, Connell and Sousa 1983, Tilman 1996, Dudgeon et al. 2010). Chapter 3 was motivated by the widely accepted concept that kelp forests and sea urchin barrens can exist as alternative stable states (Filbee-Dexter and Scheibling 2014). My overarching goal for Chapter 3 was to evaluate whether the formation of the mosaic resulted in a departure of community structure from the long-standing configuration, and whether the trajectory of community structure broadly aligned with the alternative stable state hypothesis. I found that, beginning in 2013, the entire forest community departed from a six-year cluster and drifted into a new position in multivariate space. However, variation in community trajectory was highly variable at the site-level, and the cohesion of community structure trajectory was separated by sampling regions (Carmel, Monterey Bay). These results suggest that kelp forest community structure may persist in a stable state for multiple years, but that environmental (e.g., marine heatwaves) and biotic (loss of predators, sea urchin outbreaks) perturbations can rapidly shift the community to alternative stable states. In this chapter, the nature of the biotic and environmental perturbations is central to disentangling evidence for an alternative stable state versus a phase shift. The marine heatwave has since abated, and the physio-chemical environment before and after the perturbation appears much the same. This satisfies the Connell and Sousa requirement for one environment that supports more than one stable end-state (Connell and Sousa 1983). Moreover, the results presented in this chapter highlight that departures from long-standing community configurations may be difficult to reverse (Knowlton 2004). Time will tell whether the system persists in this alternative state beyond multiple generations of a key interactor, the purple sea urchin, another requirement for alternative stable states of the community (Connell and Sousa 1983).

Although my dissertation addresses several hypotheses related to the mechanisms that structure and maintain ecological communities, it also yields many more unanswered questions as avenues for future research. First, research to determine the drivers of scale dispersion of mosaics in formerly continuous systems will be useful in identify the continuity of change. Formerly continuous systems that turn into spatial mosaics may be an early warning sign of collapse (Dakos et al. 2011), but more research is needed on whether the dynamics of spatially heterogenous systems are punctuated or continuous (deYoung et al. 2008). Second, although I show several reciprocal feedbacks between a resource mosaic and grazer and predator foraging behavior, research to determine how prey condition affects predator foraging behavior in other systems is needed. To date, only a few examples of flexibility in predator assessment of prey condition exist (Huggard 1993, Page and Ryan 2005, Holmes and McCormick 2009). Given the important community-level implications of predator preference for energetically profitable prey identified in this study, future complementary studies in other systems would shed light on the ubiquity and generality of this phenomenon. Finally, this study identified clear departures in community structure associated with the onset of sea urchin barrens, but further research specifically aimed at identifying whether state shifts in kelp forests result in functional degradation or trophic restructuring is needed (O’Connor and Byrnes 2014, Tilman et al. 2014, Gabara et al. 2021). The entire loss of a foundation species in the barrens state of the ecosystem certainly speaks to the question of trophic or functional reordering. Indeed, the ability for sea urchins to switch from foraging on detritus to active herbivory (and potentially carnivory in extreme food limited environments, Wangensteen et al. 2011) highlights the need for broad and detailed assessments of trophic complexity inside and outside of sea urchin barrens.

This dissertation highlights how the synergistic effects of climate and punctuated biotic and environmental perturbations feedback to alter the strength of top-down and bottom-up control, and can erode persistent community configurations. With increasing biodiversity loss worldwide and rapid climate-induced changes, there is a pressing need to understand how shifts in species interactions will alter the structure and functioning of communities and ecosystems. By examining effects of changes in grazer and predator behavior in the wake of a sea star epizootic and marine heatwave, my research expands understanding of the mechanisms that organize and maintain the structure and stability and ecological communities.

Appendices

Appendix 1: Supplementary material for Chapter 1

Supplementary Tables T1-T2

Table T1. Growth transition probabilities for 10 size-classes of sea urchins calculated using a Tanaka growth function and model parameters derived from Ebert 2010.

$$G = \left[\begin{array}{cccccccccc}
 & S_1 & S_2 & S_3 & S_4 & S_5 & S_6 & S_7 & S_8 & S_9 \\
S_1 & 0.1295 & 0 & 0 & 0 & 0 & 0 & 0 & 0 & 0 \\
S_2 & 0.8705 & 0.0010 & 0 & 0 & 0 & 0 & 0 & 0 & 0 \\
S_3 & 0 & 0.9990 & 0.4392 & 0 & 0 & 0 & 0 & 0 & 0 \\
S_4 & 0 & 0 & 0.5608 & 0.8437 & 0 & 0 & 0 & 0 & 0 \\
S_5 & 0 & 0 & 0 & 0.1563 & 0.9311 & 0 & 0 & 0 & 0 \\
S_6 & 0 & 0 & 0 & 0 & 0.0689 & 0.9523 & 0 & 0 & 0 \\
S_7 & 0 & 0 & 0 & 0 & 0 & 0.0477 & 0.9594 & 0 & 0 \\
S_8 & 0 & 0 & 0 & 0 & 0 & 0 & 0.0406 & 0.9669 & 0 \\
S_9 & 0 & 0 & 0 & 0 & 0 & 0 & 0 & 0.0331 & 0.9754 \\
S_{10} & 0 & 0 & 0 & 0 & 0 & 0 & 0 & 0 & 0.0246
\end{array}\right]$$

Table T2. Summary of parameter estimates from a Bayesian state space demographic model fit to survey data. The posterior distributions of each parameter are described by the mean, standard deviation (sd), 5% and 95% quantiles, the effective sample size (n_eff), and the r-hat statistic.

Parameter	mean	sd	5%	95%	n_eff	r-hat
τ	35.00	2.40	31.00	39.00	100.00	1.10
$\overline{\phi_D}$	5.20	0.86	4.00	6.80	22.00	1.30
$\overline{\phi_S}$	-1.00	1.00	-3.40	-0.03	9.20	2.30
$\overline{\phi_R}$	-0.36	0.33	-0.82	0.23	18.00	1.50
σ_D	0.91	1.40	0.02	4.90	6.90	3.00
σ_S	0.76	0.52	0.11	1.70	34.00	1.30
σ_R	0.91	0.50	0.22	1.90	31.00	1.20

Supplementary Figures S1-S4

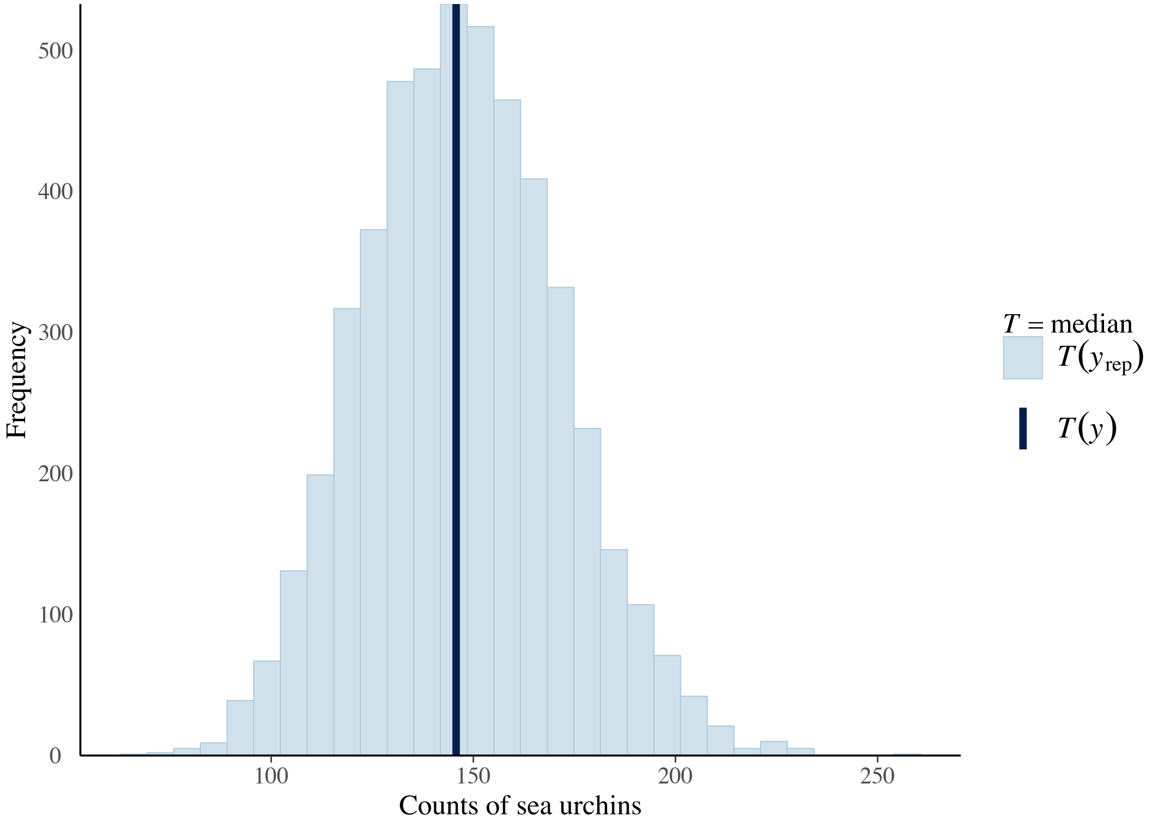

Figure S1. Mean observed sea urchin counts (black bar) compared to a frequency distribution of out-of-sample predictions from the model (observed value should be in the center for a well-fit model).

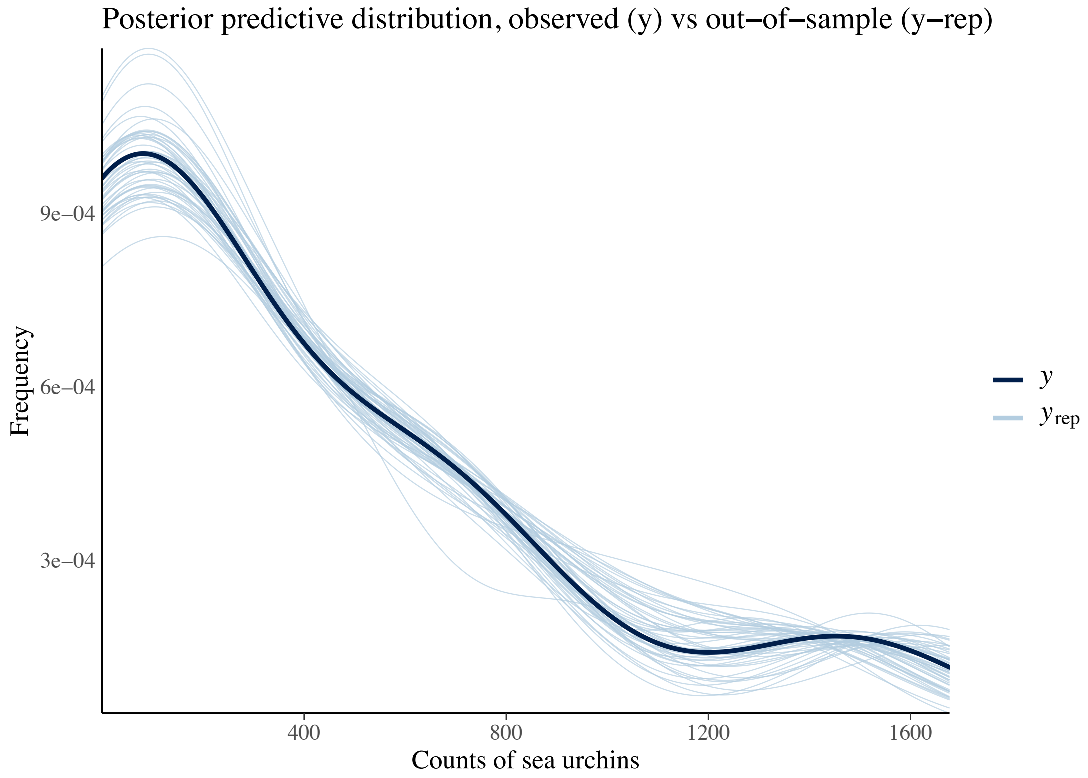

Figure S2. Posterior predictive check plot for Bayesian state-space model depicting the density of observed counts of sea urchins, with light blue lines showing out-of-sample predictions.

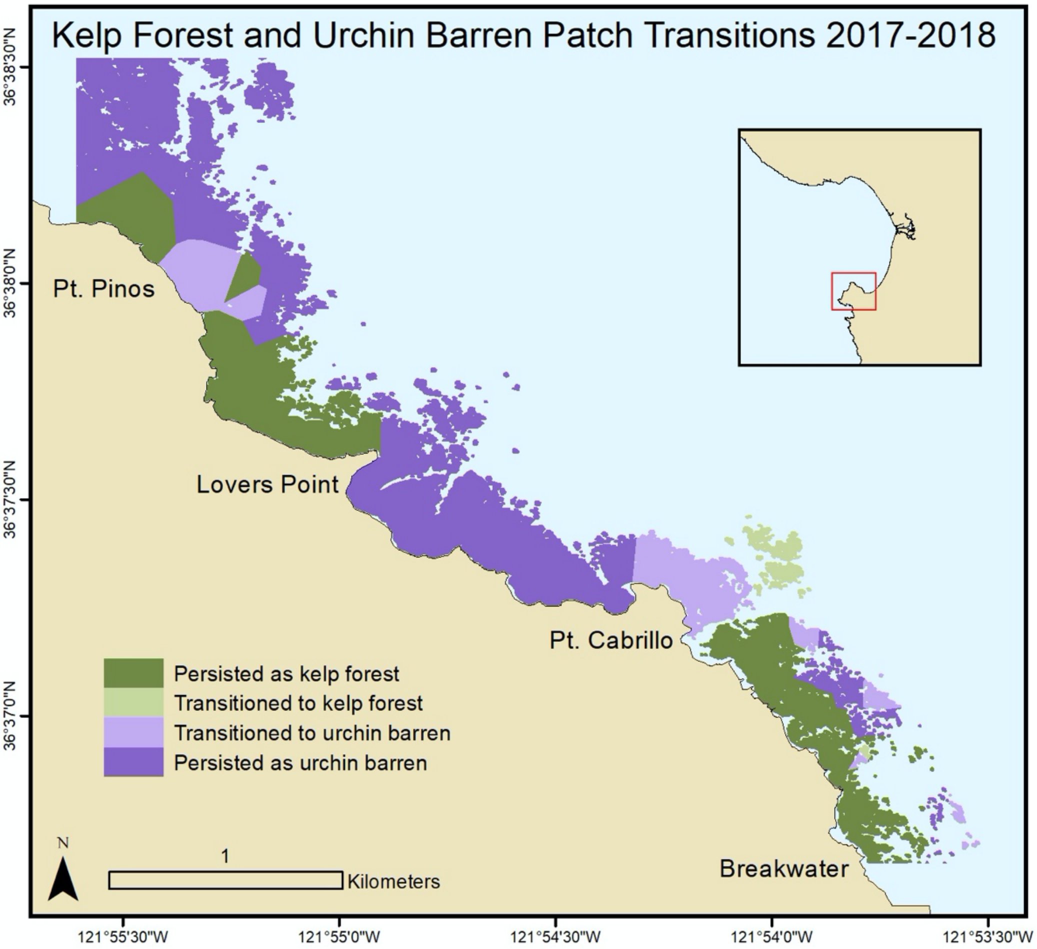

Figure S3. Patch transition dynamics across the 2017-2018 sampling periods interpolated using Thiessen polygons constrained to rocky reef substratum. Figure produced by Linnea Gullikson as part of an undergraduate student thesis at the University of California, Santa Cruz.

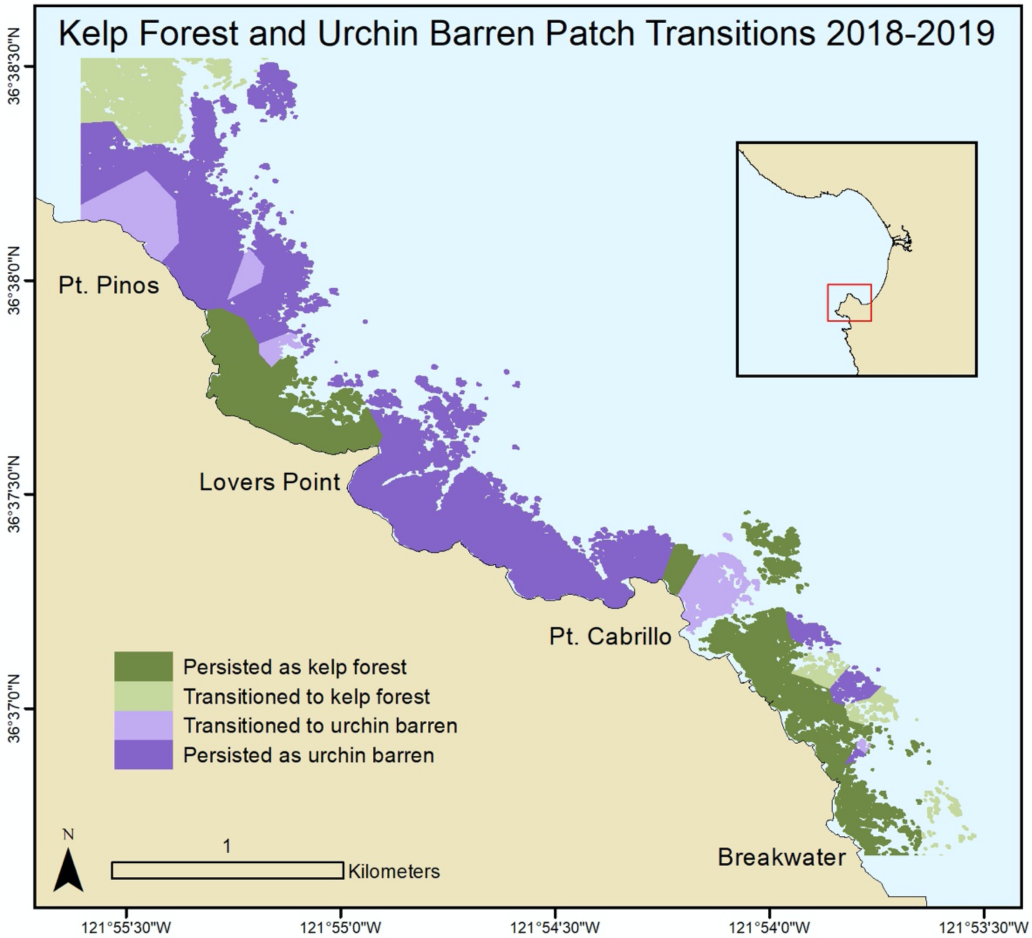

Figure S4. Patch transition dynamics across the 2018-2019 sampling periods interpolated using Thiessen polygons constrained to rocky reef substratum. Figure produced by Linnea Gullikson as part of an undergraduate student thesis at the University of California, Santa Cruz.

Appendix 2: Supplementary material for Chapter 2

Supplementary Methods

Time-series analysis of factors leading to the formation of the mosaic. I used a multivariate correlation analysis to determine the sign (positive or negative) and strength (slope) of the relationship between *Pycnopodia* density, density of exposed purple sea urchins, kelp density, and sea otter abundance in Monterey Bay, California. The analysis revealed an inverse relationship between *Pycnopodia* density and exposed purple sea urchin density ($P < 0.0001$, $ß = -0.28$), a positive relationship between *Pycnopodia* and kelp density ($P < 0.0001$, $ß = 0.13$), and a strongly positive relationship between exposed purple sea urchins and sea otter abundance ($P < 0.0001$, $ß = 0.73$). I then used a cross-correlation analysis to determine whether a time-lag occurred between the initiation of these events, but found that the model was centered at zero, indicating that these events likely began at or around the year 2014. Although these events likely initiated simultaneously, the otter, kelp, and urchin response continued for at least three years.

Emergence of urchins following the demise of *Pycnopodia.* The exponential increase in the density of exposed purple sea urchins is explained almost entirely by the emergence of urchins from refuge in crevices that then made them detectible by divers. This behavioral response is evidenced by the dramatic increase in numbers across the entire size distribution of urchins. Counts (i.e., density) of 3 cm (approx. two years old) to 8 cm (several years old) urchins uniformly increased over a magnitude of 600% between 2013 and 2014. These size classes are too large to have settled from the plankton later than 2013, and the increase occurred across all of the survey sites, negating immigration into the survey area. However, a recruitment event may have occurred post-emergence (after 2014) that further led to the observed exponential increase in sea urchin counts.

State space model for estimating population trends. The annual census counts of independent otters and dependent pups, collected between 1990 and 2018 (Hatfield et al. 2019), provide a time-series of relative abundance indices for each area of the coast. Because the sea otter census is conducted as an exhaustive, un-corrected count with no associated measurement of uncertainty, the annual counts cannot be interpreted as a true estimate of abundance (Hatfield et al. 2019). In previous analyses of sea otter population trends, maximum likelihood or Bayesian approaches have been used to infer the underlying population dynamics while accounting for observer error (Tinker et al. 2006, Tinker et al. 2021). Here I describe a Bayesian state-space model used to infer trends in southern sea otter abundance within each of three coastal regions: Santa Cruz, Monterey, and Big Sur (see Figure S10). The model explicitly incorporates demographic processes and allows for both observer error (measurement uncertainty) in the raw counts of independents and pups, as well as stochasticity (variation across years) in underlying vital rates. By utilizing an age-structured, demographically explicit process model, realistic levels of variation in the underlying trends are estimated and constrained to demographically feasible limits.

Process model. Here I describe a simplified, female-only demographic model, with structure and parameter value ranges according to previously published demographic models for southern sea otters (Eberhardt 1995, Gerber et al. 2004, Tinker et al. 2006, Tinker et al. 2021). The model includes for age classes of independent otters: 3 subadult year classes (6mo – 1.5yr, 1.5 – 2.5yr, and 2.5-3.5yr) and a 4th multi-year class for adults that spans all ages >3.5yr. Independent otter age classes begin at 6 months because that is the average age at which dependent pups are weaned by females (Riedman et al. 1994), and dependent pups are not tracked as a separate class but rather incorporated into the adult reproductive term (Tinker et al. 2006) as described below. While reproduction is continuous and only weakly seasonal in southern sea otters (Jameson and Johnson 1993), reproductive processes are discretized for model tractability such that adult females are assumed to become pregnant at the beginning of an annual time step, give birth halfway through the year, and then wean the pup (if it survives) at the end of the time step, at which time the 6mo pup recruits to the first subadult year class.

Stage-specific survival rates are described using an instantaneous hazards approach: for adults (stage 4), the annual *per-capita* survival rate is estimated as:

$$S_a = \exp\left(-\exp\left(-h_0 + \alpha\right)\right) \tag{0.1}$$

where h_0 is a constant representing baseline log-hazards (set to -3 to correspond to maximum survival of 0.95, based on previous studies (Gerber et al. 2004)); and α is the mean log-hazard ratio for adults, estimated by fitting the model to survey data. For simplicity and model tractability, the model assumes that stochasticity primarily affects subadult survival and has minimal effects on adult survival. Sub-adult survival rates are thus calculated as:

$$S_{sa,t} = \exp\left(-\exp\left(h_0 + \gamma + \varepsilon_{\gamma,t}\right)\right), \quad \varepsilon_{\gamma,t} \sim normal\left(0, \sigma_\gamma\right) \qquad (0.2)$$

where γ is the mean log-hazard ratio for subadults and $\varepsilon_{\gamma,t}$ is a normally distributed random parameter representing the effects of environmental stochasticity in year *t*, and has a mean of 0 and standard error of σ_γ (a parameter to be estimated). The survival of pups from birth to weaning is also assumed to be affected by environmental stochasticity, with annual deviations from the mean value assumed to be partially correlated and partially independent of subadult survival:

$$S_{p,t} = \exp\left(-\exp\left(h_0 + \phi + \varepsilon_{\gamma,t} + \varepsilon_{\phi,y}\right)\right), \quad \varepsilon_{\phi,t} \sim normal\left(0, \sigma_\phi\right) \qquad (0.3)$$

where ϕ is an estimated parameter (representing the mean log-hazard ratio for dependent pups) and $\varepsilon_{\phi,t}$ is a normally distributed random effects term representing environmental stochasticity in year *t*, with mean of 0 and standard error σ_ϕ, (a parameter to be estimated).

The annual *per-capita* reproductive contributions of adult females to the first female subadult year class in year *t* are calculated as:

$$R_t = S_a \times \left(br/2\right) \times S_{p,t} \qquad (0.4)$$

where *br* is the annual birth rate, which we held fixed at 1 (Tinker et al. 2019). Equation 1.4 also assumes a 50:50 sex ratio of pups, and that pup survival to weaning is conditional upon the survival of its mother (S_a). Combining these vital rates, the annual change in abundance (n) of each of the 4 age-classes in the population is calculated through the following 4 recursive equations:

$$\begin{aligned} n_{1,t} &= n_{4,t-1} \times R_t \\ n_{2,t} &= n_{1,t-1} \times S_{sa,t-1} \\ n_{3,t} &= n_{2,t-1} \times S_{sa,t-1} \\ n_{4,t} &= \left(n_{3,t-1} \times S_{sa,t-1}\right) + \left(n_{4,t-1} \times S_a\right) \end{aligned} \tag{0.5}$$

The total expected number of independent otters in year t, $N_{\text{exp,t}}$, is calculated as the sum of the individuals in each of the 4 age classes,

$$N_{\exp,t} = \sum_{i=1}^{4} n_{i,t} \tag{0.6}$$

To calculate the expected number of pups that could be counted in a survey, several complications need to be accounted for. First, not all the pups born in a year are available to be counted at the time of the spring survey, as some will have already been weaned or died, and others will not yet have been born. The parameter ρ is defined as the proportion of pups produced in year t that were born within the 6-mo. period immediately before the survey. Of those pups, a certain proportion will die before weaning (described by 1-$S_{p,t}$); however, not all of those deaths will have occurred by the time of the survey, as most pups counted in spring surveys are 2mo. or younger. Incorporating both these adjustments the expected number of pups is:

$$P_{\exp,t} = n_{4,t}\left[\rho \times \left(\frac{br}{2}\right) \times \left(S_{p,t}\right)^{\frac{1}{3}}\right] \tag{0.7}$$

Finally, I assessed the hypothesis that there was a substantial change in mean survival rates over the study period, potentially associated with the surge in prey abundance described in this study. To evaluate this possibility the model was expanded to estimate two sets of age-specific log hazard rates, [α_1, γ_1 , ϕ_1] and [α_2, γ_2, ϕ_2], with each set corresponding to a different partition of years within the study period. While the *a priori* expectation was that a change in survival rates likely occurred sometime around 2014, the model did not enforce a particular temporal break, but rather allowed to be data driven. Specifically, I defined a vector sw_y having length Y (the number of years of the study) and with integer values of 1 or 2. For years where sw_y= 1, the first set of age-specific hazard rates are applied, while for years where sw_y= 2 the second set of age-specific hazard rates are applied. I evaluated multiple configurations of the sw_y vector corresponding to different temporal sequences of hazard rates: we allowed for up to 2 temporal breaks in demographic conditions (i.e., the possibility of a change from a series of 1's to a series of 2's, and the possibility of a later change from a series of 2's back to a series of 1's) and also evaluated a "null model" where all years experienced the same set of hazard rates. For each model configuration the differences in log hazard rates between the two sets of demographic conditions are calculated as:

$$\begin{aligned} \delta_\alpha &= \alpha_2 - \alpha_1 \\ \delta_\gamma &= \gamma_2 - \gamma_1 \\ \delta_\phi &= \phi_2 - \phi_1 \end{aligned} \tag{0.8}$$

These log differences are informative because the proportional change in age-specific instantaneous hazard rates from one time period to another can be calculated as exp(δ).

Data fitting. I compared the observed survey counts of independents ($N_{obs,t}$) and pups ($P_{obs,t}$) to the expected values $N_{exp,t}$ and $P_{exp,t}$ generated by the process model, using Markov Chain Monte Carlo (MCMC) methods to find the parameter values most likely to have produced the observed data. Previous analyses of sea otter surveys have found that counts are over-dispersed relative to a Poisson distribution (Tinker et al. 2019), and thus can be described using negative binomial distributions:

$$N_{obs,t} \sim negative\_binomial\left(mean = N_{\exp,t}, \tau_N\right) \quad (0.9)$$

$$P_{obs,t} \sim negative\_binomial\left(mean = P_{\exp,t}, \tau_P\right) \quad (0.10)$$

where τ_N and τ_P are inverse-dispersion (or precision) parameters estimated during model fitting. Weak priors were set for all parameters, including half-Cauchy priors (*cauchy*(0,1)) for standard error (σ) and prevision parameters (τ), half-normal priors (*normal*(0,1)) for α, γ and ϕ parameters, and a beta prior (*beta*(1,1)) for ρ. For each model fit 20 independent chains were conducted, saving a total of 10,000 posterior samples after a burn-in of 1000 samples.

The program R (R.Core.Team 2014) and STAN (Carpenter et al. 2017) were used to code and fit the state space model. Model convergence was evaluated by graphical examination of trace plots and by ensuring the R-hat statistic was less than 1.05 for all parameters. Model goodness of fit was evaluated via graphical posterior predictive checks (Appendix 2 Figure S4), whereby the distributions of out-of-sample predictions generated by the model were compared with observed data (Gelman et al. 2000). To determine the best-supported number and timing of temporal breaks in demographic conditions (switches between alternative sets of hazard rates), models were fit with many alternative configurations of the sw_y vector. For each fit, the posterior distributions of the log-likelihoods of observed data were calculated, which were used to compute the “Leave-out-one Information Criteria”, or LooIC (Vehtari et al. 2017). LooIC diagnostics were evaluated to ensure goodness of fit (all Pareto k estimates < 0.5) and to select the model with the lowest LooIC value as the best-supported temporal sequence of vital rates for that region. Tabular summaries of the posterior distributions of parameters are reported from the best-supported model for the Monterey region (Appendix 2 Table T1), and density plots of the mean and 90% credible interval (CI) of δ_α, δ_γ, and δ_ϕ for all 3 regions (Appendix 2 Figure S5). The model estimated values of $N_{exp,t}$ and $P_{exp,t}$ were used to plot trends in abundance of pups and independent sea otters over the study period in Monterey (Appendix 2 Figure S3) and for comparing trends in total abundance between Santa Cruz, Monterey and Big Sur (Appendix 2 Figure S4, S5).

Supplementary Table T1

Table T1. Summary of parameter estimates from a Bayesian state space demographic model fit to survey data from the Monterey study area (see SI methods for parameter definitions and dynamics). The posterior distributions of each parameter are described by the mean, standard deviation, 2.5% and 97.5% quantiles (which bound the 95% CI), the effective sample size (n_eff) and the R-hat statistic, which should be close to 1 if the model converged appropriately resulting in well-mixed chains.

Parameter	mean	sd	2.50%	97.50%	n_eff	R-hat
s_g	0.3656	0.1613	0.1215	0.7429	734.6	1.022
s_f	0.3835	0.224	0.1125	0.9351	426.2	1.043
t_N	149.6	85.89	54.66	350.7	6026	1.001
t_P	41.94	188.9	9.374	167.8	4813	1.001
r	0.6913	0.0429	0.6125	0.7826	1536	1.008
a_1	0.9319	0.2666	0.2915	1.303	2511	1.008
a_2	0.2213	0.1714	0.0076	0.6272	9149	0.999
g_1	1.569	0.2519	1.142	2.093	4619	1.003
g_2	0.5824	0.296	0.1097	1.244	8245	1.001
f_1	2.145	0.387	1.494	2.977	2121	1.009
f_2	1.071	0.4379	0.3311	2.019	8525	1.001
d_a	-0.7105	0.3204	-1.209	0.02943	3411	1.005
d_g	-0.9863	0.3974	-1.722	-0.1645	5993	1.002
d_f	-1.074	0.5825	-2.165	0.1258	2976	1.005

Supplementary Figures S1-S12

Figure S1. Subtidal rocky reef survey sites along the Monterey Peninsula, California, USA.

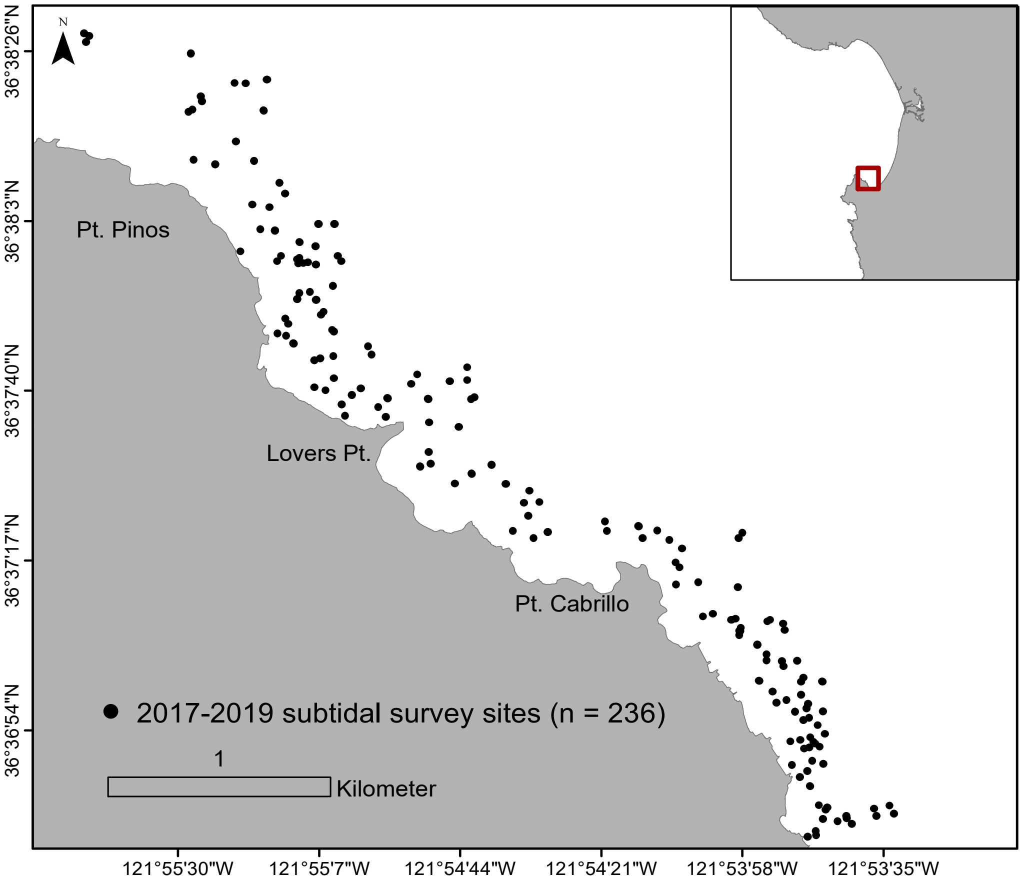

Figure S2. Subtidal survey sites (panel A) from 2018 showing the relationship between kelp density (panel B), urchin density (panel C), and gonad index (panel D). Black triangles show sea otter-sea urchin focal patches. The data in panels B-D were interpolated from 121 randomly sampled subtidal locations (both 'reference' and 'urchin focal patch' sites were sampled using the same protocol) using inverse distance weighting in ArcGIS. All interpolated maps are constrained to rocky reef in the 5–20 meters depth range.

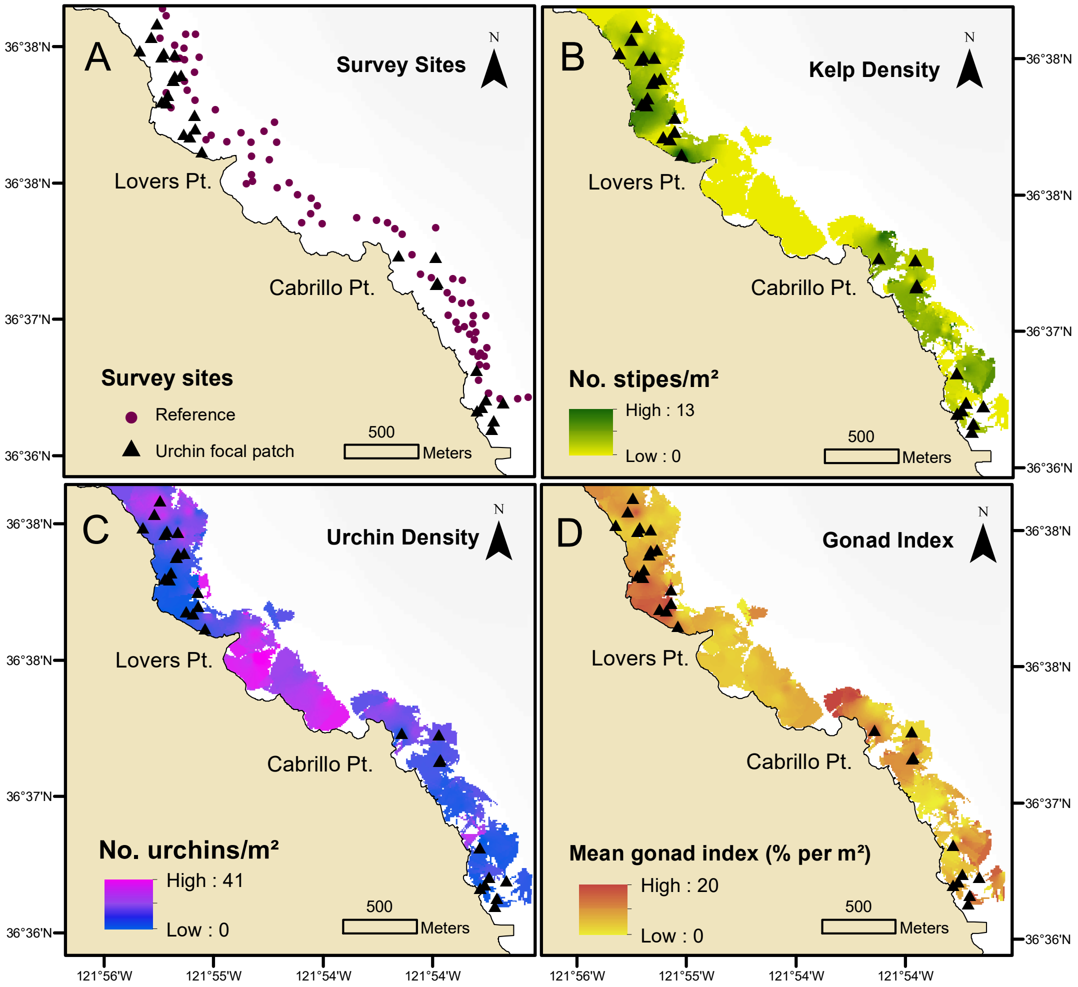

Figure S3. Trends in abundance of independent otters (blue line) and an index of pup production (orange line) for the Monterey study area, as estimated by a Bayesian state space model. The shaded band represent the 95% credible intervals (CI) around the mean estimated values.

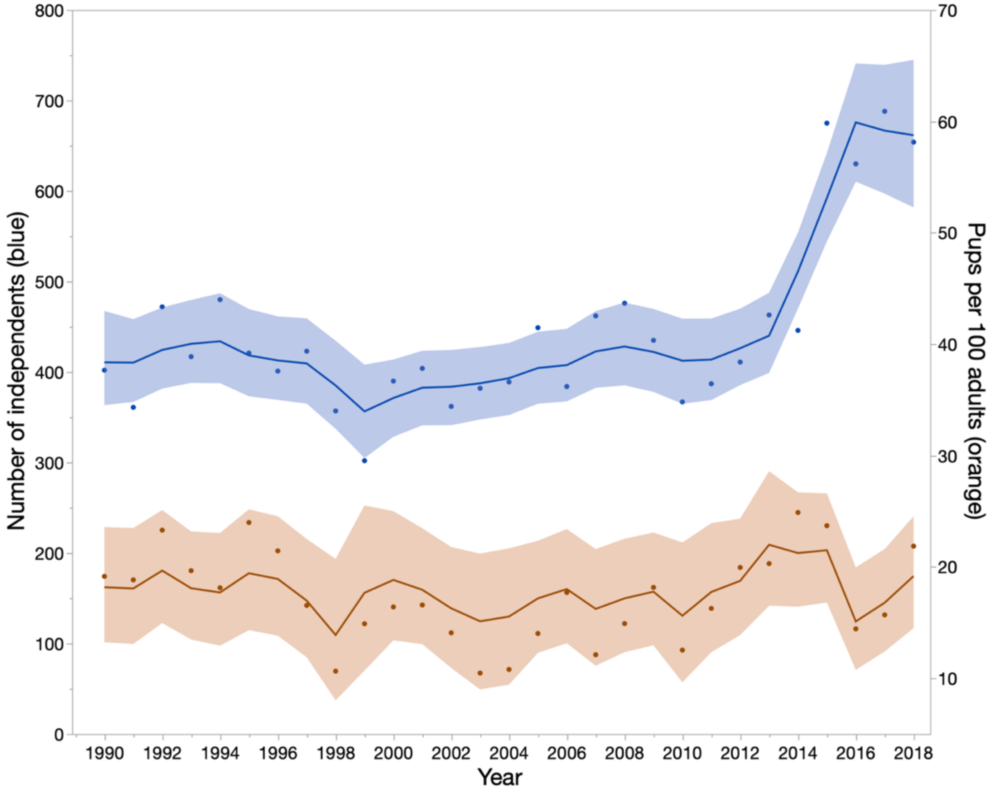

Figure S4. Posterior distributions for δ parameters estimated by a state space model fit to sea otter survey data from Santa Cruz (panel A), Monterey (panel B) and Big Sur (panel C). Each δ value represents the difference between log hazard rates for different time periods (indicated in the plot titles), and are calculated separately for adults (α), subadults (γ) and pups (ϕ).

A) Comparison of hazard rates, 2013–18 vs. pre–2013, Santa Cruz

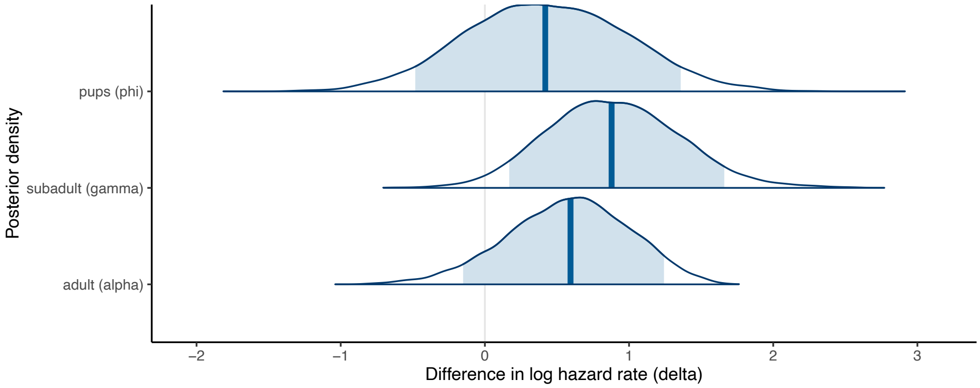

B) Comparison of hazard rates, 2014–16 vs. pre–2014, Monterey

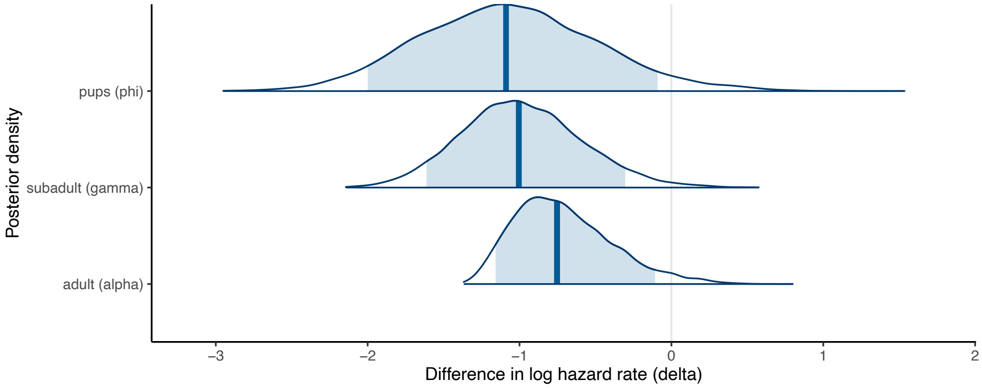

C) Comparison of hazard rates, 2014–18 vs. pre–2014, Big Sur

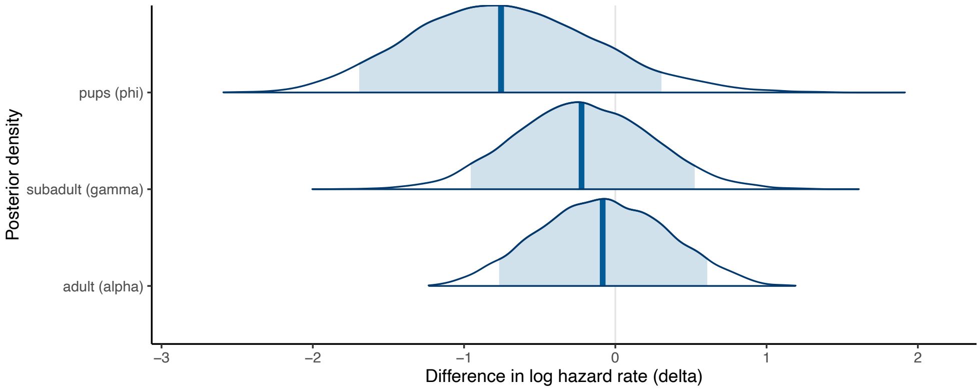

Figure S5. Trends in total abundance of sea otters for Santa Cruz (green line), Monterey (orange line), and Big Sur (blue line) as estimated by a Bayesian state space model. Each shaded band represents the 95% credible intervals (CI) around the mean estimated values.

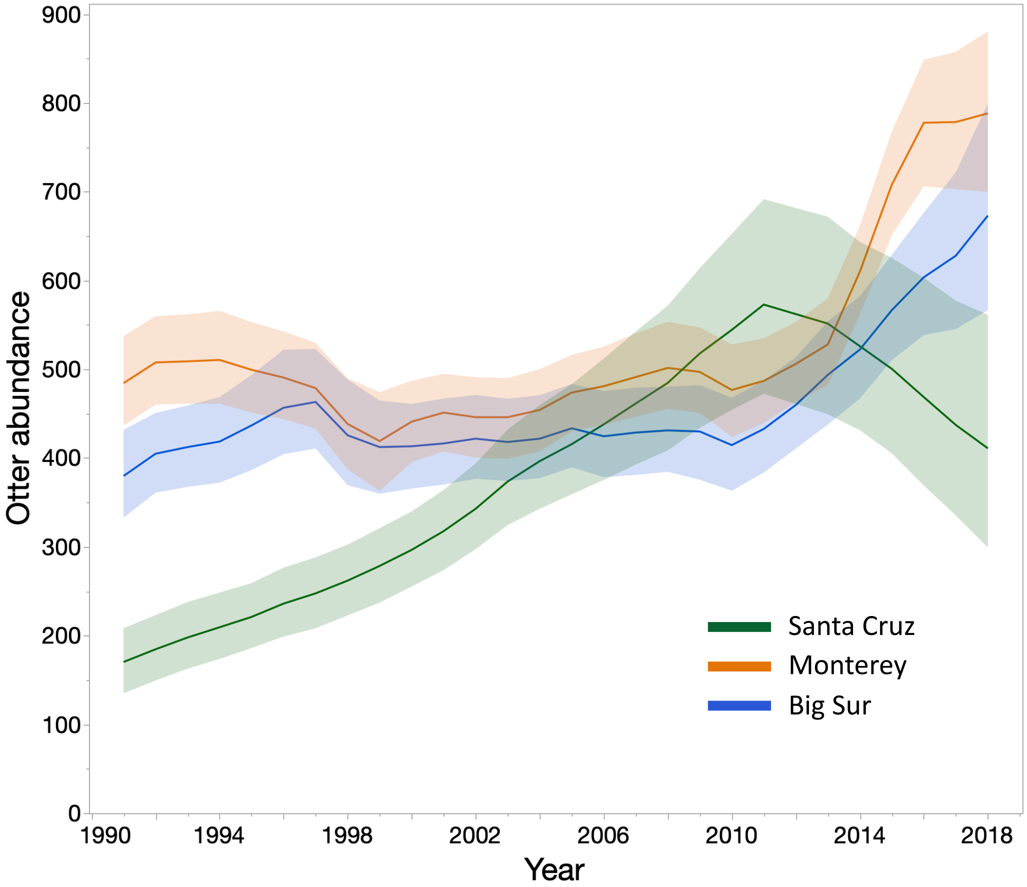

Figure S6. Dietary mean proportion of sea urchins for sea otters specializing on individual prey items before (2000-2013) and after (2014-2018) the urchin outbreak. Error bars are 95% confidence intervals surrounding the mean.

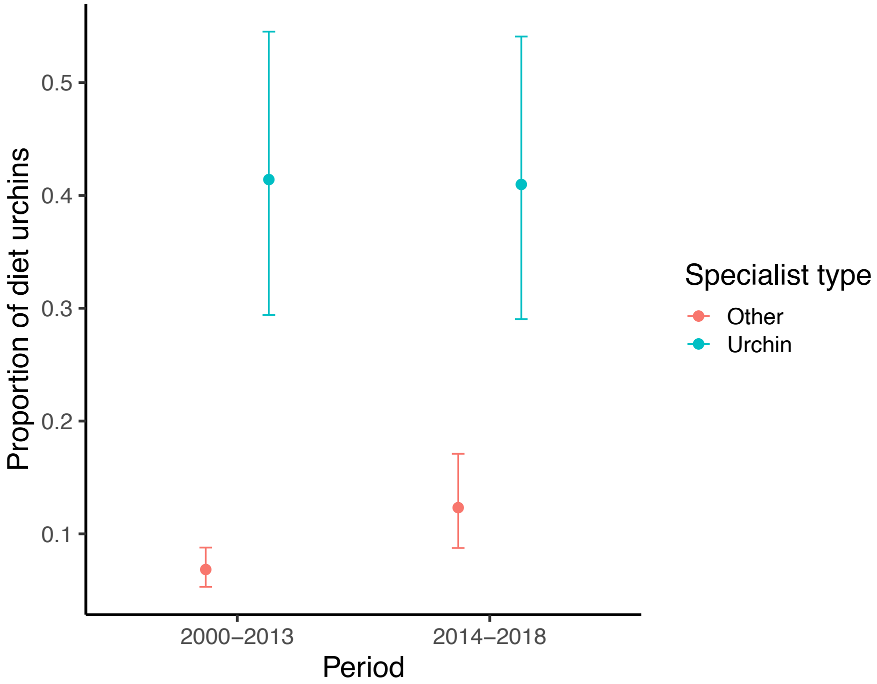

Figure S7. Population-level dietary mean proportion of sea urchins in sea otter diets before (2000-2013) and after (2014-2018) the urchin outbreak. Error bars are 95% confidence intervals surrounding the mean.

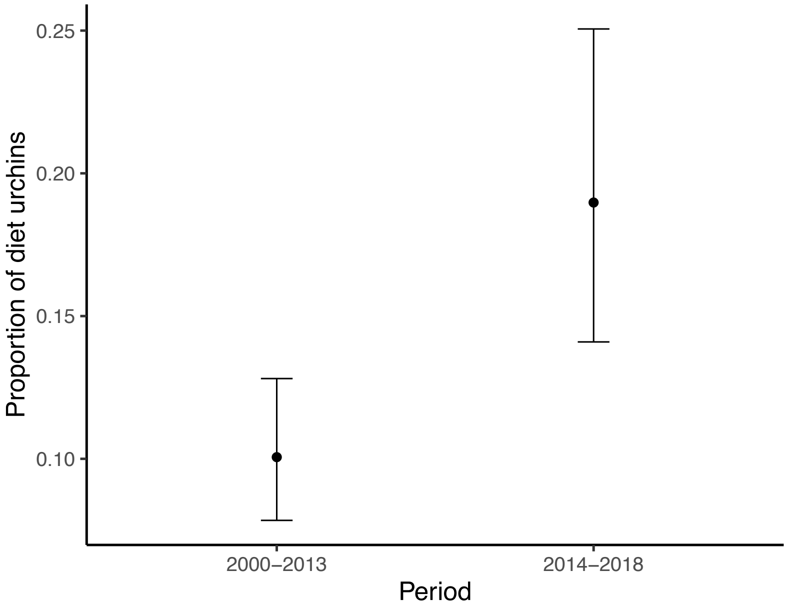

Figure S8. Estimated proportional contributions to southern sea otter diets of urchins, mussels, and urchins and mussels combined, based on observational data collected in the Monterey study area during two time periods: 2000-2013, and 2014-2018. Relative dietary abundance is measured in terms of the proportion of total consumed biomass contributed by each prey type, based on fitting a Monte Carlo-based re-sampling model to observational field data collected from foraging otters (15), and incorporating the empirically derived functional relationships between prey diameter (estimated by observers via comparison with known paw widths) and edible biomass.

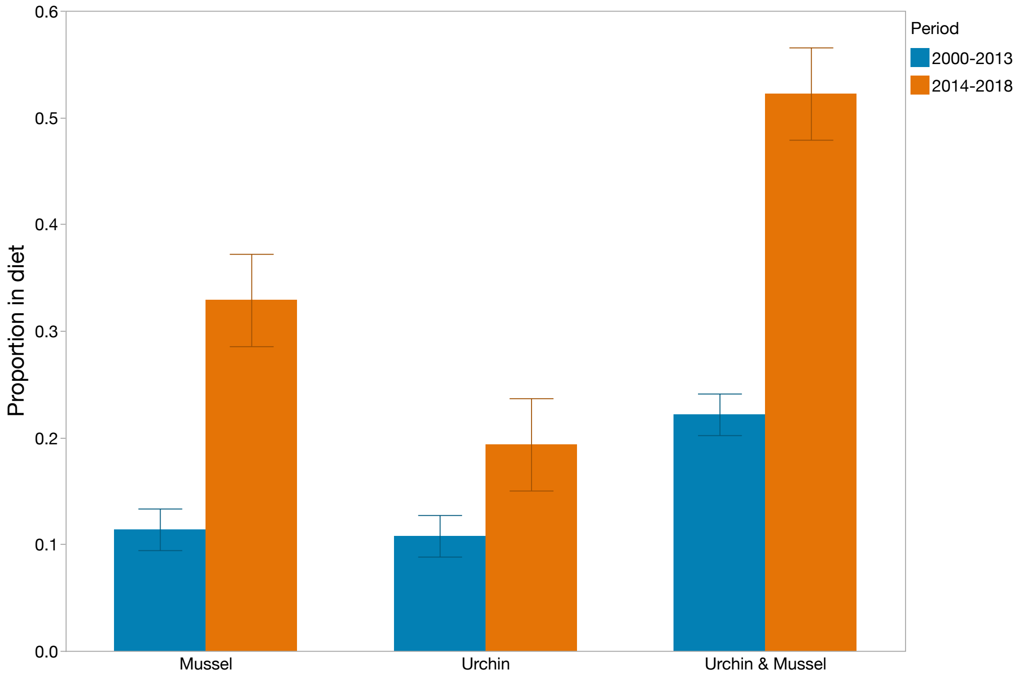

Each error bar is constructed using ±Standard Error.

Figure S9. Subtidal radial sampling design. Each line radiating from the center of the site represents a 5-meter long transect with two 1-m^2 quadrats (16 quadrats per site). Quadrats were randomly stratified in order to avoid over or under-sampling by accounting for increasing arc length with increasing distance from the center of the site. The radial sampling design was selected in order to compliment shore observations of sea otter foraging, where a sub-bout was recorded at the surface as any number of repetitive dives made within a 10-meter diameter zone.

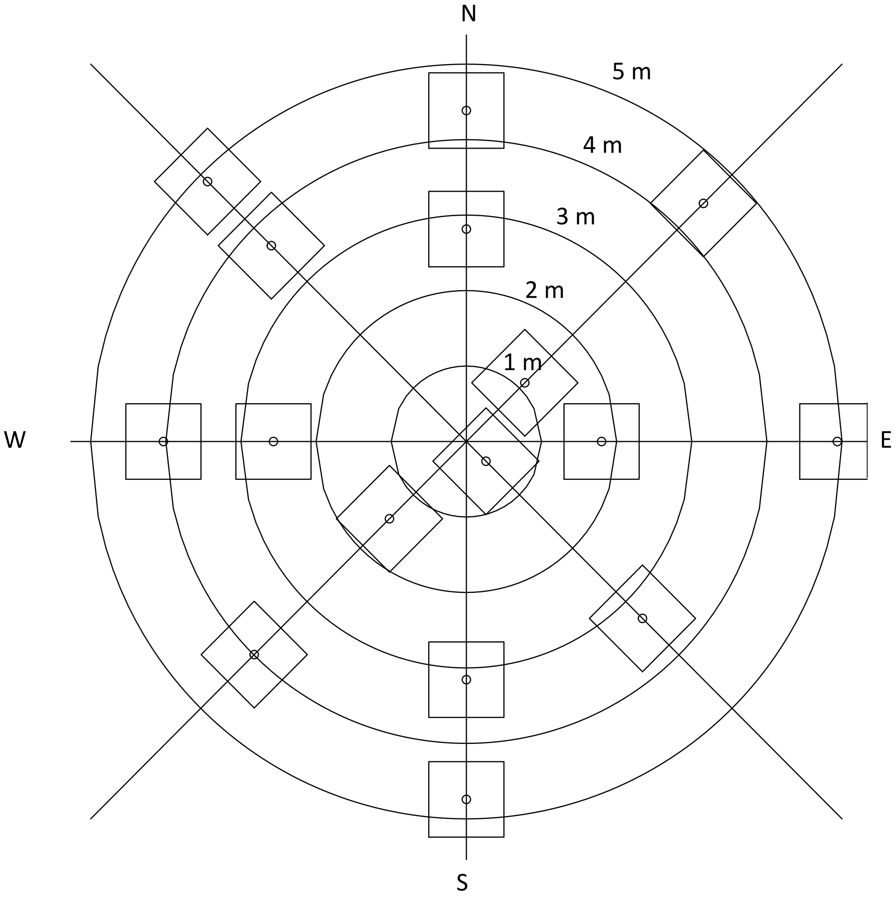

Figure S10. Sea otter population survey regions along the central coast of California, USA.

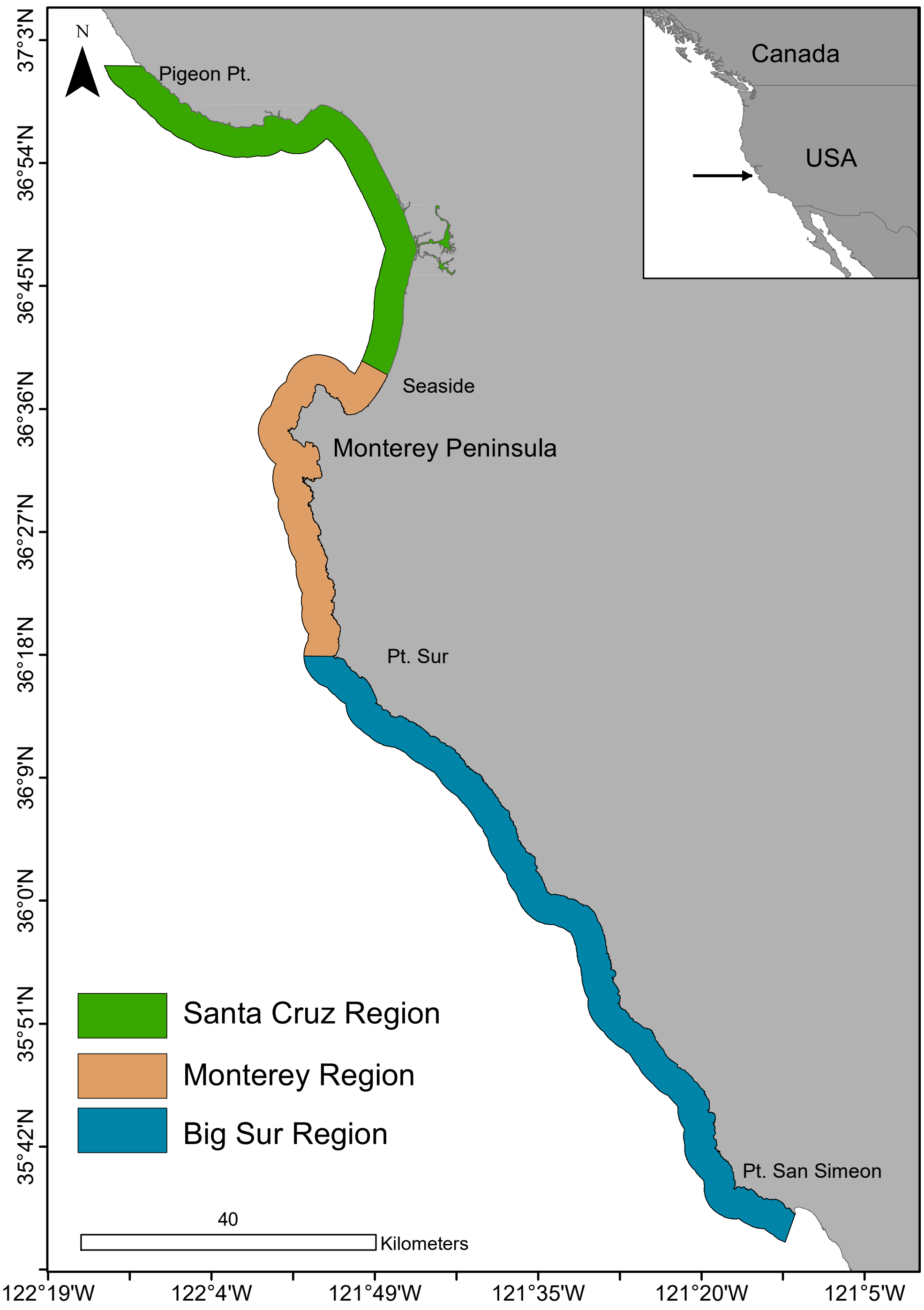

Figure S11. Relative kelp stipe density (A), proportion of exposed (i.e., active foraging) urchins (B), mean urchin density (C), and mean gonad index (D) between reference survey sites (green) and sea otter focal patches (orange) with 95% confidence intervals surrounding each mean.

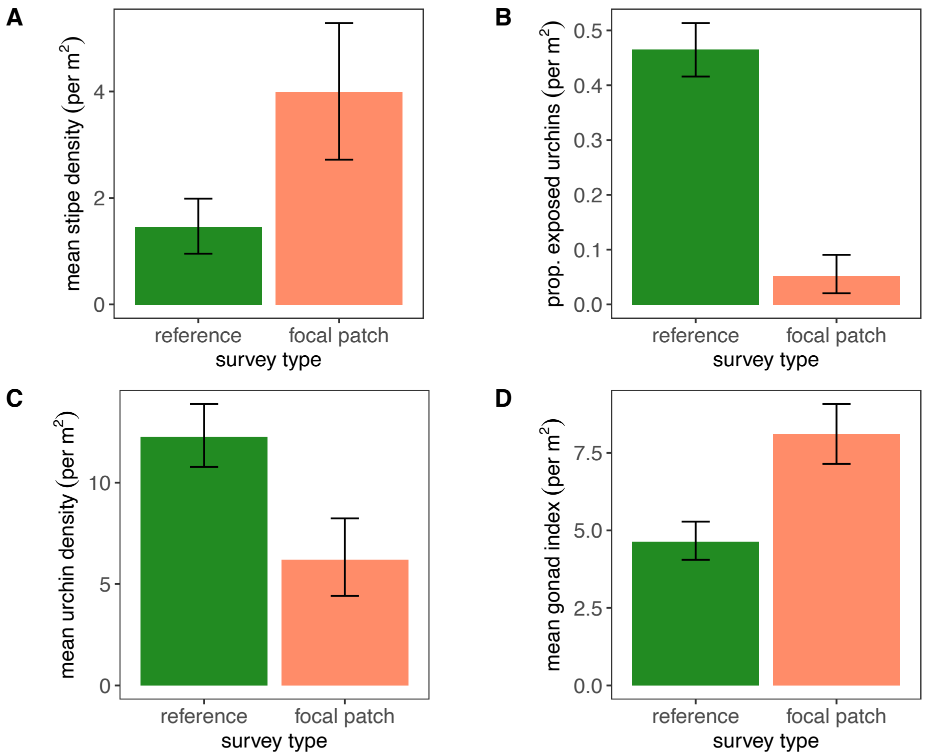

Figure S12. Posterior predictive check plots for a Bayesian state-space model fit to sea otter survey data from the Monterey region. Panel A) shows the mean observed value of independent otters from all surveys (vertical black line) compared to a frequency distribution of out-of-sample predictions from the model (the observed value should be in the center of the distribution for a well-fit model). Panel B) shows a density plot of observed counts across years, with grey lines showing replicate density plots for out-of-sample predictions.

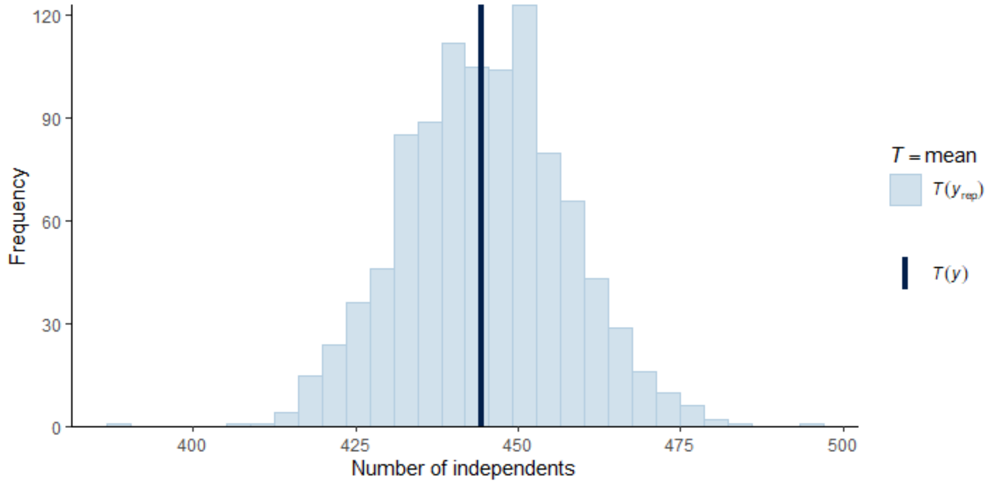

A) Mean observed abundance vs distribution of out-of-sample predictions

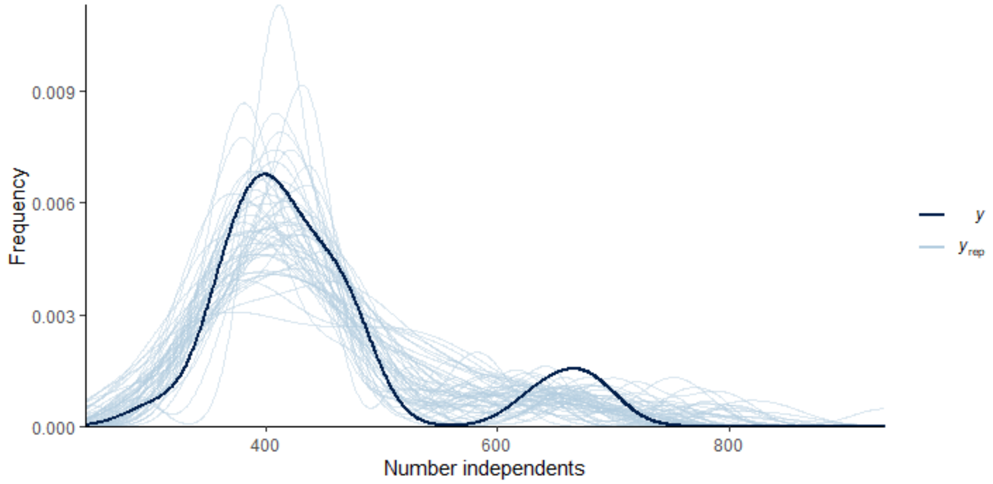

B) Posterior predictive distribution, observed vs out-of-sample predictions

Appendix 3: Supplementary material for Chapter 3

Supplementary Tables T1-T3

Table T1. Taxa recorded on PISCO surveys and included in the multivariate analyses. Order-level taxa and morphological groupings are noted in the Species column where appropriate.

Category	Genus	Species
FISH	Atherinopsidae	spp
FISH	Aulorhynchus	flavidus
FISH	Brachyistius	frenatus
FISH	Caulolatilus	princeps
FISH	Chromis	punctipinnis
FISH	Cymatogaster	aggregata
FISH	Embiotoca	jacksoni
FISH	Embiotoca	lateralis
FISH	Girella	nigricans
FISH	Halichoeres	semicinctus
FISH	Heterostichus	rostratus
FISH	Hexagrammos	decagrammus
FISH	Hypsurus	caryi
FISH	Hypsypops	rubicundus
FISH	Medialuna	californiensis
FISH	Ophiodon	elongatus
FISH	Oxyjulis	californica
FISH	Oxylebius	pictus
FISH	Paralabrax	clathratus
FISH	Paralabrax	nebulifer
FISH	Phanerodon	furcatus
FISH	Rhacochilus	toxotes
FISH	Rhacochilus	vacca
FISH	Rhinogobiops	nicholsii
FISH	Scorpaenichthys	marmoratus
FISH	Sebastes	atrovirens
FISH	Sebastes	atrovirens,carnatus, chrysomelas,caurinus
FISH	Sebastes	auriculatus
FISH	Sebastes	carnatus
FISH	Sebastes	caurinus
FISH	Sebastes	chrysomelas
FISH	Sebastes	melanops
FISH	Sebastes	miniatus
FISH	Sebastes	mystinus
FISH	Sebastes	paucispinis
FISH	Sebastes	serranoides,flavidus
FISH	Sebastes	serranoides,flavidus,

		melanops
FISH	Sebastes	serriceps
FISH	Sebastes	spp
FISH	Semicossyphus	pulcher
ALGAE	Costaria	costata
ALGAE	Dictyoneurum	californicum/reticulatum
ALGAE	Eisenia	arborea
ALGAE	Laminaria	farlowii
ALGAE	Laminaria	setchellii
ALGAE	Nereocystis	luetkeana
ALGAE	Pleurophycus	gardneri
ALGAE	Pterygophora	californica
ALGAE	Sargassum	horneri
ALGAE	Stephanocystis	osmundacea
INVERT	Anthopleura	sola
INVERT	Anthopleura	xanthogrammica
INVERT	Aplysia	californica
INVERT	Apostichopus	californicus
INVERT	Apostichopus	parvimensis
INVERT	Balanus	nubilus
INVERT	Cancer	spp
INVERT	Centrostephanus	coronatus
INVERT	Ceratostoma	foliatum
INVERT	Crassadoma	gigantea
INVERT	Cribrinopsis	albopunctata

Table T2. Species typified in the before period (2007-2012) that distinguish separation between Carmel and Monterey. Table values in the Carmel and Monterey columns are reported as the average distances based on the results of an analysis of similarity percentages (for the top 70% of species driving observed separation) on the normalized (z-score) counts. Order-level and morphological groupings are reported in the Species column where applicable.

Group	Genus	Species	Carmel	Monterey	Contrib. %	Total %
ALGAE	Pleurophycus	gardneri	0.674	-0.187	2.04	2.04
FISH	Sebastes	auriculatus	0.242	-0.0593	2.01	4.05
FISH		Embiotocidae young-of-year	0.242	-0.0593	2.01	6.06
FISH	Atherinopsidae	spp	0.242	-0.0593	2.01	8.07
INVERT	Metridium	spp	-0.0593	0.242	2.01	10.07
COVER		Clam	-0.0593	0.242	2.01	12.07
COVER		Brown Algae	0.445	-0.0825	1.98	14.05
FISH	Girella	nigricans	-0.164	0.413	1.91	15.96
INVERT	Mediaster	aequalis	1.37	-0.394	1.87	17.83
FISH	Embiotoca	lateralis (young-of-year)	0.197	-0.0637	1.81	19.64
ALGAE	Costaria	costata	0.24	-0.0628	1.72	21.36
FISH	Aulorhynchus	flavidus	0.441	0.107	1.72	23.08
FISH	Cymatogaster	aggregata	0.175	-0.042	1.68	24.76
COVER	Desmarestia	spp	0.795	-0.255	1.68	26.44
COVER		Bare Sand	-0.357	0.791	1.58	28.01
INVERT	Anthopleura	xanthogrammica	0.175	-0.153	1.56	29.58
COVER		Sediment/Mud	0.19	0.0759	1.45	31.03
FISH	Sebastes	pinniger (young-of-year)	0.235	-0.0108	1.44	32.47
INVERT	Stylaster	californicus	0.321	-0.254	1.41	33.88
ALGAE	Dictyoneurum	californicum/reticulatum	0.199	0.395	1.39	35.27
FISH	Sebastes	miniatus	0.162	-0.227	1.36	36.63
COVER		Coralline Algae - Erect/Articulated	0.828	-0.564	1.35	37.98
INVERT	Pisaster	brevispinus	0.246	-0.103	1.35	39.33
COVER		Laminariales Holdfast (Alive)	0.767	-0.375	1.31	40.64
FISH	Hexagrammos	decagrammus	-0.14	0.238	1.29	41.92
COVER		Red Algae (Lacy Branching)	0.745	0.222	1.23	43.16
FISH	Cebidichthys	violaceus	-0.134	0.273	1.22	44.38
INVERT	Pugettia	producta	-0.0555	0.137	1.21	45.58
COVER		Red Algae (Leaf-Like)	-0.171	0.884	1.19	46.77

INVERT	Ceratostoma	foliatum	-0.466	0.0575	1.15	47.92
INVERT	Tethya	californiana	0.623	-0.3	1.15	49.07
COVER		Sponge	0.684	-0.212	1.13	50.2
COVER		Barnacle	-0.183	0.336	1.12	51.32
COVER		Red Algae (Cylindrical Branches)	-0.278	0.711	1.1	52.43
ALGAE	Eisenia	arborea	0.38	-0.263	1.07	53.49
COVER		Red Algae (Branching Flat Blade)	-0.0944	0.904	1.07	54.56
FISH	Sebastes	paucispinis	0.131	-0.208	1.06	55.62
INVERT	Loxorhynchus/ Scyra	crispatus/acutifrons	-0.282	0.686	1.04	56.65
COVER		Tunicate -Solitary	-0.153	0.212	1.04	57.69
COVER		Macrosystis Holdfast (Dead)	0.401	0.0217	1.03	58.72
FISH	Heterostichus	rostratus	-0.0841	0.129	1.01	59.73
ALGAE	Pterygophora	californica	0.688	-0.542	0.99	60.71
INVERT	Haliotis	walallensis	0.236	-0.112	0.97	61.69
COVER	Diopatra/ Chaetopterus	spp	0.013	-0.0448	0.96	62.65
COVER		Anemone	0.262	-0.306	0.9	64.47
COVER	Stephanocystis	osmundacea	-0.132	0.387	0.88	65.35
INVERT	Pugettia	richii	-0.175	0.263	0.86	66.21
INVERT	Pisaster	giganteus	-0.135	0.819	0.83	67.04
INVERT	Patiria	miniata	0.417	0.951	0.8	67.84
FISH	Scorpaenichthys	marmoratus	-0.16	0.0437	0.79	68.64
INVERT	Cribrinopsis	albopunctata	0.427	-0.599	0.78	69.42
COVER		Shell Debris	-0.546	0.3	0.78	70.2

Table T3. Species typified in the after period (2015-2020) that distinguish separation between Carmel and Monterey. Table values in the Carmel and Monterey columns are reported as the average distances based on the results of an analysis of similarity percentages (for the top 70% of species driving observed separation) on the normalized (z-score) counts. Order-level and morphological groupings are reported in the Species column where applicable.

Group	Genus	Species	Carmel	Monterey	Contrib. %	Total %
INVERT	Dermasterias	imbricata	1.15	-0.438	1.47	1.47
INVERT	Megastraea	undosa	0.212	-0.0593	1.42	2.89
FISH	Sebastes	nebulosus (young-of-year)	0.212	-0.0593	1.42	4.31
FISH	Embiotoca	jacksoni (young-of-year)	0.212	-0.0593	1.42	5.73
INVERT	Crassadoma	gigantea	0.262	-0.0352	1.41	7.14
FISH	Chromis	punctipinnis	0.421	-0.051	1.41	8.55
INVERT	Pomaulax	gibberosus	0.771	-0.151	1.39	9.94
FISH	Sebastes	hopkinsi (young-of-year)	0.24	0.0316	1.39	11.33
INVERT	Lytechinus	pictus	-0.119	0.394	1.35	12.68
FISH	Oxyjulis	californica (young-of-year)	-0.107	0.332	1.34	14.01
FISH	Chromis	punctipinnis (young-of-year)	-0.0679	0.224	1.34	15.35
FISH	Rhacochilus	vacca (young-of-year)	-0.0593	0.196	1.33	16.68
INVERT	Pachycerianthus	fimbriatus	-0.0593	0.196	1.33	18.02
FISH	Semicossyphus	pulcher (young-of-year)	0.175	0.107	1.32	19.34
INVERT	Kelletia	kelletii	-0.0186	0.353	1.31	20.65
FISH	Sebastes	rosaceus (young-of-year)	0.291	-0.103	1.31	21.96
COVER	Salmacina	tribranchiata	0.0286	0.386	1.26	23.22
FISH	Semicossyphus	pulcher	-0.0312	0.573	1.24	24.46
COVER	Thylacodes	squamigerus	-0.0344	0.707	1.23	25.69
COVER	Phragmatopoma	californica	-0.196	0.45	1.21	26.9
ALGAE	Laminaria	farlowii	-0.111	0.207	1.2	28.1
INVERT	Strongylocentrotus	purpuratus	0.543	0.305	1.18	29.28
FISH	Oxylebius	pictus (young-of-year)	0.0938	0.0812	1.18	30.46
FISH	Sebastes	serriceps (young-of-year)	0.186	0.117	1.18	31.63
INVERT	Aplysia	californica	-0.134	0.349	1.16	32.79
ALGAE	Nereocystis	luetkeana	0.0715	0.0277	1.14	33.93
INVERT	Apostichopus	californicus	0.82	-0.244	1.13	35.06
INVERT	Pisaster	ochraceus	0.352	-0.15	1.12	36.18
INVERT	Anthopleura	sola	-0.368	0.635	1.12	37.3
INVERT	Mesocentrotus	franciscanus	0.24	0.748	1.11	38.41
INVERT	Balanus	nubilus	-0.0103	0.544	1.1	39.51
COVER		Bare Rock	0.483	0.253	1.08	40.59

INVERT	Cucumaria	spp	0.405	0.0238	1.07	41.67
INVERT	Henricia	leviuscula	0.782	-0.447	1.06	42.73
INVERT	Haliotis	rufescens	0.386	0.005	1.03	43.76
COVER	Dodecaceria	fewkesi	0.61	-0.401	1.03	44.79
INVERT	Cribrinopsis	albopunctata	0.716	-0.555	1.01	45.79
COVER	Corynactis	californica	0.543	0.0785	0.99	46.79
FISH	Sebastes	atrovirens,carnatus, chrysomelas,caurinus	0.13	0.247	0.99	47.77
COVER	Dictyotales	spp	0.0361	0.168	0.98	48.75
FISH	Paralabrax	clathratus	-0.158	0.391	0.96	49.71
COVER		Green Algae	0.212	-0.103	0.95	50.67
INVERT	Cryptochiton	stelleri	-0.537	0.444	0.95	51.62
COVER		Tubeworm mat	-0.239	0.39	0.95	52.57
FISH	Sebastes	carnatus	0.635	-0.576	0.95	53.52
INVERT	Apostichopus	parvimensis	0.62	0.223	0.93	54.45
FISH	Oxyjulis	californica	-0.169	0.71	0.92	55.37
FISH	Phanerodon	furcatus	-0.119	0.115	0.92	56.29
INVERT	Strongylocentrotus	purpuratus	0.9	0.452	0.9	57.19
INVERT	Cucumaria	miniata	0.431	-0.0178	0.89	58.08
FISH	Rhacochilus	vacca	0.187	0.387	0.88	58.96
FISH	Rhinogobiops	nicholsii	0.221	0.704	0.87	59.83
INVERT	Haliotis	kamtschatkana	0.45	-0.0472	0.87	60.7
FISH	Sebastes	miniatus	0.531	-0.352	0.86	61.56
COVER		Tubeworm	0.15	0.159	0.83	62.39
COVER		Bryozoan	0.0861	0.289	0.83	63.22
INVERT	Urticina	piscivora	0.423	-0.221	0.82	64.05
INVERT	Urticina	coriacea	0.313	-0.131	0.82	64.87
INVERT	Urticina	spp	0.308	-0.0108	0.8	65.66
INVERT	Megathura	crenulata	0.0765	0.657	0.78	66.45
COVER	Macrocystis	pyrifera	-0.562	0.0113	0.77	67.22
COVER		Coralline Algae - Crustose	1.21	0.16	0.77	67.99
INVERT		Cancer Crab	0.0578	0.0917	0.76	68.75
COVER		Red Algae - Encrusting	0.453	0.981	0.75	69.49
COVER		Cup Coral	0.134	0.0941	0.74	70.24

Supplementary Figures S1-S7

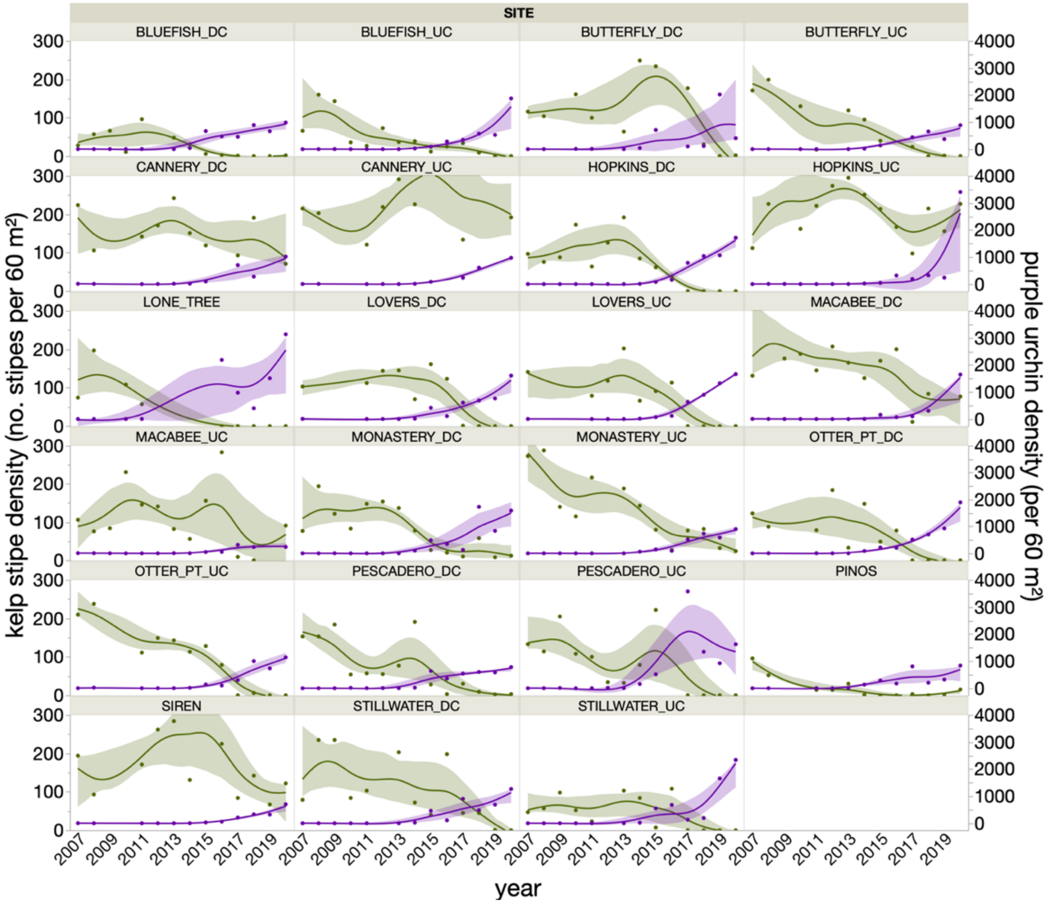

Figure S1. Temporal changes in kelp (green) and purple sea urchins (purple) at 23 sampling locations from 2007-2020. Each point represents the annual mean density for a given site fit with a cubic spline ($\lambda = 0.05$), and each shaded region depicts the 95% confidence interval.

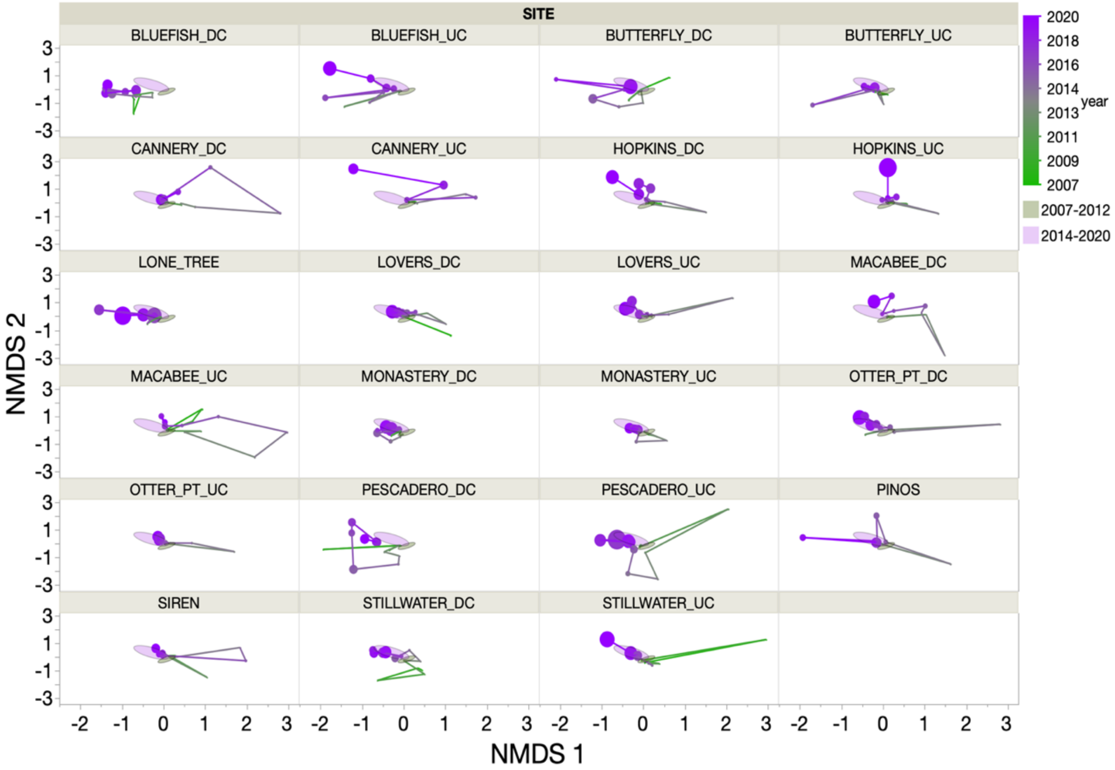

Figure S2. NMDS 2D plots for 23 sampling locations in Carmel Bay and southern Monterey Bay, California. Each line represents the trajectory of the community within a given sampling location over the 14-year study period, and bubbles over the NMDS nodes are scaled to the relative abundance of purple sea urchins (*Strongylocentrotus purpuratus*). The green ellipse denotes the 95% confidence region of community structure for all sites combined during the 2007-12 period, and the purple ellipse denotes the 95% confidence region of community structure for all sites combined during the 2014-2020 period.

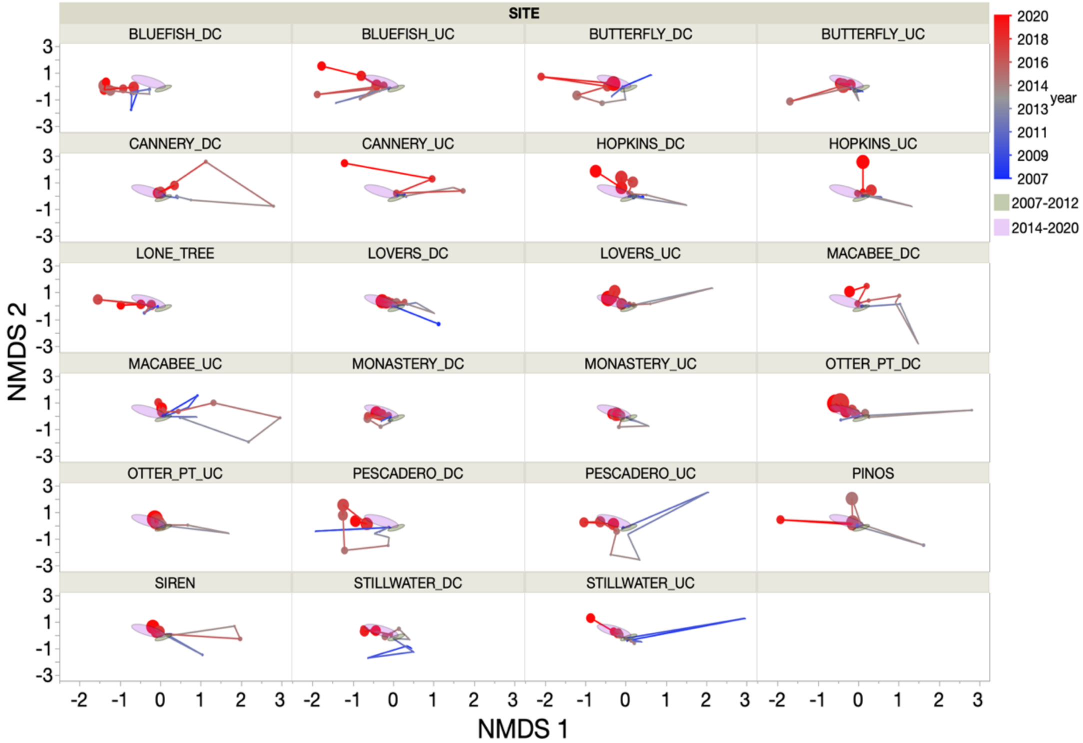

Figure S3. NMDS 2D plots for 23 sampling locations in Carmel Bay and southern Monterey Bay, California. Each line represents the trajectory of the community within a given sampling location over the 14-year study period, and bubbles over the NMDS nodes are scaled to the relative abundance of red sea urchins (*Mesocentrotus franciscanus*). The green ellipse denotes the 95% confidence region of community structure for all sites combined during the 2007-12 period, and the purple ellipse denotes the 95% confidence region of community structure for all sites combined during the 2014-2020 period.

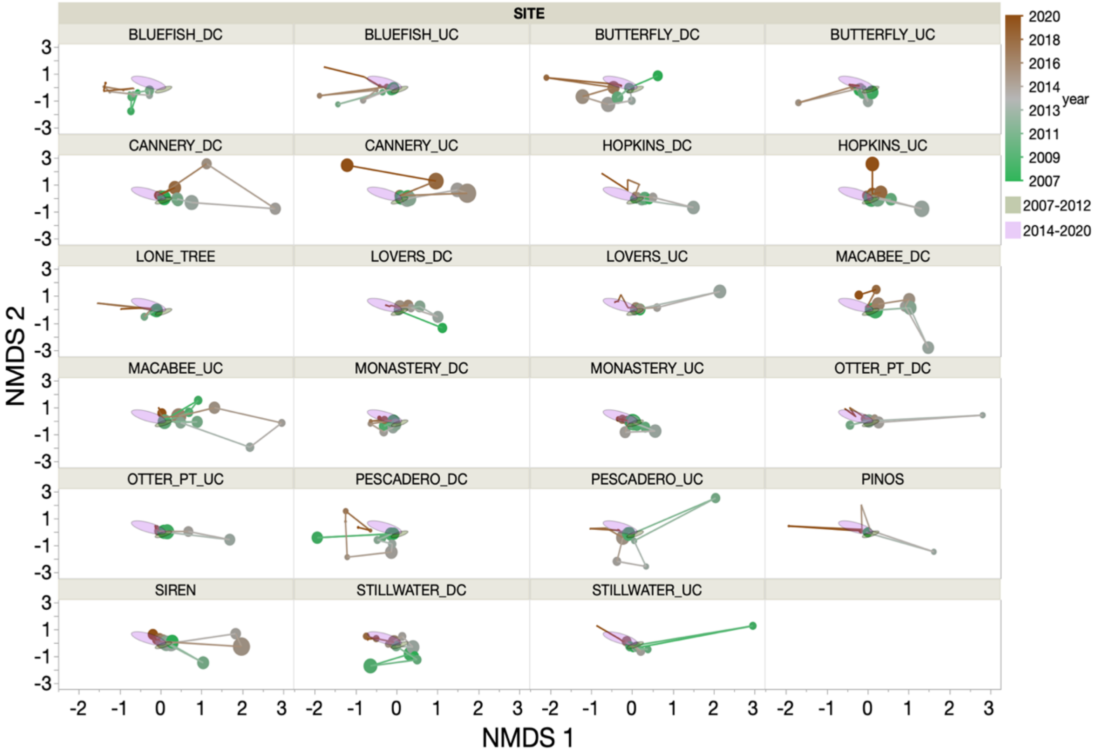

Figure S4. NMDS 2D plots for 23 sampling locations in Carmel Bay and southern Monterey Bay, California. Each line represents the trajectory of the community within a given sampling location over the 14-year study period, and bubbles over the NMDS nodes are scaled to the relative abundance of giant kelp (*Macrocystis pyrifera*). The green ellipse denotes the 95% confidence region of community structure for all sites combined during the 2007-12 period, and the purple ellipse denotes the 95% confidence region of community structure for all sites combined during the 2014-2020 period.

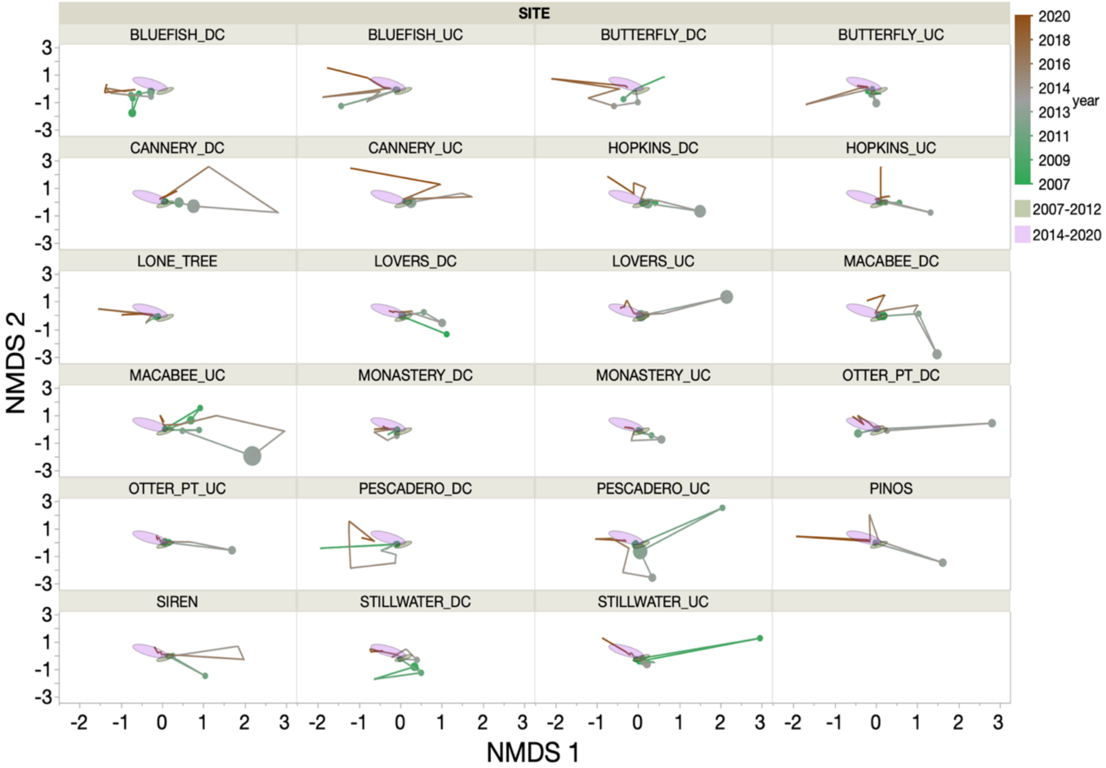

Figure S5. NMDS 2D plots for 23 sampling locations in Carmel Bay and southern Monterey Bay, California. Each line represents the trajectory of the community within a given sampling location over the 14-year study period, and bubbles over the NMDS nodes are scaled to the relative abundance of the sunflower sea star (*Pycnopodia helianthoides*). The green ellipse denotes the 95% confidence region of community structure for all sites combined during the 2007-12 period, and the purple ellipse denotes the 95% confidence region of community structure for all sites combined during the 2014-2020 period.

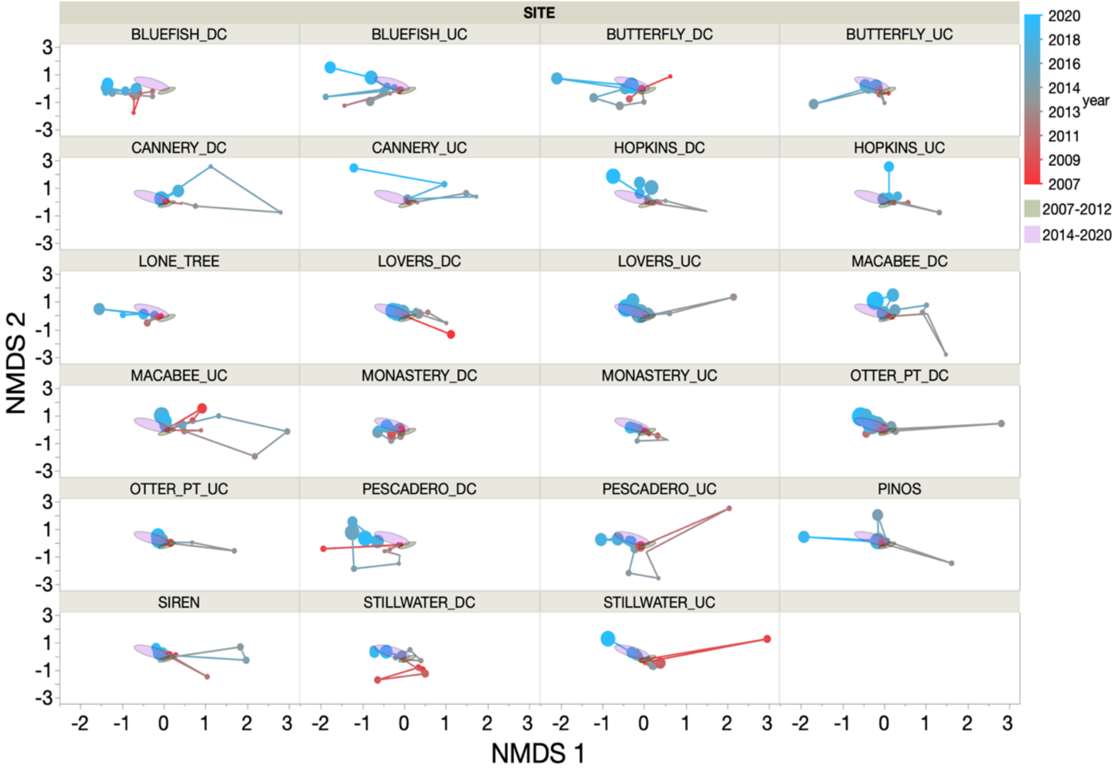

Figure S6. NMDS 2D plots for 23 sampling locations in Carmel Bay and southern Monterey Bay, California. Each line represents the trajectory of the community within a given sampling location over the 14-year study period, and bubbles over the NMDS nodes are scaled to the relative abundance of encrusting red algae. The green ellipse denotes the 95% confidence region of community structure for all sites combined during the 2007-12 period, and the purple ellipse denotes the 95% confidence region of community structure for all sites combined during the 2014-2020 period.

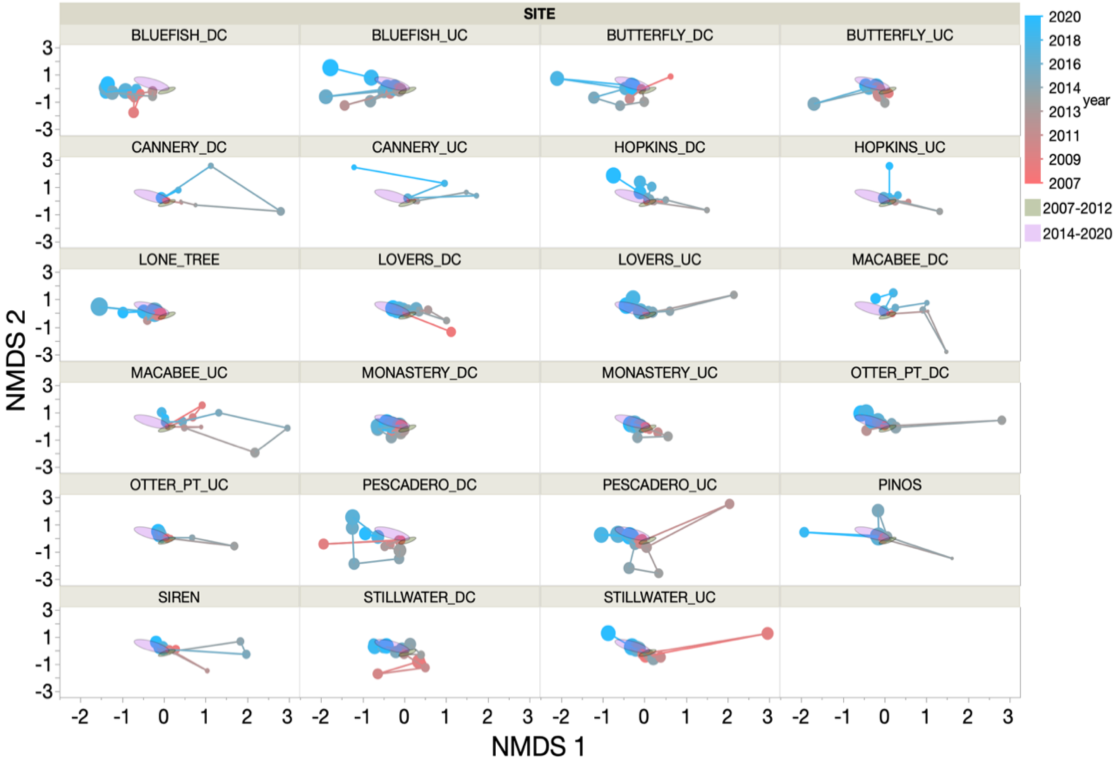

Figure S7. NMDS 2D plots for 23 sampling locations in Carmel Bay and southern Monterey Bay, California. Each line represents the trajectory of the community within a given sampling location over the 14-year study period, and bubbles over the NMDS nodes are scaled to the relative abundance of crustose coralline algae. The green ellipse denotes the 95% confidence region of community structure for all sites combined during the 2007-12 period, and the purple ellipse denotes the 95% confidence region of community structure for all sites combined during the 2014-2020 period.

Literature Cited

Arafeh-Dalmau, N., Montaño-Moctezuma, G., Martínez, J. A., Beas-Luna, R., Schoeman, D. S., & Torres-Moye, G. (2019). Extreme marine heatwaves alter kelp forest community near its equatorward distribution limit. *Frontiers in Marine Science*, *6*, 499.

Baskett, M. L., & Salomon, A. K. (2010). Recruitment facilitation can drive alternative states on temperate reefs. *Ecology*, *91*(6), 1763-1773.

Beas-Luna, R., Micheli, F., Woodson, C. B., Carr, M., Malone, D., Torre, J., ... & Torres-Moye, G. (2020). Geographic variation in responses of kelp forest communities of the California Current to recent climatic changes. *Global Change Biology*, *26*(11), 6457-6473.

Beckerman, A. P., Uriarte, M., & Schmitz, O. J. (1997). Experimental evidence for a behavior-mediated trophic cascade in a terrestrial food chain. *Proceedings of the National Academy of Sciences*, *94*(20), 10735-10738.

Beisner, B. E., Haydon, D. T., & Cuddington, K. (2003). Alternative stable states in ecology. *Frontiers in Ecology and the Environment*, *1*(7), 376-382.

Bray, J. R., & Curtis, J. T. (1957). An ordination of the upland forest communities of southern Wisconsin. *Ecological monographs*, *27*(4), 325-349.

Breshears, D. D. (2006). The grassland–forest continuum: trends in ecosystem properties for woody plant mosaics? *Frontiers in Ecology and the Environment*, *4*(2), 96-104.

Burgess, T. L., Tim Tinker, M., Miller, M. A., Bodkin, J. L., Murray, M. J., Saarinen,

J. A., ... & Johnson, C. K. (2018). Defining the risk landscape in the context of pathogen pollution: Toxoplasma gondii in sea otters along the Pacific Rim. *Royal Society open science*, *5*(7), 171178.

Burt, J. M., Tinker, M. T., Okamoto, D. K., Demes, K. W., Holmes, K., & Salomon, A. K. (2018). Sudden collapse of a mesopredator reveals its complementary role in mediating rocky reef regime shifts. *Proceedings of the Royal Society B: Biological Sciences*, *285*(1883), 20180553.

Byrnes, J., Stachowicz, J. J., Hultgren, K. M., Randall Hughes, A., Olyarnik, S. V., & Thornber, C. S. (2006). Predator diversity strengthens trophic cascades in kelp forests by modifying herbivore behaviour. *Ecology letters*, *9*(1), 61-71.

Cardinale, B. J., Srivastava, D. S., Duffy, J. E., Wright, J. P., Downing, A. L., Sankaran, M., & Jouseau, C. (2006). Effects of biodiversity on the functioning of trophic groups and ecosystems. *Nature*, *443*(7114), 989-992.

Carpenter, E. J., & Chang, J. (1988). Species-specific phytoplankton growth rates via diel DNA synthesis cycles. 1. Concept of the method. *Marine Ecology Progress Series. Oldendorf*, *43*(1), 105-111.

Carpenter, B., Gelman, A., Hoffman, M. D., Lee, D., Goodrich, B., Betancourt, M., ... & Riddell, A. (2017). Stan: a probabilistic programming language. *Grantee Submission*, *76*(1), 1-32.

Carr, M, Caselle, J. (2018). Data from “PISCO: subtidal community swath surveys.” Available at https://doi.org/10.6085/AA/PISCO_SUBTIDAL.151.2

Casini, M., Hjelm, J., Molinero, J. C., Lövgren, J., Cardinale, M., Bartolino, V., ... &

Kornilovs, G. (2009). Trophic cascades promote threshold-like shifts in pelagic marine ecosystems. *Proceedings of the National Academy of Sciences*, *106*(1), 197-202.

Chinn, S. M., Miller, M. A., Tinker, M. T., Staedler, M. M., Batac, F. I., Dodd, E. M., & Henkel, L. A. (2016). The high cost of motherhood: end-lactation syndrome in southern sea otters (*Enhydra lutris nereis*) on the Central California Coast, USA. *Journal of wildlife diseases*, *52*(2), 307-318.

Christianou, M., & Ebenman, B. (2005). Keystone species and vulnerable species in ecological communities: strong or weak interactors? *Journal of Theoretical Biology*, *235*(1), 95-103.

Clarke, K. R., & Gorley, R. N. (2015). PRIMER v7: user manual/tutorial. Primer-E Ltd, Plymouth, United Kingdom.

Connell, J. H., and Sousa, W. P. (1983). On the evidence needed to judge ecological stability or persistence. *The American Naturalist*, *121*(6), 789-824.

Conor, J. J. (1972). Gonad growth in the sea urchin, Strongylocentrotus purpuratus (Stimpson)(Echinodermata: Echinoidea) and the assumptions of gonad index methods. *Journal of Experimental Marine Biology and Ecology*, *10*(2), 89-103.

Cowen, R. K. (1983). The effects of sheephead (*Semicossyphus pulcher*) predation on red sea urchin (*Strongylocentrotus franciscanus*) populations: an experimental analysis. *Oecologia*, *58*(2), 249-255.

Cribari-Neto, F., & Zeileis, A. (2010). Beta regression in R. *Journal of Statistical*

Software, 34: 1-10.

Dakos, V., Kéfi, S., Rietkerk, M., Van Nes, E. H., & Scheffer, M. (2011). Slowing down in spatially patterned ecosystems at the brink of collapse. *The American Naturalist*, *177*(6), E153-E166.

Dayton, P. K., Currie, V., Gerrodette, T., Keller, B. D., Rosenthal, R., & Tresca, D. V. (1984). Patch dynamics and stability of some California kelp communities. *Ecological monographs*, *54*(3), 253-289.

Dayton, P. K., Tegner, M. J., Edwards, P. B., & Riser, K. L. (1998). Sliding baselines, ghosts, and reduced expectations in kelp forest communities. *Ecological Applications*, *8*(2), 309-322.

Dayton, P. K., Tegner, M. J., Parnell, P. E., & Edwards, P. B. (1992). Temporal and spatial patterns of disturbance and recovery in a kelp forest community. *Ecological Monographs*, *62*(3), 421-445.

Dayton, P. K., Mordida, B. J., & Bacon, F. (1994). Polar marine communities. *American Zoologist*, *34*(1), 90-99.

Dean, T. A., Schroeter, S. C., & Dixon, J. D. (1984). Effects of grazing by two species of sea urchins (*Strongylocentrotus franciscanus* and *Lytechinus anamesus*) on recruitment and survival of two species of kelp (*Macrocystis pyrifera* and *Pterygophora californica*). *Marine biology*, *78*(3), 301-313.

deYoung, B., Barange, M., Beaugrand, G., Harris, R., Perry, R. I., Scheffer, M., & Werner, F. (2008). Regime shifts in marine ecosystems: detection, prediction and management. *Trends in Ecology & Evolution*, *23*(7), 402-409.

Done, T. J. (1992). Phase shifts in coral reef communities and their ecological significance. *Hydrobiologia*, *247*(1), 121-132.

Dublin, H. T., Sinclair, A. R., & McGlade, J. (1990). Elephants and fire as causes of multiple stable states in the Serengeti-Mara woodlands. *The Journal of Animal Ecology*, 1147-1164.

Dudgeon, S. R., Aronson, R. B., Bruno, J. F., & Precht, W. F. (2010). Phase shifts and stable states on coral reefs. *Marine Ecology Progress Series*, *413*, 201-216.

Duffy, J. E., Cardinale, B. J., France, K. E., McIntyre, P. B., Thébault, E., & Loreau, M. (2007). The functional role of biodiversity in ecosystems: incorporating trophic complexity. *Ecology letters*, *10*(6), 522-538.

Duggins, D. O. (1983). Starfish predation and the creation of mosaic patterns in a kelp-dominated community. *Ecology*, *64*(6), 1610-1619.

Duggins, D. O., Simenstad, C. A., & Estes, J. A. (1989). Magnification of secondary production by kelp detritus in coastal marine ecosystems. *Science*, *245*(4914), 170-173.

Ebeling, A. W., Laur, D. R., & Rowley, R. J. (1985). Severe storm disturbances and reversal of community structure in a southern California kelp forest. *Marine biology*, *84*(3), 287-294.

Ebert, T. A. (1967). Negative growth and longevity in the purple sea urchin *Strongylocentrotus purpuratus* (Stimpson). *Science*, *157*(3788), 557-558.

Ebert, T. A. (1982). Longevity, life history, and relative body wall size in sea urchins. *Ecological Monographs*, *52*(4), 353-394.

Ebert, T. A. (2010). Demographic patterns of the purple sea urchin *Strongylocentrotus purpuratus* along a latitudinal gradient, 1985–1987. *Marine Ecology Progress Series*, *406*, 105-120.

Ebert, T. A., & Russell, M. P. (1988). Latitudinal variation in size structure of the west coast purple sea urchin: A correlation with headlands 1. *Limnology and Oceanography*, *33*(2), 286-294.

Eberhardt, L. L. (1995). Using the Lotka-Leslie model for sea otters. *The Journal of Wildlife Management*, 222-227.

Eisaguirre, J. H., Eisaguirre, J. M., Davis, K., Carlson, P. M., Gaines, S. D., & Caselle, J. E. (2020). Trophic redundancy and predator size class structure drive differences in kelp forest ecosystem dynamics. *Ecology*, *101*(5), e02993

Eldred, B. D. (2019). Bottom-up trait-mediated indirect effects decrease pathogen transmission in a tritrophic system. *Ecology*, *100*(1), e02551.

Estes, J. A., & Duggins, D. O. (1995). Sea otters and kelp forests in Alaska: generality and variation in a community ecological paradigm. *Ecological Monographs*, *65*(1), 75-100.

Estes, J. A., Tinker, M. T., Williams, T. M., & Doak, D. F. (1998). Killer whale predation on sea otters linking oceanic and nearshore ecosystems. *Science*, *282*(5388), 473-476.

Estes, J. A., & Palmisano, J. F. (1974). Sea otters: their role in structuring nearshore communities. *Science*, *185*(4156), 1058-1060.

Feehan, C. J., & Scheibling, R. E. (2014). Effects of sea urchin disease on coastal marine ecosystems. *Marine biology*, *161*(7), 1467-1485.

Filbee-Dexter, K., & Scheibling, R. E. (2014). Sea urchin barrens as alternative stable states of collapsed kelp ecosystems. *Marine ecology progress series*, *495*, 1-25.

Foster, M. S., & Schiel, D. R. (1985). The ecology of giant kelp forests in California: a community profile.

Fujii, J. A., Ralls, K., & Tinker, M. T. (2017). Food abundance, prey morphology, and diet specialization influence individual sea otter tool use. *Behavioral Ecology*, *28*(5), 1206-1216.

Gabara, S. S., Konar, B. H., & Edwards, M. S. (2021). Biodiversity loss leads to reductions in community-wide trophic complexity. *Ecosphere*, *12*(2), e03361.

Gelman, A., Meng, X. L., & Stern, H. (1996). Posterior predictive assessment of model fitness via realized discrepancies. *Statistica sinica*, 733-760.

Gelman, A., Goegebeur, Y., Tuerlinckx, F., & Van Mechelen, I. (2000). Diagnostic checks for discrete data regression models using posterior predictive simulations. *Journal of the Royal Statistical Society: Series C (Applied Statistics)*, *49*(2), 247-268.

Gerber, L. R., Tinker, M. T., Doak, D. F., Estes, J. A., & Jessup, D. A. (2004). Mortality sensitivity in life-stage simulation analysis: a case study of southern sea otters. *Ecological Applications*, *14*(5), 1554-1565.

Graham, M. H. (2004). Effects of local deforestation on the diversity and structure of southern California giant kelp forest food webs. *Ecosystems*, *7*(4), 341-357.

Graham, M. H., Harrold, C., Lisin, S., Light, K., Watanabe, J. M., & Foster, M. S. (1997). Population dynamics of giant kelp *Macrocystis pyrifera* along a wave exposure gradient. *Marine Ecology Progress Series*, *148*, 269-279.

Gil, M. A., Baskett, M. L., Munch, S. B., & Hein, A. M. (2020). Fast behavioral feedbacks make ecosystems sensitive to pace and not just magnitude of anthropogenic environmental change. *Proceedings of the National Academy of Sciences*, *117*(41), 25580-25589.

Hairston, N. G., Smith, F. E., & Slobodkin, L. B. (1960). Community structure, population control, and competition. *The American Naturalist*, *94*(879), 421-425.

Hamilton, S. L., & Caselle, J. E. (2015). Exploitation and recovery of a sea urchin predator has implications for the resilience of southern California kelp forests. *Proceedings of the Royal Society B: Biological Sciences*, *282*(1799), 20141817.

Harding, A. P., & Scheibling, R. E. (2015). Feed or flee: effect of a predation-risk cue on sea urchin foraging activity. *Journal of Experimental Marine Biology and Ecology*, *466*, 59-69.

Harrold, C., & Reed, D. C. (1985). Food availability, sea urchin grazing, and kelp forest community structure. *Ecology*, *66*(4), 1160-1169.

Harvell, C. D., Montecino-Latorre, D., Caldwell, J. M., Burt, J. M., Bosley, K., Keller, A., ... & Gaydos, J. K. (2019). Disease epidemic and a marine heat wave are associated with the continental-scale collapse of a pivotal predator (*Pycnopodia helianthoides*). *Science advances*, *5*(1), eaau7042.

Hatfield, B. B., Yee, J. L., Kenner, M. C., & Tomoleoni, J. A. (2019). *California sea otter (Enhydra lutris nereis) census results, spring 2019* (No. 1118). US Geological Survey.

Higginson, A. D., & Ruxton, G. D. (2015). Foraging mode switching: the importance of prey distribution and foraging currency. *Animal Behaviour*, *105*, 121-137.

Holling, C. S. (1966). The functional response of invertebrate predators to prey density. *The Memoirs of the Entomological Society of Canada*, *98*(S48), 5-86.

Holling, C. S. (1973). Resilience and stability of ecological systems. *Annual Review of Ecology and Systematics*, *4*(1), 1-23

Holmes, T. H., & McCormick, M. I. (2009). Influence of prey body characteristics and performance on predator selection. *Oecologia*, *159*(2), 401-413.

Hooper, D. U., Chapin III, F. S., Ewel, J. J., Hector, A., Inchausti, P., Lavorel, S., Lawton, J. H., Lodge, D. M., Loreau, M., Naeem, S., Schmid, B., Setala, H., Symstad, A. J., Vandermeeer, J., and Wardle, D. A. (2005). Effects of biodiversity on ecosystem functioning: a consensus of current knowledge. *Ecological Monographs*, *75*(1), 3-35.

Hopcraft, J. G. C., Sinclair, A. R. E., & Packer, C. (2005). Planning for success: Serengeti lions seek prey accessibility rather than abundance. *Journal of Animal Ecology*, *74*(3), 559-566.

Huggard, D. J. (1993). Prey selectivity of wolves in Banff National Park. I. Prey species. *Canadian Journal of Zoology*, *71*(1), 130-139.

Hunter, M. D., & Price, P. W. (1992). Playing chutes and ladders: heterogeneity and the relative roles of bottom-up and top-down forces in natural communities. *Ecology*, *73*(3), 724-732.

Jameson, R. J., & Johnson, A. M. (1993). Reproductive characteristics of female sea otters. *Marine Mammal Science*, *9*(2), 156-167.

Karatayev, V. A., & Baskett, M. L. (2020). At what spatial scales are alternative stable states relevant in highly interconnected ecosystems? *Ecology*, *101*(2), e02930.

Karatayev, V. A., Baskett, M. L., Kushner, D. J., Shears, N. T., Caselle, J. E., & Boettiger, C. (2019). Grazer behavior can regulate large-scale patterns of community states. *bioRxiv*, 722215.

Kaufman, L., & Rousseeuw, P. J. (2009). *Finding groups in data: an introduction to cluster analysis* (Vol. 344). John Wiley & Sons.

Kauffman, M. J., Brodie, J. F., & Jules, E. S. (2010). Are wolves saving Yellowstone's aspen? A landscape-level test of a behaviorally mediated trophic cascade. *Ecology*, *91*(9), 2742-2755.

Kennelly, S. J. (1989). Effects of kelp canopies on understory species due to shade and scour. *Marine Ecology Progress Series. Oldendorf*, *50*(3), 215-224.

Kenner, M. C., & Tinker, M. T. (2018). Stability and change in kelp forest habitats at San Nicolas Island. *Western North American Naturalist*, *78*(4), 633-643.

Klimley, A. P., Le Boeuf, B. J., Cantara, K. M., Richert, J. E., Davis, S. F., Van

Sommeran, S., & Kelly, J. T. (2001). The hunting strategy of white sharks (*Carcharodon carcharias*) near a seal colony. *Marine Biology*, *138*(3), 617-636.

Knowlton, N. (2004). Multiple "stable" states and the conservation of marine ecosystems. *Progress in Oceanography*, *60*(2-4), 387-396.

Konar, B., Edwards, M. S., & Estes, J. A. (2014). Biological interactions maintain the boundaries between kelp forests and urchin barrens in the Aleutian Archipelago. *Hydrobiologia*, *724*(1), 91-107.

Kriegisch, N., Reeves, S. E., Flukes, E. B., Johnson, C. R., & Ling, S. D. (2019). Drift-kelp suppresses foraging movement of overgrazing sea urchins. *Oecologia*, *190*(3), 665-677.

Krumhansl, K. A., & Scheibling, R. E. (2012). Production and fate of kelp detritus. *Marine Ecology Progress Series*, *467*, 281-302.

Krumhansl, K. A., Okamoto, D. K., Rassweiler, A., Novak, M., Bolton, J. J., Cavanaugh, K. C., ... & Byrnes, J. E. (2016). Global patterns of kelp forest change over the past half-century. *Proceedings of the National Academy of Sciences*, *113*(48), 13785-13790.

Lafferty, K. D. (2004). Fishing for lobsters indirectly increases epidemics in sea urchins. *Ecological Applications*, *14*(5), 1566-1573.

Lafferty, K. D., & Kushner, D. (2000). Population regulation of the purple sea urchin, Strongylocentrotus purpuratus, at the California Channel Islands. In *Fifth California Islands Symposium* (Vol. 99, p. 0038). Minerals Management

Service.

Levin, S. A. (1976). Spatial patterning and the structure of ecological communities. *Some Mathematical Questions in Biology*, *7*, 1-35.

Levin, S. A., & Paine, R. T. (1974). Disturbance, patch formation, and community structure. *Proceedings of the National Academy of Sciences*, *71*(7), 2744-2747.

Lewontin, R. C. (1969). The meaning of stability. In *Brookhaven symposia in biology* (Vol. 22, pp. 13-24).

Lima, S. L., & Zollner, P. A. (1996). Towards a behavioral ecology of ecological landscapes. *Trends in Ecology & Evolution*, *11*(3), 131-135.

Lindeløv, J. (2020). “mcp: An R Package for Regression with Multiple Change Points.” OSF Preprints. doi: 10.31219/osf.io/fzqxv.

Ling, S. D., Kriegisch, N., Woolley, B., & Reeves, S. E. (2019). Density-dependent feedbacks, hysteresis, and demography of overgrazing sea urchins. *Ecology*, *100*(2), e02577.

Ling, S. D., Scheibling, R. E., Rassweiler, A., Johnson, C. R., Shears, N., Connell, S. D., ... & Johnson, L. E. (2015). Global regime shift dynamics of catastrophic sea urchin overgrazing. *Philosophical Transactions of the Royal Society B: Biological Sciences*, *370*(1659), 20130269.

Loreau, M., & De Mazancourt, C. (2013). Biodiversity and ecosystem stability: a synthesis of underlying mechanisms. *Ecology Letters*, *16*, 106-115.

Lynam, C. P., Llope, M., Möllmann, C., Helaouët, P., Bayliss-Brown, G. A., &

Stenseth, N. C. (2017). Interaction between top-down and bottom-up control in marine food webs. *Proceedings of the National Academy of Sciences*, *114*(8), 1952-1957.

Malone, D. P., Koehn, K. D., Lonhart, S. I., Caselle, J. E., and Carr, M. H. (2021). Large scale, multi-decade monitoring data from kelp forest ecosystems in California and Oregon (USA). *Ecology*. In press.

Mann, K. H. (1982). Kelp, sea urchins and predators: a review of strong interactions in rocky subtidal systems of eastern Canada, 1970–1980. *Netherlands Journal of Sea Research*, *16*, 414-423.

McClanahan, T. R. (2000). Recovery of a coral reef keystone predator, *Balistapus undulatus*, in East African marine parks. *Biological Conservation*, *94*(2), 191-198.

McPherson, M. L., Finger, D. J., Houskeeper, H. F., Bell, T. W., Carr, M. H., Rogers-Bennett, L., & Kudela, R. M. (2021). Large-scale shift in the structure of a kelp forest ecosystem co-occurs with an epizootic and marine heatwave. *Communications biology*, *4*(1), 1-9.

Mehta, C. R., & Patel, N. R. (1983). A network algorithm for performing Fisher's exact test in r× c contingency tables. *Journal of the American Statistical Association*, *78*(382), 427-434.

Miller, M. A., Moriarty, M. E., Henkel, L., Tinker, M. T., Burgess, T. L., Batac, F. I., ... & Johnson, C. K. (2020). Predators, disease, and environmental change in the nearshore ecosystem: mortality in southern sea otters (*Enhydra lutris* *nereis*) from 1998–2012. *Frontiers in Marine Science*, *7*, 582.

Nichols, K. D., Segui, L., & Hovel, K. A. (2015). Effects of predators on sea urchin density and habitat use in a southern California kelp forest. *Marine Biology*, *162*(6), 1227-1237.

May, R. M. (1973). Stability in randomly fluctuating versus deterministic environments. *The American Naturalist*, *107*(957), 621-650.

Muller, C. H. (1940). Plant succession in the Larrea-Flourensia climax. *Ecology*, *21*(2), 206-212.

Newsome, S. D., Tinker, M. T., Monson, D. H., Oftedal, O. T., Ralls, K., Staedler, M. M., ... & Estes, J. A. (2009). Using stable isotopes to investigate individual diet specialization in California sea otters (*Enhydra lutris nereis*). *Ecology*, *90*(4), 961-974.

Nicholson, T. E., Mayer, K. A., Staedler, M. M., Fujii, J. A., Murray, M. J., Johnson, A. B., ... & Van Houtan, K. S. (2018). Gaps in kelp cover may threaten the recovery of California sea otters. *Ecography*, *41*(11), 1751-1762.

O'Connor, M. I., & Byrnes, J. E. K. (2013). Biodiversity and ecosystem function: Does pattern influence process. *Marine Community Ecology and Conservation. Sinauer, Sunderland, MA*, 109-130.

Okamoto, D. K., Schroeter, S. C., & Reed, D. C. (2020). Effects of ocean climate on spatiotemporal variation in sea urchin settlement and recruitment. *Limnology and Oceanography*, *65*(9), 2076-2091.

Oksanen, L., Fretwell, S. D., Arruda, J., & Niemela, P. (1981). Exploitation ecosystems in gradients of primary productivity. *The American Naturalist*, *118*(2), 240-261.

Ovadia, O., & Schmitz, O. J. (2002). Linking individuals with ecosystems: experimentally identifying the relevant organizational scale for predicting trophic abundances. *Proceedings of the National Academy of Sciences*, *99*(20), 12927-12931.

Pace, M. L., Cole, J. J., Carpenter, S. R., & Kitchell, J. F. (1999). Trophic cascades revealed in diverse ecosystems. *Trends in ecology & evolution*, *14*(12), 483-488.

Page, R. A., & Ryan, M. J. (2005). Flexibility in assessment of prey cues: frog-eating bats and frog calls. *Proceedings of the Royal Society B: Biological Sciences*, *272*(1565), 841-847.

Parnell, P. E., Fumo, J. T., Lennert-Cody, C. E., Schroeter, S. C., & Dayton, P. K. (2017). Sea urchin behavior in a Southern California kelp forest: food, fear, behavioral niches, and scaling up individual behavior. *Journal of Shellfish Research*, *36*(2), 529-543.

Petraitis, P. S., & Dudgeon, S. R. (2004). Detection of alternative stable states in marine communities. *Journal of Experimental Marine Biology and Ecology*, *300*(1-2), 343-371.

Pearse, J. S. (2006). Ecological role of purple sea urchins. *Science*, *314*(5801), 940-941.

Pearse, J. S., & Hines, A. H. (1987). Long-term population dynamics of sea urchins in a central California kelp forest: Rare recruitment and rapid decline. *Marine Ecology Progress Series. Oldendorf*, *39*(3), 275-283.

Pickett, S. T., & White, P. S. (Eds.). (2013). *The ecology of natural disturbance and patch dynamics*. Elsevier.

Pinna, S., Piazzi, L., Ceccherelli, G., Castelli, A., Costa, G., Curini-Galletti, M., ... & Bonaviri, C. (2020). Macroalgal forest vs sea urchin barren: patterns of macro-zoobenthic diversity in a large-scale Mediterranean study. *Marine environmental research*, *159*, 104955.

Poloczanska, E. S., Brown, C. J., Sydeman, W. J., Kiessling, W., Schoeman, D. S., Moore, P. J., ... & Richardson, A. J. (2013). Global imprint of climate change on marine life. *Nature Climate Change*, *3*(10), 919-925.

Power, M. E., Matthews, W. J., & Stewart, A. J. (1985). Grazing minnows, piscivorous bass, and stream algae: dynamics of a strong interaction. *Ecology*, *66*(5), 1448-1456.

Raymond, W. W., Tinker, M. T., Kissling, M. L., Benter, B., Gill, V. A., & Eckert, G. L. (2019). Location-specific factors influence patterns and effects of subsistence sea otter harvest in Southeast Alaska. *Ecosphere*, *10*(9), e02874.

Real, L. A. (1979). Ecological determinants of functional response. *Ecology*, *60*(3), 481-485.

Reed, D. C., & Foster, M. S. (1984). The effects of canopy shadings on algal recruitment and growth in a giant kelp forest. *Ecology*, *65*(3), 937-948.

Reed, D. C., Kinlan, B. P., Raimondi, P. T., Washburn, L., Gaylord, B., & Drake, P.

T. (2006). A metapopulation perspective on the patch dynamics of giant kelp in Southern California. In *Marine metapopulations* (pp. 353-386). Academic Press.

Riedman, M. L., Estes, J. A., Staedler, M. M., Giles, A. A., & Carlson, D. R. (1994). Breeding patterns and reproductive success of California sea otters. *The Journal of wildlife management*, 391-399.

Risk, M. J. (1972). Fish diversity on a coral reef in the Virgin Islands. *Atoll Research Bulletin*.

Rogers-Bennett, L., & Catton, C. A. (2019). Marine heat wave and multiple stressors tip bull kelp forest to sea urchin barrens. *Scientific reports*, *9*(1), 1-9.

Rosenzweig, M. L. (1973). Exploitation in three trophic levels. *The American Naturalist*, *107*(954), 275-294.

Russell, M. P. (1987). Life history traits and resource allocation in the purple sea urchin Strongylocentrotus purpuratus (Stimpson). *Journal of Experimental Marine Biology and Ecology*, *108*(3), 199-216.

Sala, E., & Zabala, M. (1996). Fish predation and the structure of the sea urchin Paracentrotus lividus populations in the NW Mediterranean. *Marine ecology progress series*, *140*, 71-81.

Selden, R. L., Gaines, S. D., Hamilton, S. L., & Warner, R. R. (2017). Protection of large predators in a marine reserve alters size-dependent prey mortality. *Proceedings of the Royal Society B: Biological Sciences*, *284*(1847), 20161936.

Scheffer, M. (2004). *Ecology of shallow lakes* (Vol. 22). Springer Science & Business Media.

Scheffer, M., Carpenter, S., Foley, J. A., Folke, C., & Walker, B. (2001). Catastrophic shifts in ecosystems. *Nature*, *413*(6856), 591-596.

Scheffer, M., & Carpenter, S. R. (2003). Catastrophic regime shifts in ecosystems: linking theory to observation. *Trends in ecology & evolution*, *18*(12), 648-656.

Scheffer, M., Bascompte, J., Brock, W. A., Brovkin, V., Carpenter, S. R., Dakos, V., ... & Sugihara, G. (2009). Early-warning signals for critical transitions. *Nature*, *461*(7260), 53-59.

Scheibling, R. E., & Hamm, J. (1991). Interactions between sea urchins (*Strongylocentrotus droebachiensis*) and their predators in field and laboratory experiments. *Marine Biology*, *110*(1), 105-116.

Scheibling, R. E. (1996). The role of predation in regulating sea urchin populations in eastern Canada. *Oceanologica Acta*, *19*(3-4), 421-430.

Scheibling, R. E., & Lauzon-Guay, J. S. (2010). Killer storms: North Atlantic hurricanes and disease outbreaks in sea urchins. *Limnology and Oceanography*, *55*(6), 2331-2338.

Schmitz, O. J., Beckerman, A. P., & O’Brien, K. M. (1997). Behaviorally mediated trophic cascades: effects of predation risk on food web interactions. *Ecology*, *78*(5), 1388-1399.

Schmitz, O. J. (1998). Direct and indirect effects of predation and predation risk in old-field interaction webs. *The American Naturalist*, *151*(4), 327-342.

Schröder, A., Persson, L., & De Roos, A. M. (2005). Direct experimental evidence for alternative stable states: a review. *Oikos*, *110*(1), 3-19.

Selden, R. L., Gaines, S. D., Hamilton, S. L., & Warner, R. R. (2017). Protection of large predators in a marine reserve alters size-dependent prey mortality. *Proceedings of the Royal Society B: Biological Sciences*, *284*(1847), 20161936.

Sheaves, M. (2009). Consequences of ecological connectivity: the coastal ecosystem mosaic. *Marine Ecology Progress Series*, *391*, 107-115.

Sih, A., Cote, J., Evans, M., Fogarty, S., & Pruitt, J. (2012). Ecological implications of behavioural syndromes. *Ecology letters*, *15*(3), 278-289.

Smale, D. A. (2020). Impacts of ocean warming on kelp forest ecosystems. *New Phytologist*, *225*(4), 1447-1454.

Smith, J. G., & Garcia, S. C. (2021). Variation in purple sea urchin (*Strongylocentrotus purpuratus*) morphological traits in relation to resource availability. *PeerJ*, *9*, e11352.

Smith, J. G., Tomoleoni, J., Staedler, M., Lyon, S., Fujii, J., & Tinker, M. T. (2021). Behavioral responses across a mosaic of ecosystem states restructure a sea otter–urchin trophic cascade. *Proceedings of the National Academy of Sciences*, *118*(11).

Spyksma, A. J., Taylor, R. B., & Shears, N. T. (2017). Predation cues rather than resource availability promote cryptic behaviour in a habitat-forming sea urchin. *Oecologia*, *183*(3), 821-829.

Stachowicz, J. J., Bruno, J. F., & Duffy, J. E. (2007). Understanding the effects of marine biodiversity on communities and ecosystems. *Annu. Rev. Ecol. Evol. Syst.*, *38*, 739-766.

Staver, A. C., Archibald, S., & Levin, S. A. (2011). The global extent and determinants of savanna and forest as alternative biome states. *Science*, *334*(6053), 230-232.

Steneck, R. S., Graham, M. H., Bourque, B. J., Corbett, D., Erlandson, J. M., Estes, J. A., & Tegner, M. J. (2002). Kelp forest ecosystems: biodiversity, stability, resilience and future. *Environmental conservation*, 436-459.

Steneck, R. S. (2013). Sea urchins as drivers of shallow benthic marine community structure. In *Developments in Aquaculture and Fisheries Science* (Vol. 38, pp. 195-212). Elsevier.

Sutherland, J. P. (1990). Perturbations, resistance, and alternative views of the existence of multiple stable points in nature. *The American Naturalist*, *136*(2), 270-275.

Tanaka, M. (1982). A new growth curve which expresses infinitive increase. *Publications of Amakusa Maine Biological Laboratory*, *6*, 167-177.

Tegner, M. J., & Levin, L. A. (1983). Spiny lobsters and sea urchins: analysis of a predator-prey interaction. *Journal of Experimental Marine Biology and Ecology*, *73*(2), 125-150.

Terborgh, J., & Estes, J. A. (Eds.). (2013). *Trophic cascades: predators, prey, and the changing dynamics of nature*. Island press.

Thometz, N. M., Tinker, M. T., Staedler, M. M., Mayer, K. A., & Williams, T. M. (2014). Energetic demands of immature sea otters from birth to weaning: implications for maternal costs, reproductive behavior and population-level trends. *Journal of Experimental Biology*, *217*(12), 2053-2061.

Thometz, N. M., Staedler, M. M., Tomoleoni, J. A., Bodkin, J. L., Bentall, G. B., & Tinker, M. T. (2016). Trade-offs between energy maximization and parental care in a central place forager, the sea otter. *Behavioral Ecology*, *27*(5), 1552-1566.

Tilman, D. (1996). Biodiversity: population versus ecosystem stability. *Ecology*, *77* (2), 350-363.

Tilman, D., Isbell, F., & Cowles, J. M. (2014). Biodiversity and ecosystem functioning. *Annual review of ecology, evolution, and systematics*, *45*, 471-493.

Tinker, M. T., Bentall, G., & Estes, J. A. (2008). Food limitation leads to behavioral diversification and dietary specialization in sea otters. *Proceedings of the National Academy of Sciences*, *105*(2), 560-565.

Tinker, M. T., Doak, D. F., Estes, J. A., Hatfield, B. B., Staedler, M. M., & Bodkin, J. L. (2006). Incorporating diverse data and realistic complexity into demographic estimation procedures for sea otters. *Ecological Applications*, *16*(6), 2293-2312.

Tinker, M. T., Guimaraes Jr, P. R., Novak, M., Marquitti, F. M. D., Bodkin, J. L., Staedler, M., ... & Estes, J. A. (2012). Structure and mechanism of diet specialisation: testing models of individual variation in resource use with sea otters. *Ecology letters*, *15*(5), 475-483.

Tinker, M. T., & Hatfield, B. B. (2016). *California sea otter (Enhydra lutris nereis) census results, Spring 2016* (No. 1018). US Geological Survey.

Tinker, M. T., Hatfield, B. B., Harris, M. D., & Ames, J. A. (2016). Dramatic increase in sea otter mortality from white sharks in California. *Marine Mammal Science*, *32*(1), 309-326.

Tinker, M. T., Tomoleoni, J., LaRoche, N., Bowen, L., Miles, A. K., Murray, M., ... & Randell, Z. (2017). *Southern sea otter range expansion and habitat use in the Santa Barbara Channel, California* (No. 2017-1001). US Geological Survey.

Tinker, M.T., Tomoleoni, J.A., Weitzman, B.P., Staedler, M., Jessup, D., Murray, M.J., Miller, M., Burgess, T., Bowen, L., Miles, A.K. and Thometz, N., (2019). Southern sea otter (*Enhydra lutris nereis*) population biology at Big Sur and Monterey, California--Investigating the consequences of resource abundance and anthropogenic stressors for sea otter recovery (No. 2019-1022). US Geological Survey.

Tinker, M. T., Yee, J. L., Laidre, K. L., Hatfield, B. B., Harris, M. D., Tomoleoni, J. A., ... & Miles, A. K. (2021). Habitat Features Predict Carrying Capacity of a Recovering Marine Carnivore. *The Journal of Wildlife Management*, *85*(2), 303-323.

Trussell, G. C., Matassa, C. M., & Ewanchuk, P. J. (2017). Moving beyond linear food chains: trait-mediated indirect interactions in a rocky intertidal food web. *Proceedings of the Royal Society B: Biological Sciences*, *284*(1851), 20162590.

Vásquez, J. A., & Buschmann, A. H. (1997). Herbivore-kelp interactions in Chilean subtidal communities: a review. *Revista Chilena de Historia Natural*, *70*(1), 41-52.

Vehtari, A., Gelman, A., & Gabry, J. (2017). Practical Bayesian model evaluation using leave-one-out cross-validation and WAIC. *Statistics and computing*, *27*(5), 1413-1432.

Vivian-Smith, G. (1997). Microtopographic heterogeneity and floristic diversity in experimental wetland communities. *Journal of Ecology*, 71-82.

Werner, E. E., & Peacor, S. D. (2003). A review of trait-mediated indirect interactions in ecological communities. *Ecology*, *84*(5), 1083-1100.

Wangensteen, O. S., Turon, X., García-Cisneros, A., Recasens, M., Romero, J., & Palacín, C. (2011). A wolf in sheep's clothing: carnivory in dominant sea urchins in the Mediterranean. *Marine Ecology Progress Series*, *441*, 117-128.

Watanabe, J. M., & Harrold, C. (1991). Destructive grazing by sea urchins Strongylocentrotus spp. in a central California kelp forest: potential roles of recruitment, depth, and predation. *Marine Ecology Progress Series. Oldendorf*, *71*(2), 125-141.

Watson, J., & Estes, J. A. (2011). Stability, resilience, and phase shifts in rocky subtidal communities along the west coast of Vancouver Island, Canada. *Ecological Monographs*, *81*(2), 215-239.

Wiens, J. A. (1995). Landscape mosaics and ecological theory. In *Mosaic landscapes and ecological processes* (pp. 1-26). Springer, Dordrecht.

Witman, J. D., Smith, F., & Novak, M. (2017). Experimental demonstration of a trophic cascade in the Galápagos rocky subtidal: effects of consumer identity and behavior. *PloS one*, *12*(4), e0175705.

Worm, B., Barbier, E. B., Beaumont, N., Duffy, J. E., Folke, C., Halpern, B. S., Jackson, J. B., Lotze, H. K., Micheli, F., Palumbi, S. R., Sala, E., Selkoe, K. A., Stachowicz, J. J., and Watson, R. (2006). Impacts of biodiversity loss on ocean ecosystem services. *Science*, *314*(5800), 787-790.

Young, M., Cavanaugh, K., Bell, T., Raimondi, P., Edwards, C. A., Drake, P. T., ... & Storlazzi, C. (2016). Environmental controls on spatial patterns in the long-term persistence of giant kelp in central California. *Ecological Monographs*, *86*(1), 45-60.